Title	**Atmospheric correction and related issues**
Version	0.1
Author(s)	R. Santer and O. Aznay
and affiliation(s)	ADRINORD
Modification history	First draft: 30/06/2011 This issue: 8/12/2011
Distribution	Public report

Acronyms

5S	Simulation of the Satellite Signal in the Solar Spectrum
6S	Second Simulation of the Satellite Signal in the Solar Spectrum
AA	Azimuth Angle
ABB/BOMEM	ABB BOMEM Inc (*www.bomem.com*)
AC	Atmospheric Correction
ADRINORD	Association pour le Développement de la Recherche et de l'Innovation dans le NORD
AE	Adjacency Effect
AERONET	Aerosol RObotic NETwork (http://aeronet.gsfc.nasa.gov/)
ALM	ALMulcantar
AOT	Aerosol optical thickness
ATBD	Algorithm Theorical Basis Document
BOA	Bottom Of Atmosphere
CC	Coast Colour project (http://coastcolour.org/about.html)
DB	Data Base
ENVISAT	ENVIronmental SATellite
ESA	European Space Agency (*www.**esa**.int)*
FR	Full Resolution
ICOL	Improve Contrast between Ocean and Land
IOPA	Inherent Optical Property of Aerosol
ISECA	Information System on the Eutrophication of our Coastal Areas
L1	Level 1
L2	Level 2
LUT	Look Up Table
MEGS	MEris Ground Segment
MERIS	Medium Resolution Imaging Spectrometer (ESA Envisat)
MERIS IPF	MERIS Instrument Processing Facility
MERISAT	MERIS Atmospheric Table

NIR	Near Infra Red
ODESA	**Optical Data processor of the European Space Agency**
PPL	Principal Plane
ROI	Region Of Interest
ROT	Rayleigh Optical Thickness
RR	Reduced Resolution
RTC	Radiative Transfer Code
SAM	Standart Aerosol Model
SO	Successive Order
SSA	Solar Azimuth Angle
SZA	Solar Zenith Angle
TN	Technical note
TOA	Top Of the Atmosphere
VZA	View Zenith Angle
WOPAER	Name of a software t-o derive the aerosol phase function

Executive summary:

In the frame of the atmospheric correction for ocean colour sensors, the objective in ISECA is to improve the algorithm through a better knowledge in the 2Sea region of the aerosol optical properties and the development of the radiative transfer tools to include these properties in the processing chain. One second aspect is to correct from the adjacency effect which occurs in the vicinity of the land. The ICOL software provides this correction.

General introduction

The role of ADRINORD in the preparation of A2 is to propose an algorithm chain to process the Earth Observation data, here the “ocean colour” sensors with a key instrument: MERIS onboard of ENVISAT.

The processing chain starts at level 1. This level 1 corresponds to relevant pieces of information on:

(i) The time and the geometry of observation.

(ii) The meteorological data at the time of overpass

(iii) The flags (information on the nature of the pixel: classification, quality assessment,…)

(iv) The radiometry (signal in different spectral bands)

The standard processing chain at level2 returns:

(i) The L1 general information

(ii) Additional flags on the quality of the product

(iii) The reflectance of the water body

(iv) Water products such as the chlorophyll-a and suspended matter content

These L2 product algorithms are global, i.e. based on universal optical properties and general assumptions. For ISECA, we want to develop a regional approach adapted to our 2Seas maritime ROI.

The first step of the L2 processor is to perform the atmospheric correction, going from the top of the atmosphere to the bottom for an effective observation of the ocean body. During the preparation phase, we did the following steps:

(i) Define a protocol to know the optical properties of the aerosols from in situ measurements; The in situ measurements are collected in a global network (AERONET) of radiometers (Cimel) and several stations are present in the 2Seas area. The objective was to define a protocol to analyse the data, implement it and process data to evaluate the performances. This action is reported in annex 1.

(ii) Using the above optical properties of the aerosols, we realize software to simulate the satellite signal. The objective here is first to have reference model to simulate satellite measurements and second to generate tables to be used in a processing chain. This simulator is described in annex 2.

(iii) The contrast of a satellite image is affected at coast line by the so called adjacency effects. The photons reflected by the high reflective land can contribute by atmospheric scattering to the signal observed over water. For ISECA, it is a critical issue because the directive for the water quality applies to the first nautical miles. That the reason why we developed an atmospheric correction scheme which includes this adjacency effects, annex 3.

ADRINORD

Document Title:	**The inherent optical properties of the aerosols**
Version:	1.0
Author(s):	R. Santer, O. Aznay and P. Santer Limerez
Affiliation(s):	ADRINORD, Association pour le Développement de la Recherche et de l'Innovation dans la Région Nord-Pas de Calais, Lille – France.
Modification History:	First version, July 31, 2010 Final version: January 31, 2011

Distribution: Internal

1) Introduction

The objective of this TN is to evaluate the optical properties of the aerosols in the Coast Colour ROIs in order:

(*i*) To have the suitable inputs to train the algorithms and/or to generate the required LUTs.

(*ii*) To evaluate the regional variability of the aerosol model in the frame of the regionalization of the algorithms.

The experimental tool is AERONET and we use it firstly, to identify the stations in our ROIs and secondly, to derive climatology based on the AOTs.

The theoretical tool is WOPAER, a software package developed at ADRINORD, to derive the aerosol phase functions from the sky radiance measurements provided by AERONET.

The tool to analyze these aerosol phase functions is IOPA to provide, at the end in all the MERIS bands, the inherent optical properties of the aerosols.

2) AERONET and the ROIs

AERONET is a globally distributed network of automated ground-based instruments and data archive system, developed to support the aerosol community. The instruments used are CIMEL spectral radiometers (E-318) that measure the spectral extinction of the direct Sun radiance (Holben *et al.*, 1998). The aerosol optical depths are determined using the *Beer-Bouguer* Law in several spectral bands.

The CIMEL is designed to conduct atmospheric studies, and particularly to determine the aerosol optical properties. It is equipped with four standard filters: 1020 nm, 870 nm, 675 nm and 440 nm. Thanks to two collimators (*i.e.*, sun and sky) located between the wheel of the filter and the electronic box, this instrument offers three scanning protocols: (*a*) *sun*, (*b*) *alm*, and (*c*) *ppl*. For the *sun* mode, the CIMEL selects the *sun* collimator and aims at the sun to measure the light extinction in each of the four filters. The AOTs at 440 nm, 675 nm and 870 nm are then derived from these measurements. For the *alm* mode, the sun-photometer tracks the sun and acquires measurements of downwelling radiance at the solar zenith angle using its *sky* collimator, with a complete azimuthal rotation (75 azimuth viewing angles). For the *ppl* mode, the instrument firstly points to the sun then collects radiance measurements in the principal plane (or solar plane) for 40 zenith viewing angles. For the last two scanning modes, the sky radiances are acquired in each of the four filters.

2.1) Selection of the AERONET stations

To better characterize the natural variability of the aerosols, we selected different coastal areas providing a wide range of aerosols components. A detailed description of the selected AERONET sites is available in the appendix 1.

UR-1 region I : 40°N-65°N, 20°W-O and 50°N-65°N, 5°W-15°E

North Sea

enes (58N,8E)
Date: 23-APR-2000; Latest Date: 25-APR-2010
oland (54N,7E)
Date: 10-AUG-1993; Latest Date: 27-APR-2010
burg (53N,9E),
Date: 08-AUG-1996; Latest Date: 26-APR-2010
Hague (52N,4E),

Date: 04-NOV-2001; Latest Date: 01-JUN-2006
ende (51N,2E),
Date: 14-JUN-2001; Latest Date: 04-DEC-2009
kerque (51N,2E),
Date: 30-NOV-2002; Latest Date: 26-APR-2010

English Channel

nion (48N,3W),
Date: 30-OCT-2004; Latest Date: 20-MAY-2009

Bay of Biscay

chon (44N,1W),
Date: 23-OCT-2008; Latest Date: 26-APR-2010
RDEAUX (44N,0W),
Date: 14-MAY-2001; Latest Date: 07-FEB-2003
ritz (43N,1W)
Date: 09-OCT-1996; Latest Date: 09-OCT-2001

Celtic Sea

e_Head (50N,4W)
Date: 23-DEC-1996; Latest Date: 17-JUN-2000

Irish Sea

e_Head (53N,9W),
Date: 02-NOV-2002; Latest Date: 23-FEB-2004

UR-2 region II : 57°N-66°N, 15°E-31°E

Baltic

av_Dalen_Tower (58N,17E)
Date: 16-JUL-2004; Latest Date: 06-OCT-2009
and (57N,18E)
Date: 01-JAN-1993; Latest Date: 18-MAY-2004
inki_Lighthouse (59N,24E)
Date: 16-MAY-2006; Latest Date: 13-NOV-2009

UR-3 region III : 30°N-48°N, 12°E-42°E

Eastern Mediterranean & Black Sea

stopol (44N,33E)
Date: 05-MAY-2006; Latest Date: 26-APR-2010
-METU-ERDEMLI (36N,34E)

Date: 06-JAN-1993; Latest Date: 27-APR-2010
Ziona (31N,34E)

Date: 02-JAN-1993; Latest Date: 27-APR-2010
omi (40N,22E)
Date: 16-JUL-2006; Latest Date: 29-OCT-2007
ENS-NOA (37N,23E)
Date: 07-APR-2008; Latest Date: 26-APR-2010

FORTH_CRETE (35N,25E)
Start Date: 07-AUG-1992; Latest Date: 26-APR-2010
Lampedusa (35N,12E)
Start Date: 05-JAN-2000; Latest Date: 26-APR-2010
Tremiti (42N,15E)
Start Date: 05-AUG-2007; Latest Date: 10-SEP-2008
Venise (45N,12E)
Start Date: 20-DEC-1992; Latest Date: 26-APR-2010

UR-4 region IV :
Atlantic and Mediterranean costs of Morocco

Atlantic cost

Tenerife (28N,16W)
Start Date: 24-JUN-1997; Latest Date: 24-JUL-1997
Dahkla (23N,15W)
Start Date: 04-JUN-1997; Latest Date: 08-NOV-2005

UR-5 region V : 42°N-52°N, 52°W-69°W

Acadia

Chebogue_Point (43N,66W)
Start Date: 28-JUN-2004; Latest Date: 26-AUG-2004
Halifax (44N,63W)
Start Date: 26-JUN-2002; Latest Date: 26-APR-2010
Sable_Island (43N,60W)

Mont_Joli (48N,68W)
Start Date: 24-JUN-1999; Latest Date: 14-MAR-2002

UR-6 region VI: 34°N-41°N, 70°N-79°W

Chesapeake Bay

MVCO (41N,70W)
Start Date: 07-NOV-2001; Latest Date: 27-APR-2010
Sandy_Hook (40N,73W)
Start Date: 27-MAY-1996; Latest Date: 24-OCT-1996
SERC (38N,76W)
Start Date: 22-NOV-1994; Latest Date: 27-APR-2010
Hog_Island (37N,75W)
Start Date: 08-JUL-1993; Latest Date: 11-JUL-1996
COVE_SEAPRISM (36N,75W)
Start Date: 19-APR-2005; Latest Date: 06-NOV-2009
EOPACE2 (36N,75W)
Start Date: 19-FEB-1999; Latest Date: 10-FEB-2000

UR-7 region VII: 41°N-49°N, 122°W-127°W

Oregon (and Washington??)

Saturn_Island (48N,123W)
Start Date: 08-SEP-1994; Latest Date: 27-APR-2010

UR-8 region VIII: 33.5°N-34.5°N, 119.4°W-120.5°W

Plumes and Blooms

San_Nicolas (33N,119W)
Start Date: 06-JUN-1997; Latest Date: 16-MAR-2010

Table 1: Distribution of AERONET sites per region.

In order to take account for the new ROIs, listed in table 2, we indicate first when it corresponds to an adjacent site of the initial selection, and second we identify the AERONET stations included in the additional ROIs. All the new sites are covered excepted # 18 and 19 in the Arctic Ocean.

UR	Name of the ROI	Adjacent UR	AERONET station

13	Red Sea	3	Eilat (29N,34E)
14	Indonesian		Puspiptec (6S,106E)
15	Beibu Bay	11	Bach Long Vy (20N,107E)
16	Namibian Waters		Swakopmund (22S,14E)
17	Cape Verde	4	Capo Verde (20N,107E)
18	Lena Delta and New Siberian Islands		none
19	Kara Sea		none
20	Central California	8	Monterey (36N,121W)
21	French Guyana & Amazon Delta	9	Bragansa (0S,46W)
22	South India		GOA INDIA (15N,73E)
23	Antares-Ubatuba	9	Sao Paulo (23S,46W)
24	Lake Erie & Lake St. Clair	5	Windsor B (few data; 42N,82W)

Table 2: *Distribution of new AERONET sites per region (UR).*

2.2) The AERONET climatology

A full climatology based on AERONET level 2.0 products (quality assured data and monthly averaged) namely the aerosol optical thicknesses (AOTs) is available in appendix 2. We displayed in Figure 1 a representative climatology of three different coastal areas. The latters present local aerosol models: continental [a; UR-1,2,3,11], mono-dispersed [b; UR-5,3,6,7,8] and maritime [c;UR-4].

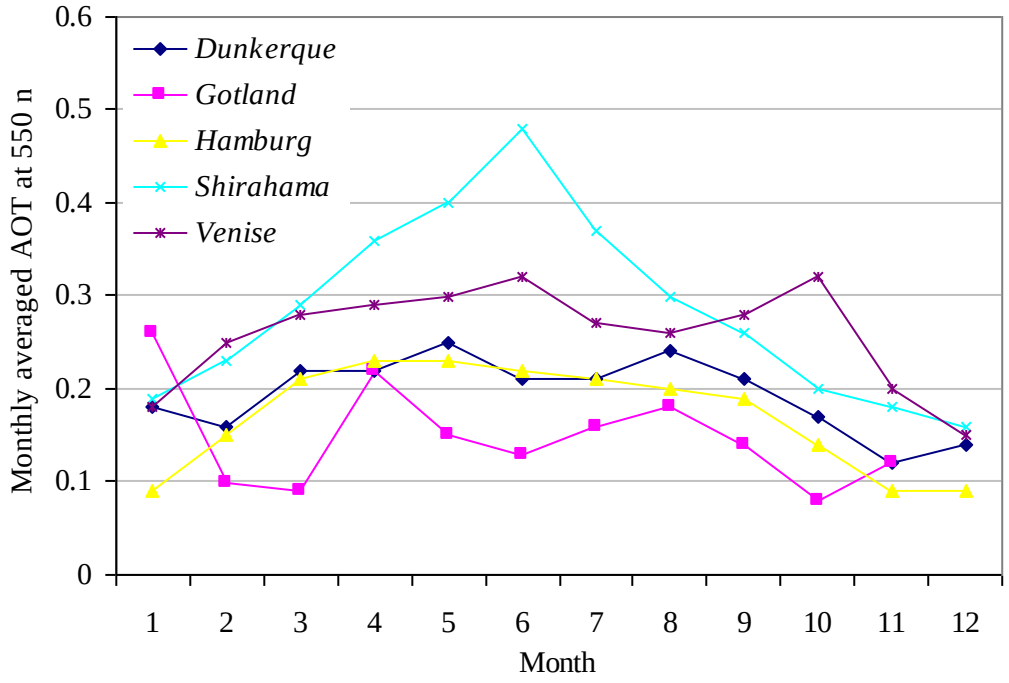
Monthly averaged AOT at 550 n
0.6
0.5
0.4
0.3
0.2
0.1
0
Dunkerque
Gotland
Hamburg
Shirahama
Venise
1
2
3
4
5
6
7
8
9
10
11
12
Month

(a)

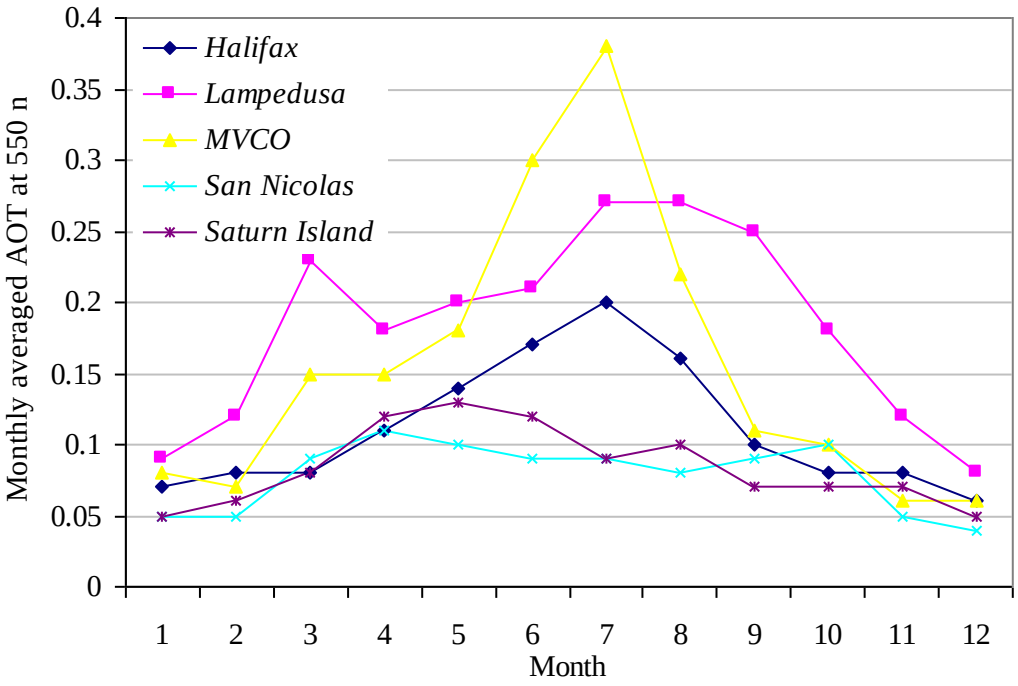
Monthly averaged AOT at 550 n
0.4
0.35
0.3
0.25
0.2
0.15
0.1
0.05
0
Halifax
Lampedusa
MVCO
San Nicolas
Saturn Island
1
2
3
4
5
6
7
8
9
10
11
12
Month

(b)

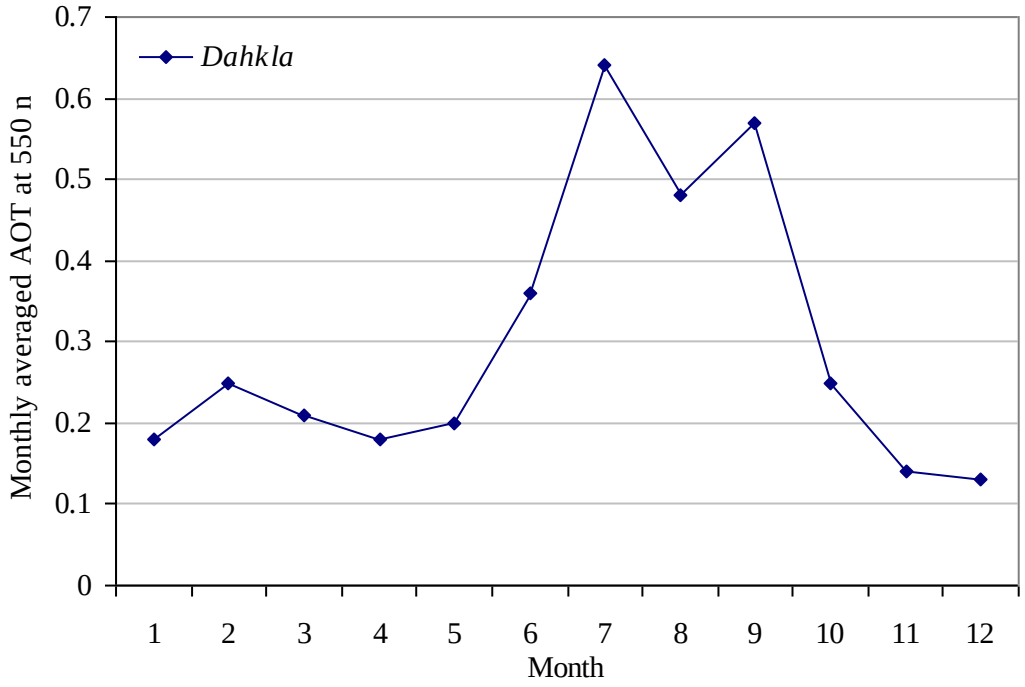

(c)

Figure 1: *Annual climatology based on AERONET level 2.0 products for three coastal types areas.*

3) Aerosol inherent optical properties

The AERONET network has already been used in many previous studies for validating the inherent optical properties (IOPs) of aerosols. The IOPs are generally computed from microphysical properties using Mie's theory (Mie, 1908). Many recent studies link the uncertainties on these IOPs with the use of aerosol climatology based on microphysical properties.

3.1) From the extinction measurement

In this section, we adopt the same approach as developed in section 2.2; however, for a more detailed study, we used AERONET level 2.0 products with a higher temporal resolution (all points). We displayed in Figure 2, the distribution of the AOT (left side) and the *Angstrom* coefficient (α; right side). The AOT distribution is displayed for three wavelengths (440, 675 and 870 nm) while the distribution of the Angstrom coefficient is displayed for two spectral windows (440-675 and 675-870). We can distinguish three kind of aerosol particles for these coastal areas: a continental aerosol model (Figure 2*a*) defined by an *Angstrom* coefficient ranging from -1.5 to -2 (80 % of the data), a mono-dispersed aerosol model (Figure 2*b*) defined by two *Angstrom* coefficients ranging from -1.7 to -2.5 (70 % of the data) and ranging from -0.3 to -1.2 (65 % of the data) and a maritime

aerosol model (Figure 2*c*) defined by an *Angstrom* coefficient ranging from -0.3 to -0.7 (80 % of the data). Coastal areas where the continental model is mainly observed (Figure 2*a*) present lower visibility than the two other coastal areas.

A deeper analysis of Figure 2*b* indicates that the dynamic of the two *Angstrom* exponents α(440,675) and α(675,870) derived from CIMEL extinctions, at 675 nm and 440 nm and at 870 nm and 675 nm, respectively, varies strongly. As a consequence, the regular aerosol size distribution cannot be representative of the local aerosols over these sites. If we are only concerned by the aerosol remote-sensing over ocean, then α(675,870) will have to be employed. Atmospheric correction in the near-infrared (NIR) region needs some refinements in the selection of the standard aerosol models. The other coastal areas (Figure 2*a* & 2*c*) represent a much more standard situation in which, through the small variation in α, a regular aerosol model appears to be more acceptable to describe the aerosols.

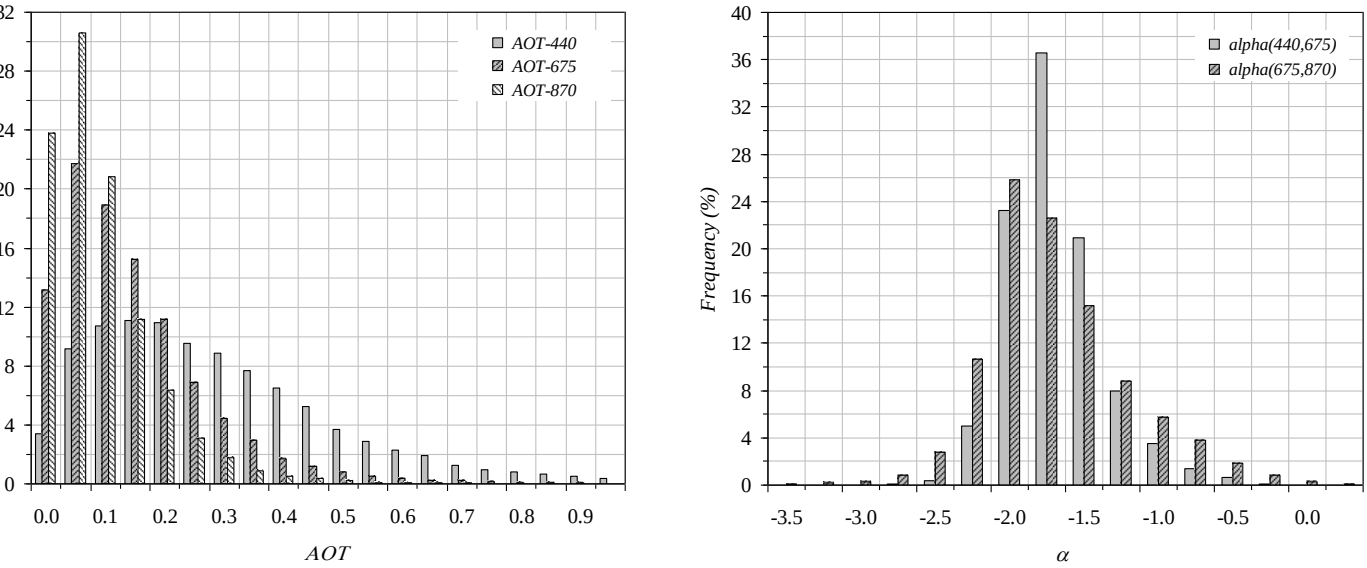

(a)

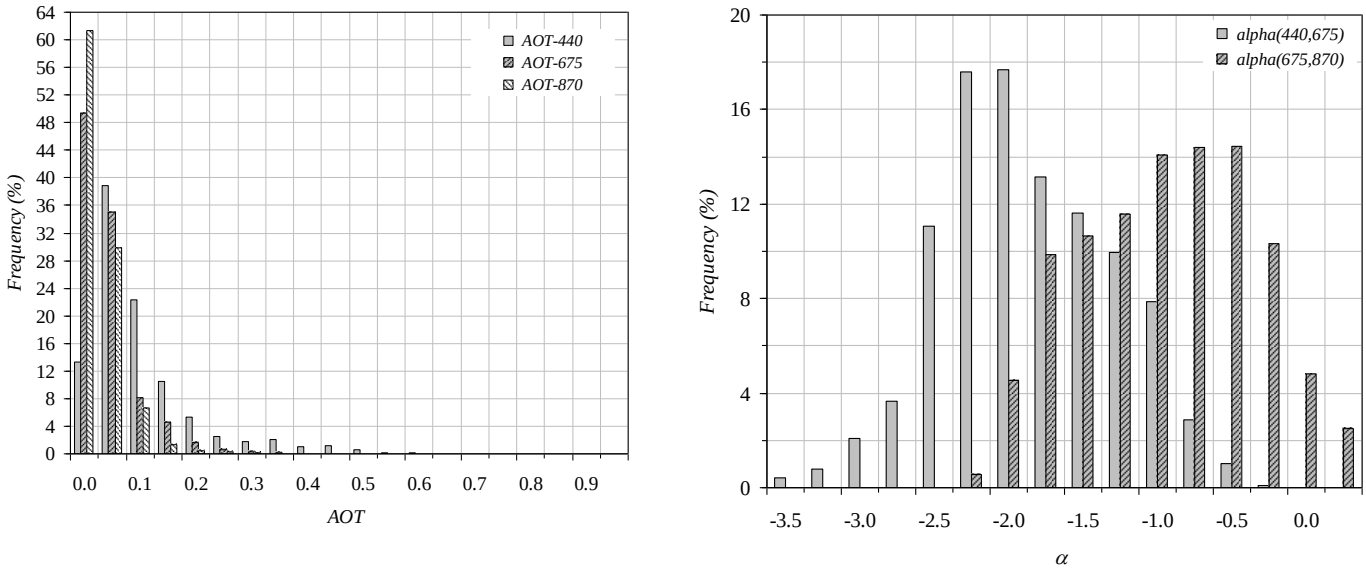

(b)

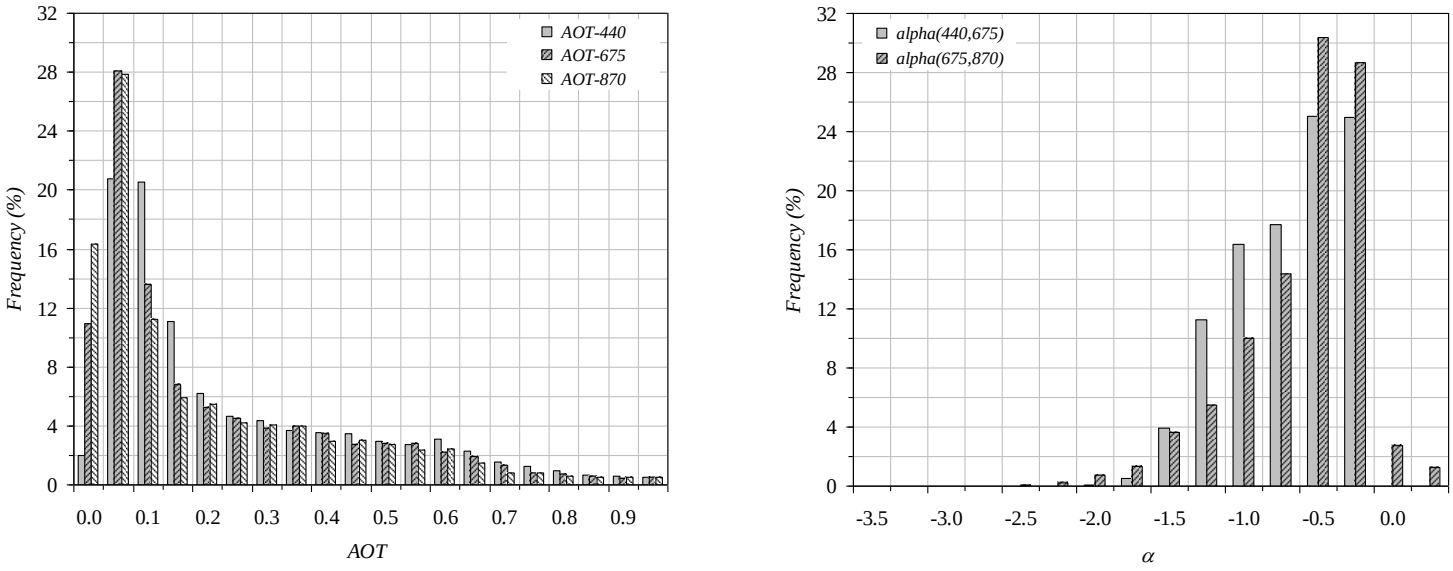

(c)

Figure 2: *Distribution of the AOT and the Angstrom coefficient for the three selected areas.*

3.2) From the sky radiance

An alternative use of the CIMEL sky radiance is to retrieve the aerosol phase function (APF) times the single scattering albebo (SSA): *ωo.Pa* (Santer *and* Martiny, 2003; Santer *et al.*, 2009). Therefore, the European Space Agency (ESA) undertook an action to produce a new set of aerosol models based on the interpretation of the

CIMEL sky radiances to retrieve the IOPs of aerosols, i.e. the product *ωo.Pa* (called IOPA models hereafter). This new set of aerosols models are still classified in α for values between 0 and 2.5 by step of 0.1 over land (Aznay *et al.*, 2010) and between 0 and 2.25 by step of 0.15 over ocean (Zagolski *et al.*, 2007).

3.2.1) The IOPA models as an alternative

Many studies (Aznay *and* Santer, 2008; Zagolski *et al.*, 2007) have shown that aerosol models, built up microphysical properties, lead to uncertainties on the aerosol products. Vidot *et al.*, (2008) have shown that the use of an alternative climatology, based on the IOPs (IOPA aerosol models) of the sky, improves the uncertainties on aerosols products. Moreover, application of IOPA models on MERIS images has shown that IOPA models (right side of Picture 1) reduces geophysical noise compared to SAMs models (left side of Picture 1). The following section describes these IOPA models.

11, 14, 15 and 22

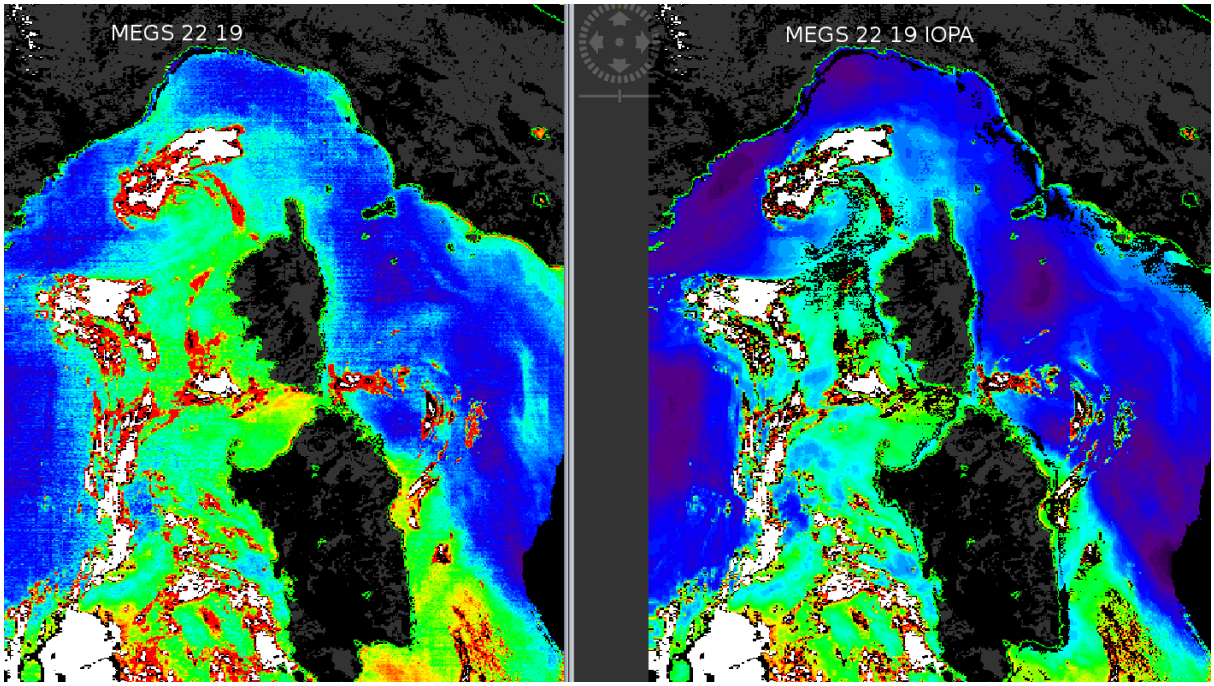

Picture 1: *Noise on the AOT at 865 nm (source: C. Mazeran from ACRI S.T).*

3.2.2) The initial IOPA data base

We briefly describe the IOPA climatology in this section. A detailed description of the IOPA models in available in Zagolski *et al.*, (2007) over oceans and in Aznay *et al.*, (2010) over lands.

In the MERIS level-2 processing, the ocean-aerosol look-up tables (LUTs) have been generated for a set of 16 aerosol models defined by an *Angstrom* exponent within the range [0; 3]. As the IOPs of the aerosols derived from the CIMEL measurements appear to be continuous versus α, we decided to characterize them by classes of α. For that, we selected the 16 classes of α from the MERIS ocean-aerosol product using a Δα of 0.15, except for the first class, for which α was fixed at 0.05, with a Δα of 0.1; Thus, using this set of classes, the retrieved APFs at 675 nm and 870 nm were averaged for the scattering angles in the range [0°; 150°] by class of α.

For each class of α and each scattering angle (Θ), we first averaged the APFs and computed the average root mean square error (*rms*), denoted σ(Θ). For each Θ, a filtering was then applied to the full set of APFs by discarding the ones for which the *rms* was greater than σ(Θ). Finally, the remaining number (<*Ni*>) of APFs was averaged for each Θ. σ(Θ) is an essential output parameter in this selection of IOP classes. In fact, it defines the error in the APF retrieval scheme, but also describes the natural variability of the APF based on a selection reduced to one parameter (i.e., the spectral dependency between two wavelengths).

Costal areas present more turbidity than the open ocean. In order to estimate the need of a specific climatology above coastal sites, we compared the existing IOPA climatology over ocean (defined by a refractive index m = 1.44) with a coastal IOPA climatology (derived from the ocean one). This comparison of the APF for three representative classes of α (-0.5, -1.5 and -2.3) at 870 nm is summarized in Figure 3.

For large particles (Figure 3*b* & 3*c*), the discrepancy between the two APF is low (< 10 %) especially in the backscattering region while for larger particles (Figure 3*a*) the discrepancy is more important due to the geophysical noise. There is clearly a need to take account for these specific areas, especially for these small particles, with a specific climatology describing with more accuracy the different aerosol models observed above these sites.

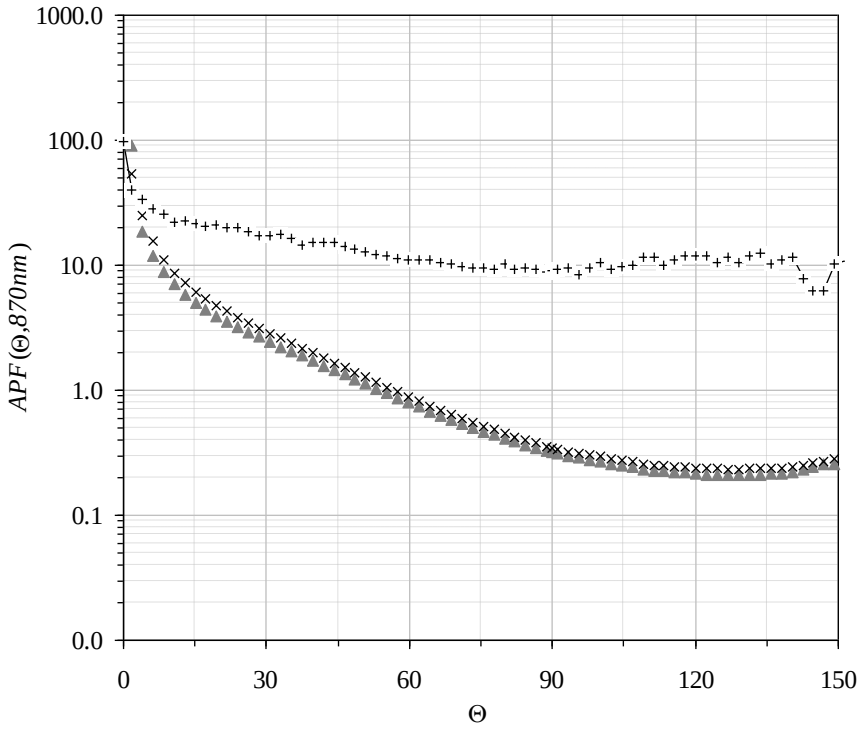
1000.0
100.0
10.0
1.0
0.1
0.0
APF(Θ,870nm)
0
30
60
90
120
150
Θ

(a)

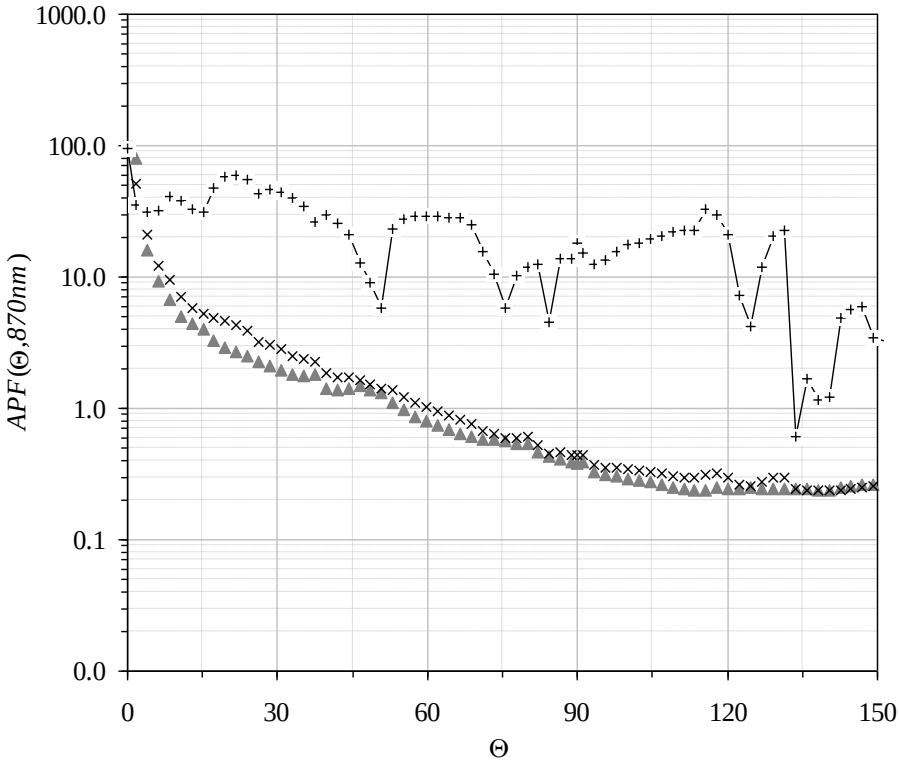
1000.0
100.0
10.0
1.0
0.1
0.0
APF(Θ,870nm)
0
30
60
90
120
150
Θ

(b)

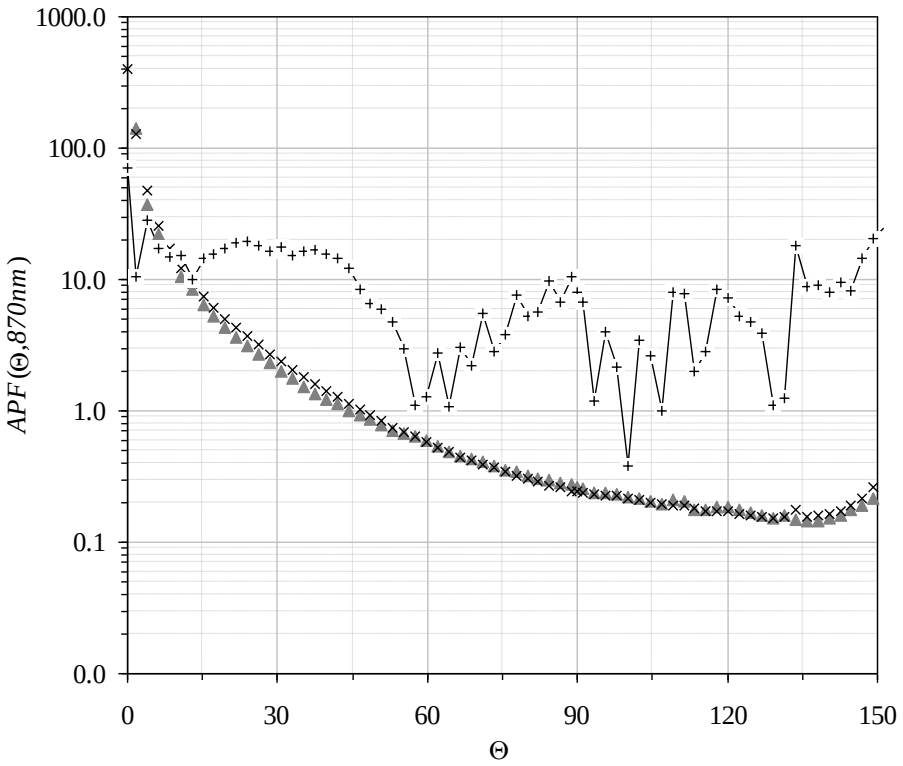

(c)

Figure 3: *Comparison between IOPA ocean and IOPA coastal climatology for three classes of alpha: α = -1.5 (a), α = -2.3 (b) and α = -0.5 (c).*

3.2.3) Consolidation of the IOPA data base

A new set of criteria aiming to improve the inversion process and ensure a data quality has been developed, tested and described in Aznay *et al.*, (2010). The inversion process is then improved:

(*i*) By using the initial set of CIMEL data sequences

(*ii*) By discarding the sequences for which the relative difference between measured and simulated

sky radiances at 440 nm is larger than 20 percent

(*iii*) By removing the sequences for which the angular symmetry in the *alm* geometry is not respected

(*iv*) By interrupting the iteration using the new convergence criteria

(*v*) By discarding the sequences for which the retrieved APF at 675 nm presents negative values

(*vi*) By filtering the sequences for which consistency between the *ppl*-derived APF and the *alm-1-*

and *alm-2*-derived APFs is not observed.

This new set has been tested on the *Venice* site and will be applied on both ocean and land IOPA climatology.

3.2.4) The regionalization of the IOPs

This study highlighted the need to take account for a specific climatology above coastal areas. To improve the aerosol products above these areas, there is clearly a need to define an optical climatology (LUTs) in the remote-sensing algorithms. In order to size these algorithms, we defined three coastal areas defined by a type of aerosol model:

(*i*) A continental aerosol model (Figure 2*a*) defined by $-1.5 < \alpha < -2$,

(*ii*) A mono-dispersed aerosol model (Figure 2*b*) defined by $-1.7 < \alpha_1 < -2.5$ and $-0.3 < \alpha_2 < -1.2$,

(*iii*) A maritime aerosol model (Figure 2*c*) defined by $-0.3 < \alpha < -0.7$;

A special effort has to be done to better describe the optical properties of small aerosols located above these coastal areas. For other aerosols, the IOPA climatology above ocean (defined by $m = 1.44$) can be used without introducing large discrepancies. We also need to evaluate the impact of the use of the IOPA climatology for located events such as Saharan or Asian dust plumes and blue aerosols.

3.2.5) The blue aerosols issue

The first MERIS L2 processing over water was conducted using *Shettle and Fenn* (SF) aerosol models for the atmospheric corrections. These initial models are the heritage of the SeaWiFS processing and are mainly relevant for the open ocean. In the coastal areas, there are experimental evidences of the presence of small aerosols which were not included in the SF aerosol models. Conversely, smaller aerosols were introduced in the aerosol retrieval over the land. For the MERIS second reprocessing, an urgent decision was taken to add the "smaller" aerosol models used over as well in the ocean aerosol remote sensing module.

The first need to refine the IOPs of the so-called blue aerosol models was evocated because the spectral interpolation from the NIR to the blue seems to over estimate the atmospheric corrections. This appreciation was confirmed during the previous IOPA contract again on the spectral dependence of the extinction but also on the atmospheric reflectance. The comparison between the *Junge* "blue" models and the IOPA "blue" model are quite substantial. The conclusion is that this blue *Junge* model should be replaced by the IOPA models.

In order to validate our IOPA "blue" aerosol models, we compared the latters with "blue" aerosol models built up microphysical properties (BIOP models). To define the IOPs of these BIOP models, the strategy is straightforward:

(i) We generate a database of IOPs for Log-normal distribution. The first model selection is m=1.44 (real part) and k=-0.003 (imaginary part) as for the 4 MODIS models; 20 value of σ: 0.2, 0.4, 0.6; 10 values of the mean radius r_m: 0.02, 0.04, 0.06, 0.08, 0.1, 0.12, 0.14, 0.16, 0.18 and 0.2 µm.

(ii) For each σ, we identify r_m which allows retrieving for a given blue aerosol model, α(665,865).

We displayed in Figure 4 the comparison on the APF between the IOPA models and the BIOP models at 870 nm. Note that BIOP01 stands for the BIOP model defined by α = 1.72, BIOP02 for the model defined by α = 1.86 and BIOP03 for the model defined by α = 2.02; the APF between the two climatologies is very close in the backscattering region..

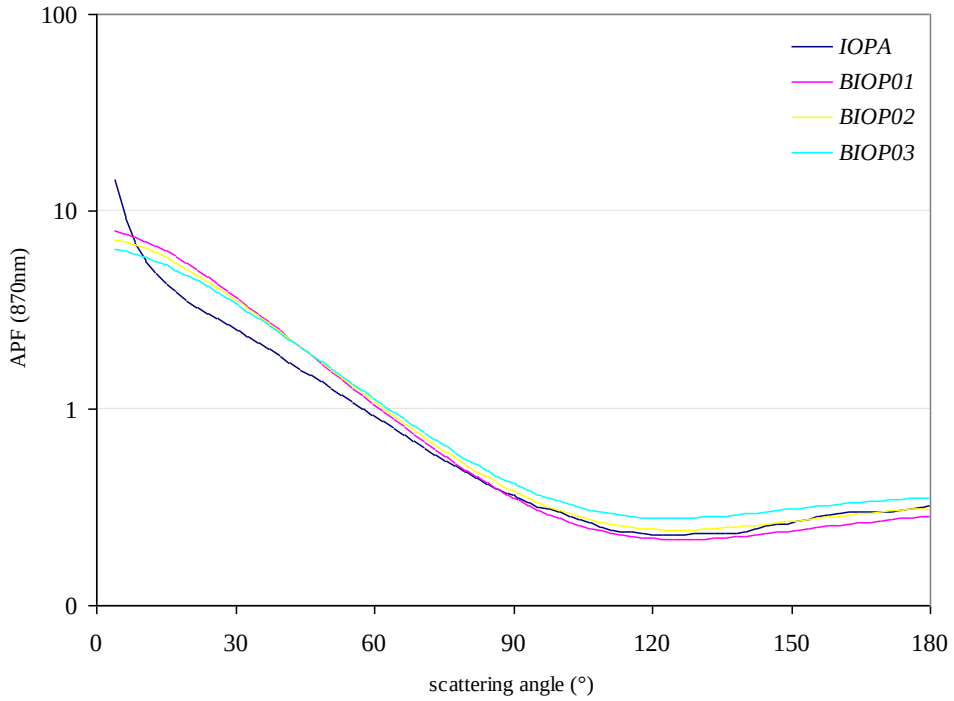

(a)

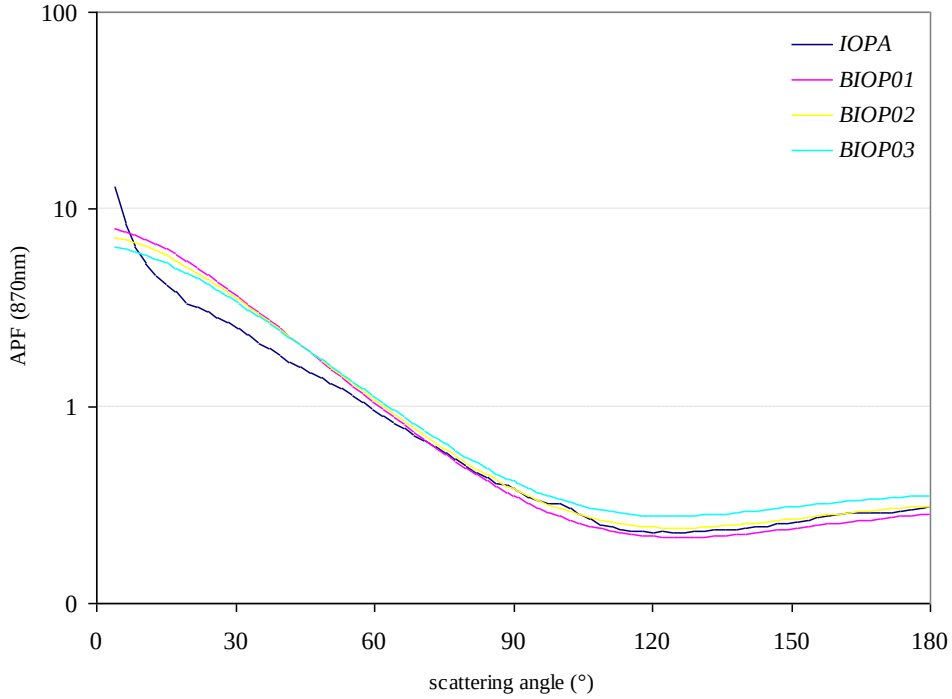

(b)

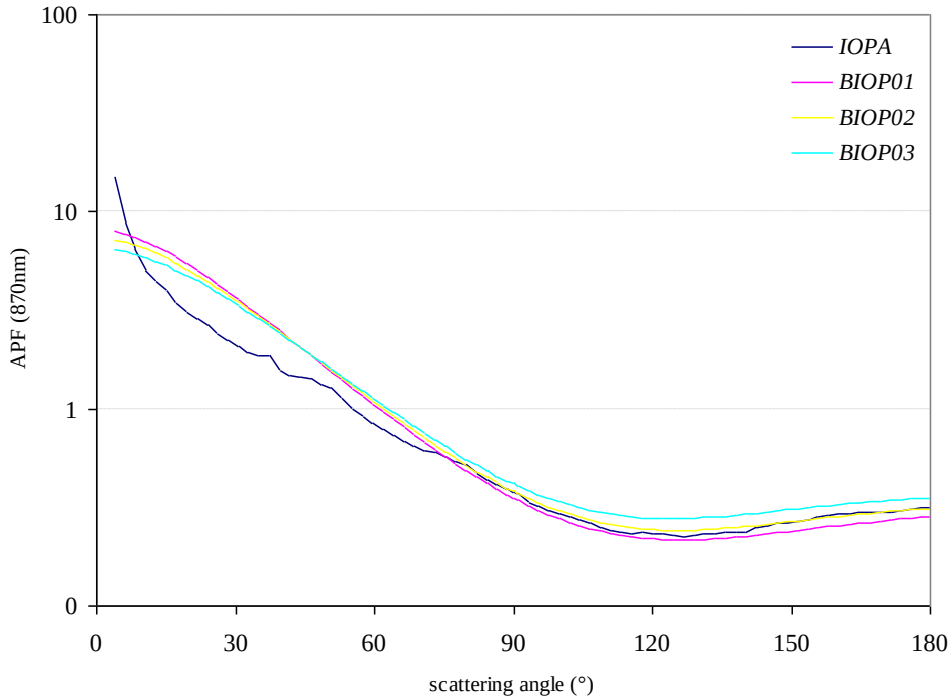

(c)

Figure 4: *Comparison of the APF at 870 nm between IOPA and BIOP climatology for three classes of alpha: α = -1.95 (a), α = -2.1 (b) and α = -2.25 (c).*

We also need to verify the spectral dependency of the extinction coefficient of our IOPA models. Indeed, as we mentioned it previously, the spectral interpolation from the NIR to the blue seems to over estimate the atmospheric corrections. We displayed in Figure 5 the comparison of the spectral dependency of the extinction coefficient (from the NIR to the blue) between IOPA and BIOP models. We can see that both climatologies have the same spectral dependency of the extinction coefficient.

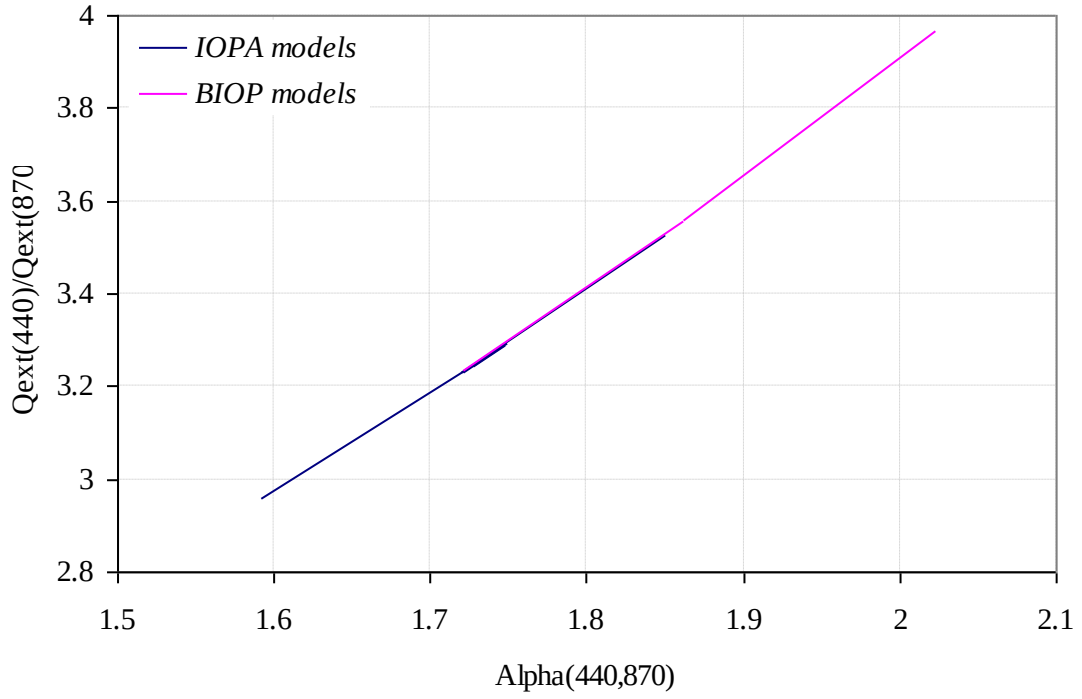

Figure 5: *Comparison of the spectral dependency of the extinction coefficient (from the NIR to the blue) between IOPA and BIOP climatologies.*

3.2.6) The Saharan and Asian (dust) aerosols issue

Two types of dust events (Saharan and Asian) are evoked in this study. Aerosols observed during these events are commonly described as absorbing aerosols.

- *Saharan dust storms:*

It has been shown in Aznay *et al.*, (2010) the occurrence of Saharan dust plumes in three different locations: Capo-Verde, Dakar and Ouagadougou. The latters also indicate that the turbid days correspond to large particles. No trend appears in the SSA, which allows us to suggest the presence of absorbing aerosols in the Saharan region. The conclusion of this study clearly indicates that we do not need to account for an additional

absorption in the presence of high Saharan aerosol loading at 440 nm. The same conclusion applies to the two other wavelengths (675 nm and 870 nm).

- *Asian dust storms:*

This dust presents more absorption than their Saharan counterparts (Dubovik *et al.*, 2002). Dust from China observed over Japan actually comprises particles with a radius of about 2 µm (Tanaka *et al.,* 1989), and measurements from Li-Jones *and* Prospero (1998) and from Arimoto *et al.* (1997) showed that these particles had a size distribution ranging from 1 µm to 5 µm. In addition, due to the combined influences of regions producing arid dusts and to the increased use of fuel, to meet the growth of the China in particular, East Asia is often the scene of peak concentration of tropospheric aerosols (Eck *et al.,* 2005). It has been shown in Aznay *et al.*, (2010) that a little absorption of 10 % has to be added to the IOPs in the case of high Asian dust loading.

The new selected AERONET site named GOA INDIA (UR-22 in Table 2). This site is characterized by very low visibility (50 % of the AOTs > 0.5 at 440 nm) and continental matérial (<α(675,870)> = 1.7). As an illustration of absorbing Asian dust, we displayed in Figure 6 the distribution of the AOT (left side) and the Angstrom coefficient (right side) for

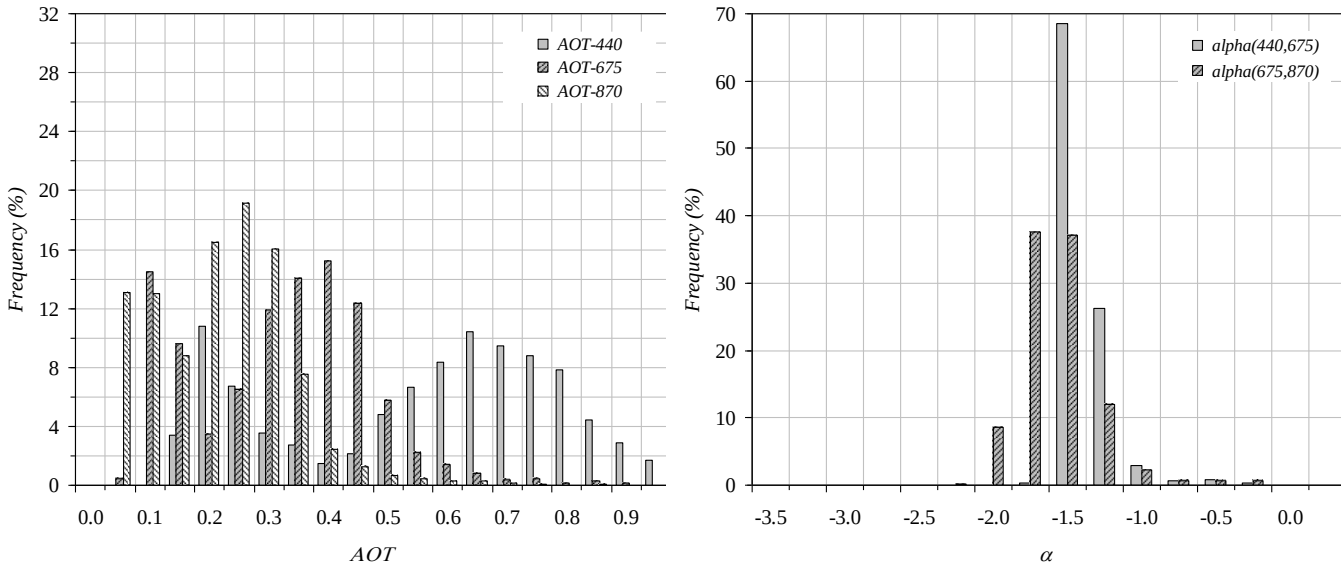

Figure 6: *Distribution of the AOT and the Angstrom coefficient for the new GOA INDIA AERONET site.*

4) Operational issues

4.1) Aerosol inherent optical properties

The UR-17 will be used to take account for Saharan dust while UR-14, 15, 22 will be used to take account for Asian dust. For the latter's, a threshold on the AOT ($\tau > 0.5$ at 440 nm) will be set to activate the local IOPA climatology (more absorbing aerosols).

5) Conclusion

In the frame of an ESA project, IOPA, ADRINORD produced a set of LUTs of the aerosol IOPs. This set covered both the coastal and the open ocean areas. For the coastal colour ROIs, we selected AERONET stations located in the Coast Colour ROIs in order to compare the IOPs of these different ROIs to the global climatology. As a result, the coastal and the global data bases do not depart significantly except for small particles.

As operational outputs, we will provide to the CC consortium this IOPA data base for a first implementation of the algorithm. These data base can be used by GKSS to train the neural network. For ADRINORD, this data base will be used to generate the LUTs of the second algorithm proposed to perform the atmospheric correction.

Depending of the performances of the atmospheric correction and to potential difficulties in some ROIs, we will evaluate the need for regionalization of the aerosol properties. The following table summarizes this regionalization of the aerosol optical properties.

6) References

ANTOINE, D., and A. MOREL, 1999. "A multiple scattering algorithm for atmospheric correction of remotely sensed ocean color (MERIS instrument): Principle and implementation for atmospheres carrying various aerosols including absorbing ones", *International Journal of Remote Sensing*, 20 (9), pp. 1875-1916.

ARIMOTO, R., B.J. RAY, N.F. LEWIS, U. TOMZA, and R.A. DUCE, 1997. "Mass-particle size distributions of atmospheric dust and the dry deposition of dust to the remote ocean", *Journal of Geophysical Research*, **102**, pp. 15867-15874.

AZNAY, O., ZAGOLSKI, F., SANTER, R., 2010. "A new Aerosol Climatology based on the Inherent Optical Properties for Remote Sensing over Land". International Journal of Remote Sensing. *In press*.

DEUZÉ, J.L., M. HERMAN, and R. SANTER, 1989. "Fourier series expansion of the transfer equation in the atmosphere-ocean system", *Journal of Quantitative Spectroscopy and Radiative Transfer*, 41 (6), pp. 483-494.

DUBOVIK, O., B.N. HOLBEN, T. LAPYONOK, A. SINYUK, M.I. MISHCHENKO, P. YANG, and I. SLUTSKER, 2002. "Non-spherical aerosol retrieval method employing light scattering by spheroids ", *Geophysical Research Letters*, **29**, pp. 541-544.

ECK, T.F., B.N. HOLBEN, O. DUBOVIK, A. SMIRNOV, P. GOLOUB, H.B. CHEN, B. CHATENET, L. GOMES, X.Y. ZHANG, S.C. TSAY, Q. JI, D. GILES, and I. SLUTSKER, 2005. "Columnar aerosol optical properties at AERONET sites in central Eastern Asia and aerosol transport to the tropical mid-Pacific", *Journal of Geophysical Research*, **110**, (*doi:10.1029/2004JD005274*).

HOLBEN, B. N., ECK, T. F., SLUTSKER, I., TANRÉ, D., BUIS, J. P., SETZER, A., VERMOTE, E., REAGAN, J. A., KAUFMAN, Y. J., NAKAJIMA, T., LAVENU, F., JANKOWIAK, I. AND SMIRNOV, A., 1998 , "AERONET—A Federated Instrument Network and Data Archive for Aerosol", *Remote Sens. Environ.*, 66, 1-16, doi:10.1016/S0034-4257(98)00031-5, 1998.

HERMAN, J. M., J.L. DEUZE, B. LAFRANCE, R. SANTER, D. TANRE, 2007. "A successive order of scattering code for solving the vector equation of transfer in the earths atmosphere with aerosols", *Journal of Quantitative Spectroscopy & Radiative Transfer 107 (2007) 479507*

LI-JONES, X., and J.M. PROSPERO, 1998. "Validation in the size distribution of non-sea-salt sulfate aerosol in the marine boundary layer at Barbados: impact of African dust", *Journal of Geophysical Research*, **103**, pp. 16073-16084.

SANTER, R., and N. MARTINY, 2003. "Sky radiance measurements for ocean colour calibration/validation", *Applied Optics*, **42** (6), pp. 896-907.

SANTER, R., F. ZAGOLSKI, and O. AZNAY, 2009. "Iterative process to derive the phase function from CIMEL measurements", *International Journal of Remote Sensing*, in press.

TANAKA, M., M. SHOBARA, T. NAKAJIMA, M. YAMANO, and K. ARAO, 1989. "Aerosol optical characteristics in the yellow sand events observed in May 1982 at Nasadaki – Part I. Observations", *Journal of the Meteorological Society of Japan*, **67** (2), pp. 267-278.

ZAGOLSKI R., SANTER R., AZNAY O., 2007. A new climatology for atmospheric correction based on the aerosol inherent optical properties. Journal of Geophysical Research, *Vol. 112, No. D14, D14208*

Annex 1:.1 AERONET Site Information Database

Helgoland (Helgoland Island, Germany)

Image 1 - A view of the sunphotometer on a with a remote controlled cover for weather protection.

Image 2 - A view of the sun photometer on a overlooking the harbor.

Image 1 **Image 2**

Site Coodinates and Elevation:	• Latitude: 54.17786° North • Longitude: 7.88736° East • Elevation: 33.0 Meters
Site Description:	• This site is located on a platform overlooking the water on Helgoland Island, Germany. Helgola very small island in the middle of the German Bight nearly 35 miles far from land. The German part of the North Sea. The island has rocky cliffs of red-colored sandstone with an altitude of 6 meters. In former times it was a sea-fortress but now it has tourism, a little fishery, a coast gua base, pilots, sea-rescue, and the home of a well-known institute for biological and zoological research.(http://www.helgoland.de)
Principal Investigator(s) Information:	• Roland Doerffer • E-mail: doerffer@gkss.de • Roland Doerffer GKSS-Research Centre Institute for Coastal Research Max-Planck-Straße D-21502 Geesthacht, Germany * Phone: 494152 871580 * E-mail: doerffer@gkss.de
Site Manager(s) Information:	• Wolfgang Cordes • Email: wolfgang.cordes@gkss.de • Wolfgang Cordes GKSS-Research Center Institute for Coastal Research Max-Planck-Straße D-21502 Geesthacht, Germany Phone: 494152 871591

	E-mail: wolfgang.cordes@gkss.de
Responsible Institution(s):	• GKSS Research Centre D-21502 Geesthacht, Germany http://www.gkss.de

Hamburg (Hamburg, Germany)

Image 1

Image 2

Image 1 - A
the instrum
site.

Image 2 - A
view of the
instrument
site.

Site Coodinates and Elevation:	• Latitude: 53.56833° North • Longitude: 9.97333° East • Elevation: 105.0 Meters
Site Description:	• This instrument is located on top of a 97 m high building, the Geomaticum, which is in the cent the city of Hamburg.
Principal Investigator(s) Information:	• Stefan Kinne • E-mail: stefan.kinne@zmaw.de • Dr. Stefan Kinne Bundesstrasse 53 20146 Hamburg Germany Tel +49 40 41173 383 Fax +49 40 41173 298 Email: Stefan.Kinne@zmaw.de
Site Manager(s) Information:	• Friedhelm Jansen • Email: friedhelm.jansen@zmaw.de • Friedhelm Jansen Max Planck Institute for Meteorology Bundesstr. 55 D-20146, Hamburg

	GERMANY Phone: 49-40-41173-256; fax: 49-40-41173-359 E-mail: friedhelm.jansen@zmaw.de
Responsible Institution(s):	• Max-Planck-Institut for Meteorology http://www.mpimet.mpg.de/en/web/index.html/

The_Hague (The Hague, Netherlands)

Image 1

Image 2

Image 1 - A the instrum the roof.

Image 2 - A view of the instrument roof.

Site Coodinates and Elevation:	• Latitude: 52.11048° North • Longitude: 4.32682° East • Elevation: 18.0 Meters
Site Description:	• This site is located in the western part of the Netherlands at about 3 km from the coast.
Principal Investigator(s) Information:	• Brent N. Holben • E-mail: Brent.N.Holben@nasa.gov • Code 614.4, Building 33 NASA Goddard Space Flight Center Greenbelt,MD 20771 USA Ph: 1-301-614-6658 Fax: 1-301-614-6695
Site Manager(s) Information:	• Henk L.M. Verhagen • Email: henk.verhagen@tno.nl • Henk L.M. Verhagen TNO - BenO (Netherlands Organisation of Applied Scientific Research, BenO) Laan van Wetenenk 501 Apeldoorn 7334 DT, The Netherlands

	Phone: +31-055 5493977 E-mail:henk.verhagen@tno.nl
Responsible Institution(s):	• Netherlands Organisation of Applied Scientific Research (TNO), Physics and Electronics Laborat (FEL), Observation Systems Division, Electro-optics Technologies Propagation * http://www.tno.nl/instit/fel/os/exp/eo_tech_propagation.html

Oostende (Oostende, Belgium)

Image 1

Image 2

Image 1 - A
the instrum

Image 2 - A
view of the
instrument

Site Coodinates and Elevation:	• Latitude: 51.22500° North • Longitude: 2.92500° East • Elevation: 23.0 Meters
Site Description:	• The instruments are installed on the roof platform of a building in Oostend, Belgium, a port cit the coast of the North Sea.
Principal Investigator(s) Information:	• Kevin Ruddick • E-mail: k.ruddick@mumm.ac.be • Kevin Ruddick Management Unit of the North Sea Mathematical Models(MUMM) MUMM, Gulledelle 100 B-1200 Brussels BELGIUM * Phone: +32-2-773-21-31 * E-mail: k.ruddick@mumm.ac.be

Site Manager(s) Information:	• Jean-Pierre De Blauwe • Email: jp.deblauwe@mumm.ac.be • Jean-Pierre De Blauwe BMM-Meetdienst Oostende Management Unit of the North Sea Mathematical Models 3e & 23e Linieregimentsplein B-8400 Oostende BELGIUM Phone: 32.59.70.01.31, Fax : 32.59.70.49.35 E-Mail: jp.deblauwe@mumm.ac.be
Responsible Institution(s):	• Management Unit of the North Sea Mathematical Models (MUMM) http://www.mumm.ac.be

Dunkerque (Dunkerque, France)

Image 1

Image 2

Image 1 - A
the instrum
all the insta
which is set
the roof of
LPCA.

Image 2 - A
view of the
instrument
measures o
south.

Site Coodinates and Elevation:	• Latitude: 51.03535° North • Longitude: 2.36812° East • Elevation: 0.0 Meters
Site Description:	• This sunphotometer site is located close to the harbor in the city of Dunkerque (approximately 000 inhabitants).
Principal Investigator(s) Information:	• Jean-Francois Leon • E-mail: leon@loa.univ-lille1.fr • Jean-Francois Leon Laboratoire d'Optique Atmospherique Cite scientifique

	bat P5, F-59655 Villeneuve d'ascq FRANCE Phone: +33 (0)3 20 43 68 19 E-mail: leon@loa.univ-lille1.fr AND • Philippe Goloub • E-mail: philippe.goloub@univ-lille1.fr • Philippe Goloub Université des Sciences et Technologies de Lille Laboratoire d'Optique Amosphérique - Bât P5 59655 Villeneuve d'Ascq - Cedex FRANCE Phone: Voice: 33.3.20.33.61.88, Fax : 33.3.20.43.43.42 e-mail : philippe.goloub@univ-lille1.fr
Site Manager(s) Information:	• Herve Delbarre • Email: herve.delbarre@univ-littoral.fr • Herve Delbarre LPCA - Laboratoire de physico-chimie de l'tatmosphere Universite du Littoral 145, avenue Maurice Schuman F-59140 Dunkerque FRANCE Phone: +33(0) 28 65 82 65 E-mail: herve.delbarre@univ-littoral.fr AND • Thierry Podvin • Email: podvin@loa.univ-lille1.fr • Thierry Podvin Laboratoire d'Optique Atmosphérique Bâtiment P5 UFR de PHYSIQUE Université des sciences et technologies de LILLE1 59650 VILLENEUVE D'ASCQ CEDEX FRANCE Phone; (33)3 .20.43.66.45 fax :(33)3.20.43.43.42 E-mail: podvin@loa.univ-lille1.fr AND • Marc Fourmentin • Email: marc.fourmentin@univ-littoral.fr • Marc Fourmentin LPCA - Laboratoire de physico-chimie de l'tatmosphere Universite du Littoral 145, avenue Maurice Schuman F-59140 Dunkerque FRANCE Email: marc.fourmentin@univ-littoral.fr Tél : +33 (0)3 28 65 82 70 Fax : +33 (0)3 28 65 82 44
Responsible Institution(s):	• LOA - Laboratoire d'Optique Atmospherique http://www-loa.univ-lille1.fr/

Lannion (Lannion, France)

Image 1

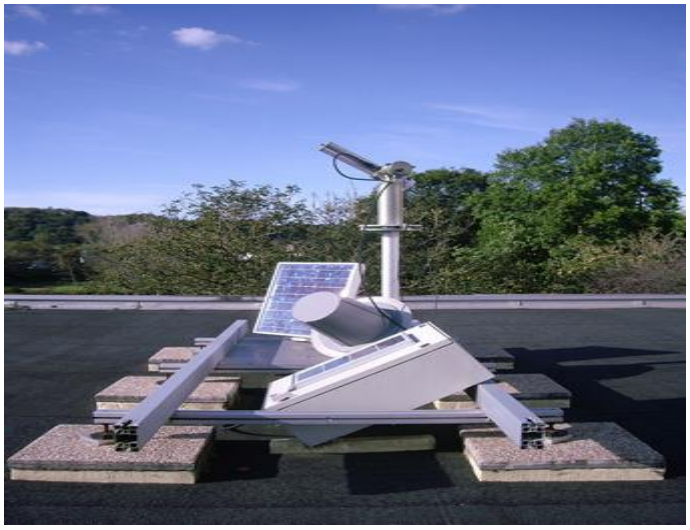

Image 2

Image 1 - V the sunphotom

Image 2 - V the sunphotom

Site Coodinates and Elevation:	• Latitude: 48.73083° North • Longitude: 3.46194° West • Elevation: 15.0 Meters
Site Description:	• Sun Photometer #345 on the top of the building (ENSSAT), near the center of the small city. No important aerosol sources. Lannion is located at 8 km of the shore.
Principal Investigator(s) Information:	• Olga Lado-Bordowsky • E-mail: Olga.Lado-Bordowsky@enssat.fr • Olga Lado-Bordowsky Laboratoire d'Optronique LIDAR & Propagation Atmosphérique ENSSAT - BP 447 6 rue de Kerampont 22305 Lannion cedex Tel: 02 96 46 66 13 Fax: 02 96 37 01 99 E-mail: Olga.Lado-Bordowsky@enssat.fr
Site Manager(s) Information:	• Olga Lado-Bordowsky • Email: Olga.Lado-Bordowsky@enssat.fr • Olga Lado-Bordowsky Laboratoire d'Optronique LIDAR & Propagation Atmosphérique ENSSAT - BP 447 6 rue de Kerampont 22305 Lannion cedex Tel: 02 96 46 66 13 Fax: 02 96 37 01 99 E-mail: Olga.Lado-Bordowsky@enssat.fr
Responsible Institution(s):	• Dr. Yvonick HURTAUD CELAR/DGA BP 57419

35174 Bruz Cedex
yvonick.hurtaud@dga.defense.gouv.fr
Tel: +33 2 99 42 96 52

Additional Photographs and Images

CAPTION	IMAGE
Image 3 - View of the sunphotometer.	

Arcachon (Arcachon, France)

Image 1

Image 2

Image 1 - V the sunphotom

Image 2 - V the sunphotom

Site Coodinates and Elevation:	• Latitude: 44.66353° North • Longitude: 1.16322° West • Elevation: 11.0 Meters
Site Description:	• The CIMEL instrument is set up in the city of Arcachon (seafront) on the roof of the Marine Station building.
Principal Investigator(s) Information:	• Nadège Martiny • E-mail: n.martiny@epoc.u-bordeaux1.fr • Nadège Martiny UMR CNRS EPOC - OASU Université de Bordeaux 1 Avenue des Facultés 33405 Talence Cedex - FRANCE Tel : (+33) 5 40 00 88 31 Fax : (+33) 5 56 84 08 48 Email : n.martiny@epoc.u-bordeaux1.fr
Site Manager(s) Information:	• Michel Leconte • Email: m.leconte@epoc.u-bordeaux1.fr • Michel Leconte UMR CNRS EPOC -OASU Station Marine d'Arcachon Université de Bordeaux 1 2 rue du Professeur Jolyet 33120 Arcachon Cedex - FRANCE Tel : (+33) 5 56 22 39 15 Fax : (+33) 5 56 83 51 04 Email : m.leconte@epoc.u-bordeaux1.fr

Responsible Institution(s):	• The CIMEL instrument has been borrowed from the Laboratoire d'Optique Atmosphérique (LOA) (Université des Sciences et Technologies de Lille) for a one-year period.

BORDEAUX (Bordeaux, France)

Image 1

Image 2

Image 1 - A
the instrum

Image 2 - A
view of the
instrument

Site Coodinates and Elevation:	• Latitude: 44.78803° North • Longitude: 0.57917° West • Elevation: 40.0 Meters
Site Description:	• This site is located on top of a water tower in a suburb south of Bordeaux.
Principal Investigator(s) Information:	• Dominique Guyon • E-mail: guyon@ferrade.bordeaux.inra.fr • Dominique Guyon INRA Centre de recherche de bordeaux Unité de recherche en Bioclimatologie BP 81, 33883 Villenave d'Ornon Cedex FRANCE * Phone: 33 5 56 84 31 86; Fax 33 5 56 84 31 35 * E-mail: guyon@ferrade.bordeaux.inra.fr
Site Manager(s) Information:	• Dominique Guyon • Email: guyon@ferrade.bordeaux.inra.fr • Dominique Guyon INRA Centre de recherche de bordeaux Unité de recherche en Bioclimatologie BP 81, 33883 Villenave d'Ornon Cedex FRANCE * Phone: 33 5 56 84 31 86; Fax 33 5 56 84 31 35 * E-mail: guyon@ferrade.bordeaux.inra.fr

Responsible Institution(s):	• CNES (Centre National d'Etudes Spatiales) http://www.cnes.fr/

Mace_Head (Galway, Ireland)

Site Coodinates and Elevation:	• Latitude: 53.33000° North • Longitude: 9.90000° West • Elevation: 20.0 Meters
Site Description:	• The World Meteorological Organisation (WMO) Global Atmosphere Watch (GAW) atmospheric research station at Mace Head is located on the west coast of Ireland. The observatory is main representative for the marine background atmosphere of the eastern North Atlantic Ocean. (http://macehead.physics.nuigalway.ie)
Principal Investigator(s) Information:	• Christoph Kleefeld • E-mail: christoph.kleefeld@nuigalway.ie • Christoph Kleefeld Atmospheric Research Group Department of Experimental Physics National University of Ireland, Galway University Road Galway Ireland Phone: +353 91 524411 ext 3437; fax +353 91 750584 E-mail: christoph.kleefeld@nuigalway.ie
Site Manager(s) Information:	• S. Gerard Jennings • Email: gerard.jennings@nuigalway.ie • Prof. Dr. S. Gerard Jennings Department of Experimental Physics, National University of Ireland, Galway University Road, Galway, Ireland Phone: +353 91 524411 E-mail: gerard.jennings@nuigalway.ie
Responsible Institution(s):	• NASA'S AERONET http://aeronet.gsfc.nasa.gov National University of Ireland, Galway http://www.nuigalway.ie/ WMO Global Atmosphere Watch http://www.wmo.ch/web/arep/gaw/gaw_home.html

Annex 1-2

AERONET Climatology, Level 2.0 - Quality Assured Data

Helgoland (N 54°10', E 07°53', Alt 33 m)

Year: 2000, 2001, 2002, 2003, 2004, 2005, 2006, 2007, 2008, 2009

Channel (nm): 1020, 870, 670, **500**, 440, 380, 340, 500 (not interpolated)

Explanation of Statistics

Aerosol optical depth at 500 nm (tau_{a500}), Angstrom exponent ($alpha_{440-870}$), precipitable water (PW), the associated standard deviations (sigma), the number of days (*N*) and months (Month) in the observation periods.

Overall Averages of	tau_{a500}	sigma	$alpha_{440-870}$	sigma	PW	sigma	*N*	Month
JAN	•••	•••	•••	•••	•••	•••	•••	•••
FEB	•••	•••	•••	•••	•••	•••	•••	•••
MAR	•••	•••	•••	•••	•••	•••	•••	•••
APR	0.26	0.10	1.23	0.40	0.96	0.29	13	2
MAY	0.19	0.12	1.10	0.36	1.39	0.40	51	6
JUN	0.16	0.09	1.19	0.44	1.62	0.44	54	8
JUL	0.18	0.10	1.42	0.40	2.16	0.44	86	8
AUG	0.21	0.15	1.18	0.41	2.09	0.47	99	9
SEP	0.20	0.14	1.12	0.41	1.77	0.46	84	9
OCT	0.13	0.09	1.07	0.45	1.32	0.45	42	7
NOV	0.12	0.03	0.72	0.32	1.39	0.29	2	1

DEC	•••	•••	•••	•••	•••	•••	•••	•••
YEAR	•••	•••	•••	•••	•••	•••	431	50

Hamburg (N 53°34', E 09°58', Alt 105 m)

Year: 2000, 2003, 2004, 2005, 2006, 2007, 2008, 2009

Channel (nm): 1020, 870, 670, **500**, 440, 380, 340, 500 (not interpolated)

Explanation of Statistics

Aerosol optical depth at 500 nm (tau_{a500}), Angstrom exponent ($alpha_{440-870}$), precipitable water (PW), the associated standard deviations (sigma), the number of days (*N*) and months (Month) in the observation periods.

Overall Averages of	tau_{a500}	sigma	$alpha_{440-870}$	sigma	PW	sigma	*N*	Month
JAN	0.09	0.04	1.07	0.41	0.56	0.20	32	6
FEB	0.15	0.10	1.28	0.34	0.50	0.20	46	6
MAR	0.21	0.17	1.38	0.39	0.72	0.24	68	7
APR	0.23	0.22	1.22	0.38	0.91	0.32	78	6
MAY	0.23	0.16	1.35	0.47	1.25	0.34	78	4
JUN	0.22	0.15	1.39	0.45	1.72	0.46	100	6
JUL	0.21	0.12	1.44	0.31	2.01	0.44	103	6
AUG	0.20	0.11	1.41	0.36	1.95	0.38	105	6
SEP	0.19	0.13	1.26	0.42	1.58	0.47	126	7
OCT	0.14	0.10	1.28	0.39	1.29	0.47	101	7
NOV	0.09	0.05	1.08	0.40	0.93	0.33	38	6

DEC	0.09	0.06	1.05	0.45	0.65	0.24	26	5
YEAR	0.17	0.06	1.27	0.14	1.17	0.54	901	72

AERONET Climatology, Level 2.0 - Quality Assured Data

The_Hague (N 52°06', E 04°19', Alt 18 m)

Year: 2001, 2002, 2003, 2004, 2005, 2006

Channel (nm): 1020, 870, 670, **500**, 440

Explanation of Statistics

Aerosol optical depth at 500 nm (tau_{a500}), Angstrom exponent ($alpha_{440-870}$), precipitable water (PW), the associated standard deviations (sigma), the number of days (*N*) and months (Month) in the observation periods.

Overall Averages of	**tau_{a500}**	**sigma**	**$alpha_{440-870}$**	**sigma**	**PW**	**sigma**	***N***	**Month**
JAN	0.12	0.04	0.96	0.56	0.75	0.33	25	4
FEB	0.16	0.08	0.95	0.41	0.61	0.30	33	3
MAR	0.23	0.12	1.12	0.41	0.73	0.29	48	4
APR	0.26	0.16	1.19	0.43	0.95	0.34	66	4
MAY	0.22	0.14	1.15	0.37	1.46	0.33	42	3
JUN	0.23	0.16	1.30	0.34	1.85	0.53	63	4
JUL	0.22	0.11	1.41	0.28	2.22	0.56	40	4
AUG	0.23	0.19	1.35	0.37	2.19	0.36	36	2
SEP	0.22	0.16	1.38	0.39	1.77	0.54	32	2
OCT	0.18	0.13	1.04	0.51	1.58	0.61	34	3

NOV	0.11	0.04	0.81	0.50	1.40	0.33	20	3
DEC	0.13	0.06	0.71	0.57	0.83	0.28	16	3
YEAR	0.19	0.05	1.12	0.23	1.36	0.58	455	39

Oostende (N 51°13', E 02°55', Alt 23 m)

Year: 2001, 2002, 2003, 2004, 2005, 2006, 2007, 2008, 2009

Channel (nm): 1020, 870, 670, **500**, 440, 380, 340, 500 (not interpolated)

Explanation of Statistics

Aerosol optical depth at 500 nm (tau_{a500}), Angstrom exponent ($alpha_{440-870}$), precipitable water (PW), the associated standard deviations (sigma), the number of days (*N*) and months (Month) in the observation periods.

Overall Averages of	tau_{a500}	sigma	$alpha_{440-870}$	sigma	PW	sigma	*N*	Month
JAN	0.11	0.05	0.98	0.45	0.73	0.34	17	3
FEB	0.21	0.15	1.43	0.40	0.68	0.25	9	1
MAR	0.30	0.31	1.04	0.42	1.03	0.48	39	3
APR	0.26	0.20	1.18	0.41	1.12	0.40	69	4
MAY	0.22	0.19	1.17	0.41	1.45	0.41	86	6
JUN	0.23	0.14	1.42	0.35	1.84	0.52	121	6
JUL	0.20	0.12	1.45	0.35	2.13	0.50	125	6
AUG	0.21	0.16	1.36	0.34	2.09	0.44	120	6
SEP	0.21	0.14	1.26	0.40	1.68	0.41	130	7

OCT	0.17	0.15	0.99	0.41	1.49	0.50	92	7
NOV	0.10	0.04	0.85	0.42	1.13	0.34	41	7
DEC	0.12	0.06	0.84	0.51	0.84	0.26	28	4
YEAR	0.19	0.06	1.16	0.22	1.35	0.51	877	60

Dunkerque (N 51°02', E 02°22', Alt 0 m)

Year: 2003, 2004, 2005, 2006, 2007, 2008, 2009

Channel (nm): 1020, 870, 670, **500**, 440, 380, 340, 500 (not interpolated), 1640

Explanation of Statistics

Aerosol optical depth at 500 nm (tau_{a500}), Angstrom exponent ($alpha_{440-870}$), precipitable water (PW), the associated standard deviations (sigma), the number of days (*N*) and months (Month) in the observation periods.

Overall Averages of	**tau_{a500}**	**sigma**	**$alpha_{440-870}$**	**sigma**	**PW**	**sigma**	***N***	**Month**
JAN	0.18	0.10	0.97	0.47	0.76	0.33	29	4
FEB	0.16	0.11	0.96	0.36	0.74	0.29	32	4
MAR	0.22	0.18	0.98	0.56	0.87	0.27	42	4
APR	0.22	0.12	1.17	0.33	1.11	0.37	41	3
MAY	0.25	0.13	1.23	0.37	1.66	0.52	58	4
JUN	0.21	0.11	1.29	0.41	1.87	0.63	65	4
JUL	0.21	0.13	1.20	0.40	2.10	0.55	90	6
AUG	0.24	0.17	1.18	0.38	2.05	0.38	76	6
SEP	0.21	0.12	1.14	0.46	1.78	0.48	103	6

OCT	0.17	0.14	1.01	0.46	1.60	0.54	79	6
NOV	0.12	0.05	0.95	0.47	1.22	0.42	38	6
DEC	0.14	0.06	1.11	0.45	0.81	0.31	31	5
YEAR	0.20	0.04	1.10	0.12	1.38	0.52	684	58

AERONET Climatology, Level 2.0 - Quality Assured Data

Lannion (N 48°43', W 03°27', Alt 15 m)

Year: 2007

Channel (nm): 1020, 870, 670, **500**, 440, 1640

Explanation of Statistics

Aerosol optical depth at 500 nm (tau_{a500}), Angstrom exponent ($alpha_{440-870}$), precipitable water (PW), the associated standard deviations (sigma), the number of days (*N*) and months (Month) in the observation periods.

Overall Averages of	**tau_{a500}**	**sigma**	**$alpha_{440-870}$**	**sigma**	**PW**	**sigma**	***N***	**Month**
JAN	•••	•••	•••	•••	•••	•••	•••	•••
FEB	•••	•••	•••	•••	•••	•••	•••	•••
MAR	0.15	0.15	1.06	0.46	0.84	0.28	14	1
APR	0.39	0.26	1.40	0.26	1.35	0.46	18	1
MAY	0.30	0.05	1.47	0.41	1.29	0.41	2	1
JUN	0.17	0.08	1.44	0.42	2.02	0.19	7	1
JUL	0.15	0.04	1.45	0.39	1.82	0.18	7	1
AUG	0.13	0.07	1.35	0.42	1.78	0.31	14	1

SEP	0.14	0.07	1.30	0.42	1.82	0.36	17	1
OCT	0.26	0.00	1.17	0.00	2.20	0.00	1	1
NOV	0.09	0.02	1.26	0.70	1.06	0.21	4	1
DEC	•••	•••	•••	•••	•••	•••	•••	•••
YEAR	•••	•••	•••	•••	•••	•••	84	9

AERONET Climatology, Level 2.0 - Quality Assured Data

Arcachon (N 44°39', W 01°09', Alt 11 m)

Year: 2008, 2009

Channel (nm): 1020, 870, 670, **500**, 440

Explanation of Statistics

Aerosol optical depth at 500 nm (tau_{a500}), Angstrom exponent ($alpha_{440-870}$), precipitable water (PW), the associated standard deviations (sigma), the number of days (*N*) and months (Month) in the observation periods.

Overall Averages of	**tau_{a500}**	**sigma**	**$alpha_{440-870}$**	**sigma**	**PW**	**sigma**	***N***	**Month**
JAN	0.12	0.04	1.00	0.49	0.99	0.35	14	1
FEB	0.12	0.05	1.09	0.38	0.88	0.31	18	1
MAR	0.12	0.07	1.03	0.46	0.79	0.22	17	1
APR	0.24	0.23	1.08	0.29	1.29	0.25	20	1
MAY	0.17	0.10	1.03	0.26	1.94	0.47	27	1
JUN	0.14	0.05	1.23	0.31	2.10	0.60	27	1
JUL	0.15	0.05	1.10	0.29	2.46	0.60	28	1

AUG	0.20	0.08	1.04	0.27	2.68	0.38	21	1
SEP	0.19	0.05	1.10	0.35	2.02	0.46	15	1
OCT	•••	•••	•••	•••	•••	•••	•••	•••
NOV	•••	•••	•••	•••	•••	•••	•••	•••
DEC	0.10	0.05	1.11	0.30	0.96	0.31	10	1
YEAR	•••	•••	•••	•••	•••	•••	197	10

BORDEAUX (N 44°47', W 00°34', Alt 40 m)

Year: 2001, 2002, 2003

Channel (nm): 1020, 870, 670, **500**, 440

Explanation of Statistics

Aerosol optical depth at 500 nm (tau_{a500}), Angstrom exponent ($alpha_{440-870}$), precipitable water (PW), the associated standard deviations (sigma), the number of days (*N*) and months (Month) in the observation periods.

Overall Averages of	**tau_{a500}**	**sigma**	**$alpha_{440-870}$**	**sigma**	**PW**	**sigma**	***N***	**Month**
JAN	0.13	0.06	1.17	0.54	0.99	0.44	32	2
FEB	0.16	0.14	0.99	0.51	1.09	0.35	13	2
MAR	0.19	0.10	1.14	0.33	1.23	0.53	18	1
APR	0.21	0.16	1.23	0.31	1.29	0.32	18	1
MAY	0.18	0.11	1.17	0.35	1.74	0.50	30	2
JUN	0.23	0.14	1.17	0.29	2.18	0.63	40	2
JUL	0.22	0.13	1.33	0.41	2.47	0.56	42	2

AUG	0.24	0.14	1.24	0.34	2.58	0.59	43	2
SEP	0.16	0.07	1.38	0.35	1.88	0.54	49	2
OCT	0.17	0.15	0.97	0.42	2.01	0.57	39	2
NOV	0.12	0.06	1.15	0.34	1.24	0.41	24	2
DEC	0.15	0.07	1.26	0.42	0.94	0.49	31	2
YEAR	0.18	0.04	1.18	0.12	1.64	0.58	379	22

AERONET Climatology, Level 2.0 - Quality Assured Data

Biarritz (N 43°28', W 01°33', Alt 0 m)

Year: 2001

Channel (nm): 870, 670, **500**, 440

Explanation of Statistics

Aerosol optical depth at 500 nm (tau_{a500}), Angstrom exponent ($alpha_{440-870}$), precipitable water (PW), the associated standard deviations (sigma), the number of days (*N*) and months (Month) in the observation periods.

Overall Averages of	**tau_{a500}**	**sigma**	**$alpha_{440-870}$**	**sigma**	**PW**	**sigma**	***N***	**Month**
JAN	•••	•••	•••	•••	•••	•••	•••	•••
FEB	•••	•••	•••	•••	•••	•••	•••	•••
MAR	•••	•••	•••	•••	•••	•••	•••	•••
APR	•••	•••	•••	•••	•••	•••	•••	•••
MAY	•••	•••	•••	•••	•••	•••	•••	•••
JUN	•••	•••	•••	•••	•••	•••	•••	•••

JUL	•••	•••	•••	•••	•••	•••	•••	•••
AUG	•••	•••	•••	•••	•••	•••	•••	•••
SEP	0.20	0.13	1.59	0.13	•••	•••	8	1
OCT	0.09	0.02	1.16	0.33	•••	•••	5	1
NOV	•••	•••	•••	•••	•••	•••	•••	•••
DEC	•••	•••	•••	•••	•••	•••	•••	•••
YEAR	•••	•••	•••	•••	•••	•••	13	2

Rame_Head (N 50°21', W 04°08', Alt 0 m)

Year: 1997, 1998

Channel (nm): 1020, 870, 670, **500**, 440, 380, 340, 500 (not interpolated)

Explanation of Statistics

Aerosol optical depth at 500 nm (tau_{a500}), Angstrom exponent ($alpha_{440-870}$), precipitable water (PW), the associated standard deviations (sigma), the number of days (*N*) and months (Month) in the observation periods.

Overall Averages of	**tau_{a500}**	**sigma**	**$alpha_{440-870}$**	**sigma**	**PW**	**sigma**	***N***	**Month**
JAN	0.05	0.03	0.28	0.06	0.40	0.09	2	1
FEB	0.12	0.07	0.84	0.27	0.96	0.36	6	1
MAR	•••	•••	•••	•••	•••	•••	•••	•••
APR	0.21	0.12	0.93	0.46	•••	•••	13	1
MAY	0.16	0.07	1.10	0.30	•••	•••	8	1
JUN	0.12	0.08	0.81	0.30	1.83	0.44	9	2

JUL	0.14	0.08	1.19	0.46	1.75	0.28	28	2
AUG	0.15	0.09	1.34	0.33	1.69	0.44	27	2
SEP	0.85	1.19	0.94	0.44	1.95	0.40	3	1
OCT	0.14	0.12	1.16	0.52	1.25	0.25	10	1
NOV	0.06	0.03	0.52	0.45	0.96	0.22	10	1
DEC	0.07	0.03	0.79	0.99	0.74	0.39	2	1
YEAR	•••	•••	•••	•••	•••	•••	118	14

AERONET Climatology, Level 2.0 - Quality Assured Data

Mace_Head (N 53°19', W 09°54', Alt 20 m)

Year: 2003, 2004

Channel (nm): 1020, 870, 670, **500**, 440, 380, 340, 500 (not interpolated)

Explanation of Statistics

Aerosol optical depth at 500 nm (tau_{a500}), Angstrom exponent ($alpha_{440-870}$), precipitable water (PW), the associated standard deviations (sigma), the number of days (*N*) and months (Month) in the observation periods.

Overall Averages of	**tau_{a500}**	**sigma**	**$alpha_{440-870}$**	**sigma**	**PW**	**sigma**	***N***	**Month**
JAN	0.04	0.00	0.59	0.00	0.84	0.00	1	1
FEB	0.06	0.02	1.00	0.80	0.58	0.08	3	1
MAR	•••	•••	•••	•••	•••	•••	•••	•••
APR	•••	•••	•••	•••	•••	•••	•••	•••
MAY	•••	•••	•••	•••	•••	•••	•••	•••

JUN	•••	•••	•••	•••	•••	•••	•••	•••
JUL	•••	•••	•••	•••	•••	•••	•••	•••
AUG	•••	•••	•••	•••	•••	•••	•••	•••
SEP	•••	•••	•••	•••	•••	•••	•••	•••
OCT	0.14	0.02	0.20	0.01	0.83	0.22	2	1
NOV	•••	•••	•••	•••	•••	•••	•••	•••
DEC	•••	•••	•••	•••	•••	•••	•••	•••
YEAR	•••	•••	•••	•••	•••	•••	6	3

ADRINORD

Technical Note

Issue: 1 Rev.: 0

Date: 15-10-2010

Page: 49

Document Title: Prediction of the MERIS TOA reflectance over water in absence of gaseous absorption and adjacency effects.

Version: 1.0

Author(s): R. Santer , O. Aznay and F. Zagolski

Affiliation(s): ULCO, Université du Littoral Côte d'Opale, Wimereux - France.

ADRINORD, Association pour le Développement de la Recherche et de l'Innovation dans la Région Nord-Pas de Calais, Lille – France.

Modification History: First version, July 31, 2010

Final version, Oct 15, 2010

Distribution: Public

1) Introduction

The reference document is the CC ATBD (Santer, 2010) which:

(*i*) Describes the 5S formalism over the ocean.

(*ii*) Expresses the needs in terms of Look Up Tables (LUTs).

(*iii*) Expresses the needs in terms of routines to generate the atmospheric functions.

(*iv*) Express es the need to have a simulator first, to validate the atmospheric corrections (ACs) and second, to conduct a sensitivity study.

Section 2 describes the LUTs generation. In section 3, we present the forward simulator with inputs/outputs and Section 4 is a quality control of the processor is based on a direct inter comparison with the outputs of the RTC. The different routines we use to compute the different atmospheric functions will be implemented as well in the AC processor. In section 5, we recall these different routines.

2) Generation of the LUTs

2.1) Modifications of the SO radiative transfer code

The vector version of the SO radiative transfer code (RTC; Deuzé *et al.*, 1989; Lenoble *et al.*, 2009) used by ABB/BOMEM to generate the MERIS LUTs is the ocean (3 layers) version. The basic outputs of the SO RTC are the top of atmosphere (TOA) normalized (with a solar irradiance equal to π) radiances for different geometries: 24 view zenith angles (VZAs) with *Gaussian* quadrature plus the nadir view and 25 azimuth angles (AAs) ranging from 0° to 180° with 7.5° step. To these TOA radiances, we first added the downwelling radiance at the bottom of the atmosphere (BOA). This SO RTC has been modified in order:

(i) To loop on the 15 MERIS spectral bands.
(ii) To loop on 16 aerosol optical thicknesses (AOTs) at 550 nm (from 0 to 1.5).
(iii) To loop on 24 solar zenith angles (SZAs).
(iv) To compute the direct and total transmittances.

The SO code uses a *Fourier* series expansion of the radiance field. The 0^{th} order gives the diffuse irradiance at surface ϕ_d^0 using the *Gaussian* quadrature as:

$$\phi_d^0 = 2\pi \sum_{j=1}^{24} a_j \mu_j L_j^0 \quad (1)$$

where the 0^{th} downwelling radiance at surface for the 24 *Gaussian* angles (cosine is μ) is weighted by the Gaussian weights a_j.

The total transmittance for the solar path is given by:

$$T(\mu_s) = \exp(-\tau / \mu_s) + \phi_d^0 / (\Pi \mu_s) \quad (2)$$

2.2) The LUTs

The updated version of SO has been run over wind-roughened sea surfaces both for a pure *Rayleigh* atmosphere and a (*Rayleigh* + aerosols) atmosphere, in the 15 MERIS spectral bands, with a standard pressure of 1013.25 hPa. The outputs of the SO code for each aerosol type are:

(i) The TOA atmospheric radiances (15 bands x 16 AOTs x 25 SZAs x 25 VZAs x 25 AAs).

(ii) The BOA atmospheric radiances (15 bands x 16 AOTs x 25 SZAs x 25 VZAs x 25 AAs).

(iii) The total and diffuse downward transmittances (15 bands x 16 AOTs x 25 SZAs).

(iv) The total and diffuse upward transmittances (15 bands x 16 AOTs x 25 SZAs).

To compute the upward transmittance applying the principle of reciprocity, we use the same code but without the Fresnel reflection and only for the $s=0^{th}$ terms of the Fourier series.

By aerosol family, for the 15 MERIS bands, the initial database (DB) is quite huge (40 Go). One first task was to reduce it. The SOS code for accuracy purpose uses the double precision. First we transform the double precision sky radiance into a single precision into a reflectance which makes a factor 2. We also have merged the different outputs (TOA radiances and downward transmittances over black ocean and upward transmittances over black land) into one file. At the end, the LUT size is about 250 Mo for one aerosol model and one wind speed. For the full DB, we have 3 wind speeds (1 m/s, 5 m/s and 10 m/s) and two aerosols families (IOPA with and without absorption).

3) Forward simulator of the atmospheric reflectance and transmittance

3.1) Inputs

The inputs are:

(i) The detector index (1 to 3700)

(ii) The geometrical conditions: SZA (0 to 90°), VZA (0 to 90°), SZA (°), VZA (°). The MERIS convention for the azimuth is used.

(iii) The barometric pressure (hPa).

(iv) The wind speed (ws).

(v) The aerosol family (*Junge*, IOPA-144). The standard CoastColor aerosol model is IOPA-144. An additional model is IOPA-144 with absorption (Santer *et al.*, 2010).

(vi) The *Angstrom* coefficient α from which the aerosol type is derived.

(vii) The AOT at 550 nm (0 to 1.5).

(viii) The water reflectance (ρw) in 13 MERIS bands.

Default values are: P=1013.25 hPa, ws=3 m/s, IOPA-144, α=-1.2, AOT(550)=0.2, ρw(15 bands) = 0.

3.2) Flowchart

We describe in this section the different steps allowing the prediction of the signal and atmospheric functions (Figure 1). Once the aerosol family is selected (*Junge* or IOPA-144 models), the Angstrom coefficient is used to select, among this aerosol family, the closest aerosol model. The wind speed is then used to select the closest value between 1, 5 and 10 m/s. The spectral dependency of the aerosol extinction is computed using the provided AOT at 550 nm.

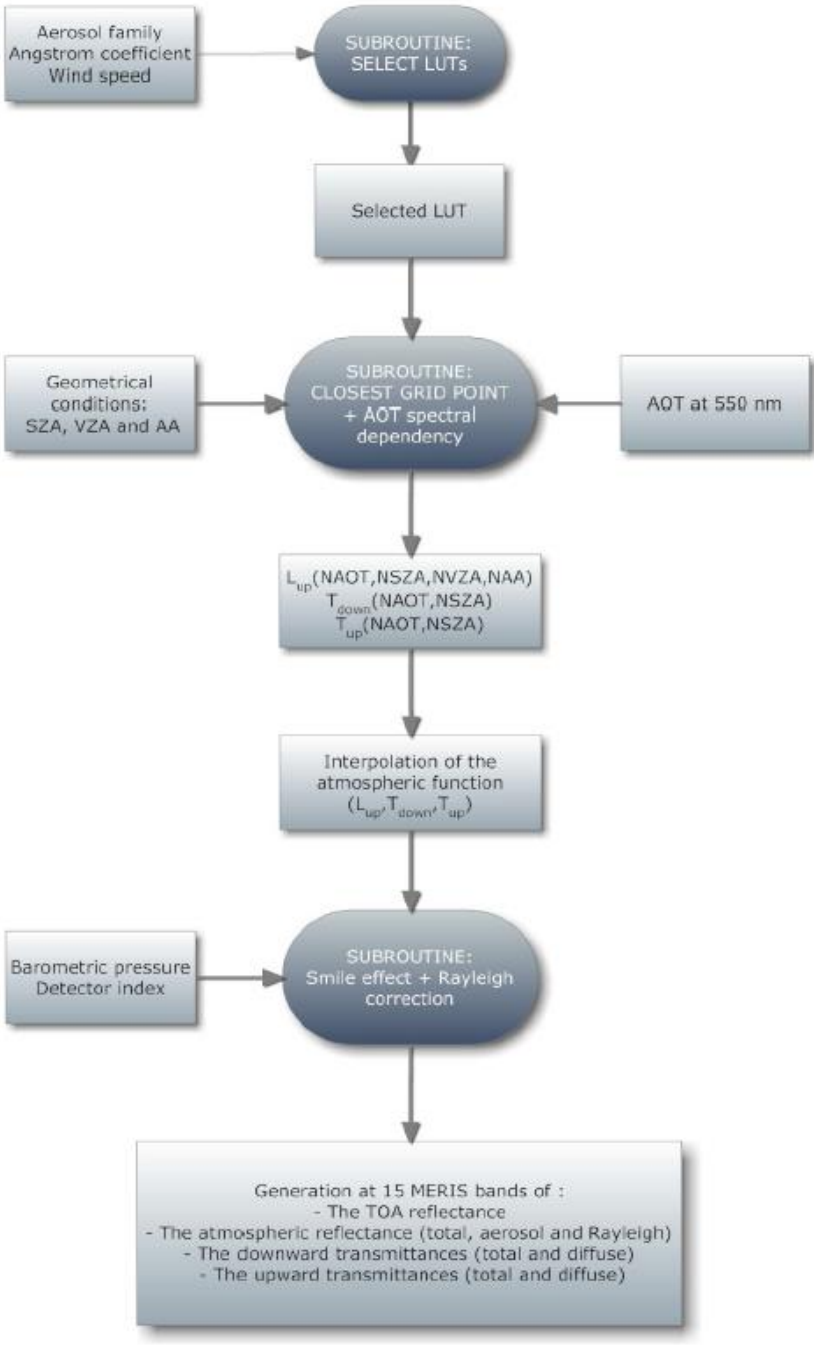

Figure 1: *Flowchart describing the generation of the TOA signal and atmospheric functions.*

The interpolations in SZA, VZA and AA are made, as it is in the MERIS IPF, for the two bracketed values of the AOT. Then, the linear interpolation of the AOT is done. The Rayleigh adjustment with the barometric pressure is done as well as the Rayleigh correction of the smile effect.

This routine returns in 13 MERIS bands the TOA atmospheric reflectance and the total and diffuse transmittances for the down-welling path and the up-welling path.

3.3) Outputs

The outputs (Annex 1.3) are divided in three parts: the first part recalls the different inputs used by the simulator. The second part provides, for each of the 15 MERIS bands, the smile effect (distance in nm from the nominal wavelength), the aerosol optical thickness and the *Rayleigh* optical thicknesses (without and with smile correction). In the third part, we provide, for the 15 MERIS bands, the different atmospheric functions:

(i) The TOA reflectance
(ii) The atmospheric reflectance
(iii) The aerosol reflectance
(iv) The *Rayleigh* reflectance
(v) The *Rayleigh* reflectance corrected by the barometric pressure and the smile
(vi) The contribution of the sun glint
(vii) The downward and upward transtances
(viii) The spherical albedos (total, aerosol and *Rayleigh*).

4) Quality control

The purpose here is to verify that our routine to compute the different scattering functions, including the coupling with the Fresnel reflection, is correct. We test it in two MERIS bands: 442 nm and 865 nm; one IOPA-144 models corresponding to α=-1.2; one aerosol vertical distribution with a scale height of 3 km and one wind speed of 5 m/s.

The different interpolations on the geometry grid are in line with the MERIS IPF and the principle of these interpolations is out of our scope. For the 1 SZA, 25 VZAs, 3 AAs and 2 AOTs, we selected grid points. The linear interpolation is checked for the 2 VZA, 2 AOTs and for one AA. The test is on the atmospheric reflectance. We recall hereafter the different values of the inputs used to perform our computations.

(i) 1 SZA: 58.46°;

(ii) 3 AOTs (560 nm): 0., 0.2 and 0.25;

(iii) 25 *Gaussian* VZAs: from 0° and 90°.

(iv) 2 VZAs: 30 and 60°.

(v) 3 AAs: 0°, 90° and 180°.

We displayed in Figure 2, the verification of the atmospheric normalized radiance at grid point. For both *Rayleigh* (in MERIS Band-2; Figure 2*a*) and aerosol (AOT = 0.2 in MERIS Band-13; Figure 2*b*) cases, the simulation of the TOA signal, compared to SO computations, is exactly the same .

In Figure 3, we checked the interpolation of the signal between to *Gaussian* VZAs (Table 1) and between to AOTs (Figure 3). The interpolation between two VZAs gives quite similar results. Even for a double interpolation (on VZA and AOT), the discrepancy on the signal between SO computation and our simulation is very low. Regarding the interpolation between two AOTs (0.2 and 0.3), the restitution of the TOA signal is very close for VZAs lower than 65°. For higher VZAs, the mean value of the discrepancy between SO computations and our estimation is lower than 0.5 % and reaches 3.5 % for VZA = 90°.

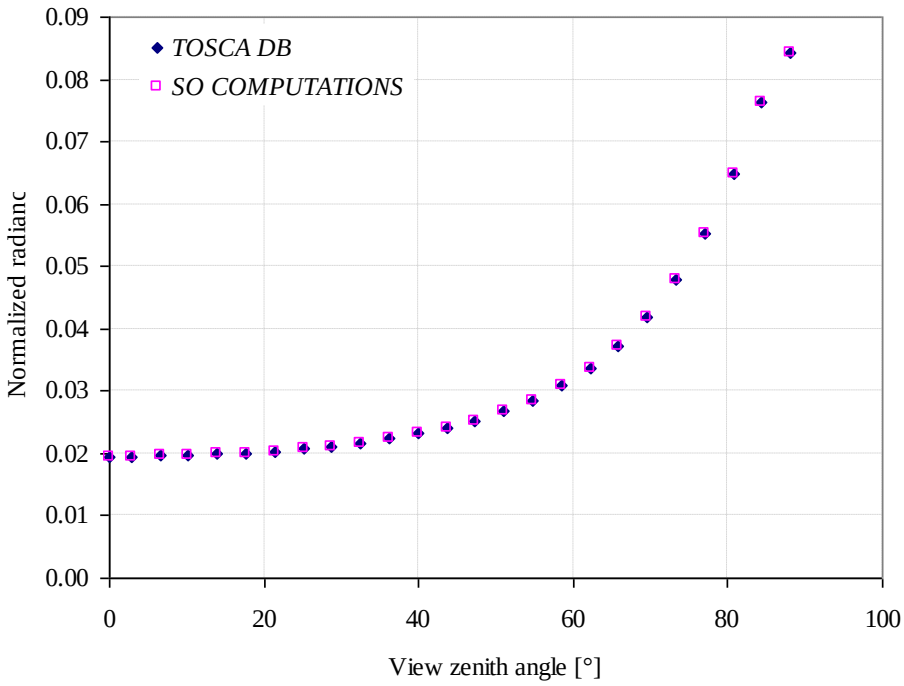

(a)

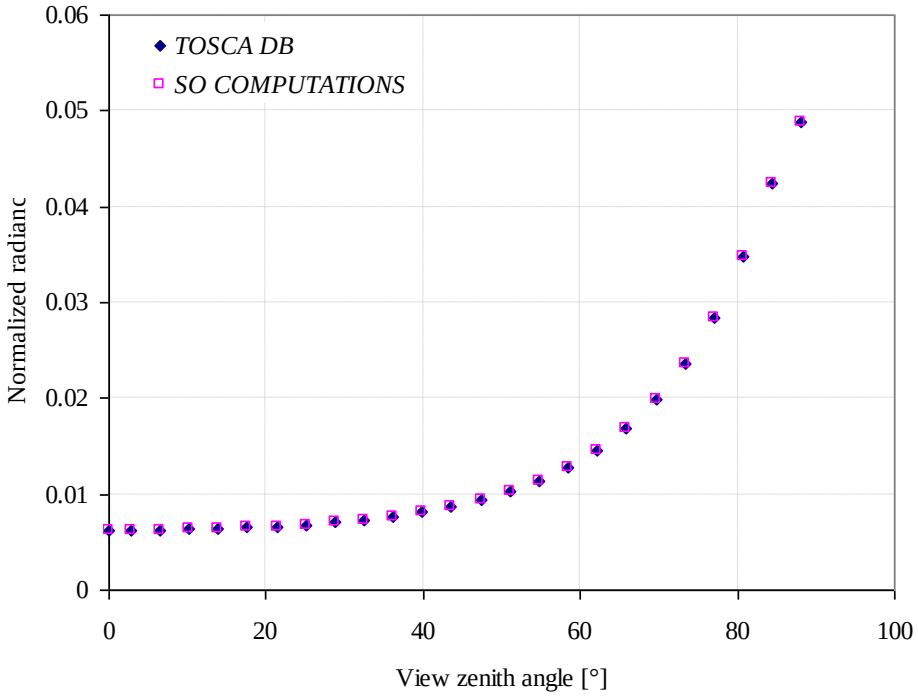

(b)

Figure 2: *Verification of the prediction of the signal at grid points:*

Rayleigh case at 442 nm (a) and aerosol case at 865 nm (b).

		MERIS band-2		MERIS band-13	
	VZA	**AOT = 0**	**AOT = 0.25**	**AOT=0**	**AOT=0.25**
TOSCA	30	0.02133	0.02786	0.00148	0.00867
	60	0.03193	0.04338	0.00229	0.01641
SO	30	0.02134	0.02785	0.00148	0.00866

	60	0.03200	0.04336	0.00230	0.01632

Table 1: *Verification of the interpolation of the normalized radiance.*

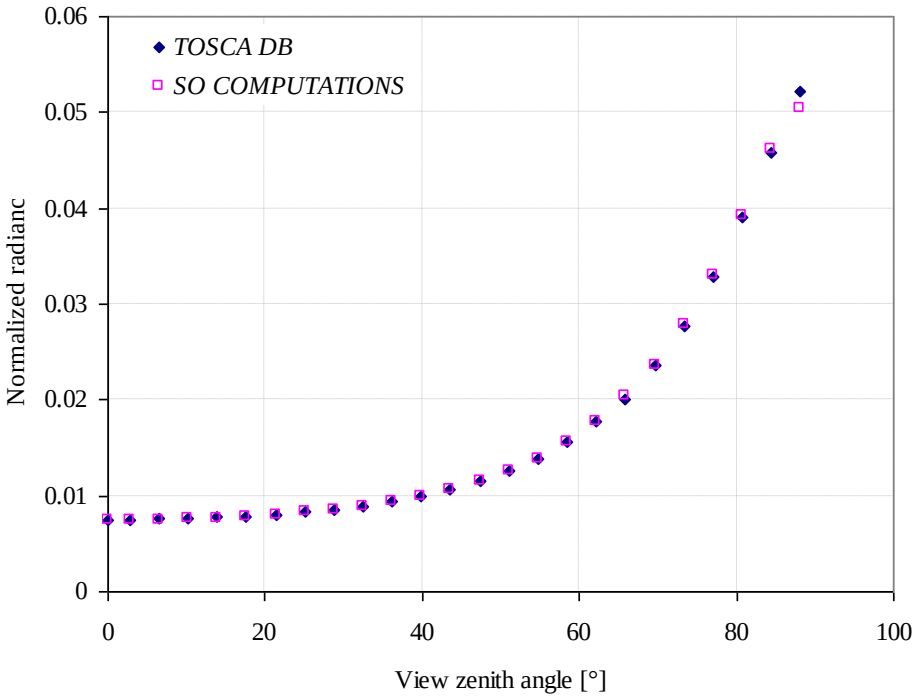

Figure 3: *Verification of the simulation of the signal at non grid points: interpolation between two AOTs.*

5) To integrate the atmospheric functions and the sunglint

All the ingredients are in the forward processor. We just focus here on specific tools we need to integrate in the CC processor. The linear interpolations between the grid points are documented in the MERIS IPF and are implemented in the forward processor.

51) Reading the grid points

Common variables are:

(i) The MERIS central wavelength for the 15 spectral bands.

(ii) The Rayleigh optical thickness for the standard barometric pressure for the 15 spectral bands.

(iii) the angular grid for the LUTs

(iv) the AOT at 550 nm for the LUTs and their spectral dependence for the 15 spectral bands.

All of this is given in annex 2.1.

5.2) Reading the LUTs

The forward processor is for one aerosol type and one wind speed, which corresponds to the initial LUTs generation. The CC processor should include upstream the two aerosol families (regular IOPA and IOPA dust) and the three wind speed. Annex 2.2 is a Fortran routine to combine the 16 aerosol types of one family for one wind speed.

5.3) Computing the direct sunglint

The Cox and Munk model is used and the subroutine is given in annex 1.2.

6) Conclusion

We defined and realized a forward simulator. The Fortran code and examples of inputs-outputs are given in annexes 1 (1.1; 1.2; 1.3). Both the code and the LUTs will be available on the CC web server to be used:

(i) To check the AC processor atmospheric routines.

(ii) To verify the correct implementation of the AC processor.

(iii) To evaluate on synthetic data bases the performances of the AC codes in the frame of the round robin exercise (See Ruddick et al, 2010).

The different elements of the forward simulator will be integrated in the CC AC processor.

References

COX, C., AND W. MUNK, 1954. Measurements of roughness of the sea surface from photographs of the sun glitter, *Journal of Optical Society in America*, 44 (11): 838-888.

DEUZÉ, J.L., M. HERMAN, and R. SANTER, 1989. "Fourier series expansion of the transfer equation in the atmosphere-ocean system", *Journal of Quantitative Spectroscopy and Radiative Transfer*, 41 (6), pp. 483-494.

LENOBLE J., M. HERMAN, J.L. DEUZÉ,, B. LAFRANCE, R. SANTER, D. TANRÉ ,. (2007). A successive order of scattering code for solving the vector equation of transfer in the earths atmosphere with aerosols *Journal of Quantitative Spectroscopy & Radiative Transfer 107 (2007) 479507*

RUDDICK K, July 2010 DUE CoastColour. Round Robin Protocol. Contribution to Technical Specification Deliverable DEL-5. Draft Version 1.0.

SANTER R.(2010). The inherent optical properties of the aerosols. Technical note to Coast Colour.

SANTER R., AZNAY O. AND SANTER-LIMEREZ P. (2010). The inherent optical properties of the aerosols. Technical note to Coast Colour.

Annex 2.1 : Inputs to the simulator

```
1.2   !Angstrom coefficient
0.2   !AOT at 560nm
58.6  !SZA
58.6  !VZA
0.    !SAA
90.   !VAA
0. 0. 0. 0. 0. 0. 0. 0. 0. 0. 0. 0. 0. 0. 0.   !RHOW(AT 15 MERIS BANDS)
1     !IDETECTOR
1013.25     !PE
```

Annex 2.2 : Fortran code of the simulator

```
************************************************************************
C *****                                                           *****
C *****  COMPUTATION OF TOA REFLECTANCES                          *****
C *****  .OVER the ocean                                          *****
C ************************************************************************

       PROGRAM rhoTOA

C -----------------------------------------------------------------------
C Parameters declaration
C -----------------------------------------------------------------------

       INTEGER NAOT,NMU,NRAA,NBAND,NAER
       PARAMETER (NRAA   = 25)     ! max nb of user azimuthal angles
       PARAMETER (NAOT   = 16)     ! nb of AOT's at 550nm
       PARAMETER (NMU    = 25)     ! nb of Gaussian angles used in SO
       PARAMETER (NBAND  = 15)     ! nb of MERIS spectral bands
       PARAMETER (NAER   = 16)     ! nb of IOPA models

       REAL P0
       PARAMETER (P0 =1013.25D0)   ! standard surface pressure [hPa]

C -----------------------------------------------------------------------
C Variables declaration
C -----------------------------------------------------------------------

       CHARACTER*80     file,file2,Gauss_file

       INTEGER          No_sza,No_phi,No_vza,No_aot2
       INTEGER          No_aot(NBAND),No_ray(NBAND)
       INTEGER          nmodel,idec,nws

       REAL thetas,thetav,phi,ws,aoti
       REAL lambda,tauR,saa,vaa,PI,xmus,xmuv,xlg
       REAL dummy,alphaC,tauRS,dP,PP,Pe

       REAL twvl(NBAND),aot(NBAND),glint(NBAND)
       REAL phi_OS(1:NRAA),AOT_OS(1:NAOT),rmu(0:NMU)
       REAL rho_ATM(NBAND),ROT(NBAND),ROTS(NBAND)
       REAL rho_ray(NBAND),rho_ray2(NBAND)
       REAL sa(NBAND,NAOT),Qnorm(16,NBAND)
       REAL sai(NBAND)

       REAL ttot(NBAND,NAOT,NMU),ttot2(NBAND,NAOT,NMU)
       REAL rad1(NBAND,NAOT,NMU,NMU,NRAA)
       REAL Tdown(NBAND),Tdirect(NBAND),Tup_ray(NBAND)
       REAL Tup(NBAND),wvlidec(3700,15),Td_up(NBAND)
       REAL rhow(NBAND),signalTOA(NBAND)
       REAL Tdirect_ray(NBAND),Td_ray_up(NBAND)
       REAL Tdirect2(NBAND)

       REAL Lup1(NAER,NBAND,NAOT,NMU,NMU,NRAA)

       REAL T_tot1(NAER,NBAND,NAOT,NMU)

       REAL T_tot21(NAER,NBAND,NAOT,NMU)

       REAL spha1(NAER,NBAND,NAOT)

C -----------------------------------------------------------------------
C Data set
C -----------------------------------------------------------------------
C ---- Set 15 MERIS wavelengths [mic.]
       DATA twvl/0.41250D0,0.44250D0,0.49000D0,0.51000D0,0.56000D0,
     &           0.62000D0,0.66500D0,0.68125D0,0.70875D0,0.75375D0,
     &           0.7610D00,0.77875D0,0.86500D0,0.88500D0,0.90000D0/
```

```
C ---- Set 15 Rayleigh Optical Thickness
       DATA ROT/0.31527978, 0.23591024, 0.15515523, 0.13171376,
     &          0.08991221, 0.05943336, 0.04472972, 0.04056213,
     &          0.03455820, 0.02694379, 0.02592163, 0.02361672,
     &          0.01545924, 0.01409880, 0.01317574/

C ---- Set 16 AOTs
       DO k=1,NAOT
       AOT_OS(k)=(k-1)/10.
       ENDDO

C ---- Set 25 azimut angles [deg.]
       DO i=1,NRAA
       phi_OS(i) = 7.5*(i-1)
       ENDDO

C ---- Set Rayleigh index
       DO i=1,NBAND
       No_ray(i) = 1
       ENDDO

C ---------------------------------------------------------------------
C Setting...
C ---------------------------------------------------------------------
C ---- Set some variables
       PI=DACOS(-1.D0)

C ---- Read wvl of the full resolution
       OPEN(1,FILE='input/smile')
       DO k=1,3700
       READ(1,*) dummy,(wvlidec(k,i),i=1,15)
       ENDDO
       CLOSE(1)

C ---- Gauss quadrature (mu angles, weigths) for atmosphere
       Gauss_file='input/gauss25'
       OPEN(1,FILE=Gauss_file)
       rmu(0)=0.D0
       DO k=1,NMU
       READ(1,*) rmu(k)
       ENDDO
       CLOSE(1)

C ---- Spectral dependence of the AOT
       Gauss_file='input/Qnorm_IOPA'
       OPEN(1,FILE=Gauss_file)
       DO j=1,16
       READ(1,*) (Qnorm(j,k),k=1,NBAND)
       ENDDO
       CLOSE(1)

C ---------------------------------------------------------------------
C Read data from input binary file
C ---------------------------------------------------------------------
C ---- Read TOA radiances and transmittances for 16 IOPA models
       OPEN(1,FILE='input/LUT_IOPA144cc_ws5',FORM='unformatted')
       DO ii=1,NAER
       READ(1) rad1
       READ(1) ttot,sa
       READ(1) ttot2
       DO i=1,NBAND
        DO j=1,NAOT
        spha1(ii,i,j) = sa(i,j)
         DO k=1,NMU
         T_tot1(ii,i,j,k) = ttot(i,j,k)
         T_tot21(ii,i,j,k) = ttot2(i,j,k)
          DO m=1,NRAA
           DO l=1,NMU
```

```
            Lup1(ii,i,j,k,l,m) =  rad1(i,j,k,l,m)
            ENDDO
           ENDDO
          ENDDO
         ENDDO
        ENDDO
        ENDDO
        CLOSE(1)

C ---------------------------------------------------------------------
C Read user inputs (interactif mode or input card)
C ---------------------------------------------------------------------

C ---- Case of interactive mode
        IF (IArgC().NE.1) THEN
C ------ Select index for aerosol family (iaer)
!        write(6,*) 'Enter the Aerosol family [1-2]:' !! iaer=1 IOPA-144
!        READ(5,*) iaer                               !! iaer=2 IOPA-144 Abs.
C ------ aerosol model
        write(6,*) 'Enter Angstroem coefficient a(778/865):'
        READ(5,*) alphaC
C ------ aerosol optical thickness
        write(6,*) 'Enter the AOT at 560 nm:'
        READ(5,*) aoti
C ------ solar zenith angle (thetas)
        write(6,*) 'Enter the solar zenith angle [Deg.]:'
        READ(5,*) thetas
C ------ view zenith angle (thetav)
        write(6,*) 'Enter the view zenith angle [Deg.]:'
        READ(5,*) thetav
C ------ azimut angle (phi) [6S convention]
        write(6,*) 'Enter the solar azimut angle [Deg.]:'
        READ(5,*) saa
        write(6,*) 'Enter the view azimut angle [Deg.]:'
        READ(5,*) vaa
C ------ marine reflectance (rhoW)
        write(6,*) 'Enter the marine reflectance at 15 wavelenghts:'
        READ(5,*) (rhow(i),i=1,NBAND)
C ------ wind speed (ws)
!        write(6,*) 'Enter the wind speed [m/S]:'
!        READ(5,*) ws
C ------ index for detector
        write(6,*) 'Enter the detector index:'
        READ(5,*) idec
C ------ barometric pressure
        write(6,*) 'Enter the barometric pressure [hPa]:'
        READ(5,*) Pe
        ENDIF

C--- Convert phi(6S) into phi(SO)
        phirad = (saa-vaa)*PI/180.
        IF (phirad .LT. 0.) phirad = phirad + 2*PI
        IF (phirad .GT. (2*PI)) phirad = phirad - 2*PI
        phi = phirad*180./PI

        IF (phi .LE. 180) THEN
        phi = 180 - phi
        ELSE
        phi = phi - 180
        ENDIF

        write(6,*)
        write(6,*) 'RECALL OF THE INPUTS:'
        write(6,*) 'ALPHA = ',alphaC
        write(6,*) 'AOT (560nm) = ',aoti
        write(6,*) 'SZA = ',thetas
        write(6,*) 'VZA = ',thetav
        write(6,*) 'PHI (OS)= ',phi
```

```
        write(6,*) 'BAROMETRIC PRESSURE = ',Pe
        write(6,*) 'IDETECTOR = ',idec
        write(6,*)

C--- Compute the direct sunglint
        xlg=0.
        CALL SUN_GLINT(thetas,thetav,phi,ws,xlg)

C--- Look for the grid point
        CALL indices(thetas,thetav,phi,aoti,
     &              xmus,xmuv,No_sza,No_vza,No_phi,No_aot2)

        write(6,*) 'num. indices: SZA VZA PHI AND AOT'
        write(6,*) No_sza,No_vza,No_phi,No_aot2
        write(6,*)

C ---------------------------------------------------------------------
C Select the aerosol model and associated LUTs file
C ---------------------------------------------------------------------
        CALL select_model(alphaC,nmodel)

C--- Compute the spectral depedency of the extinction
C--- IOPA models
        DO i=1,NBAND
        aot(i) = aoti*Qnorm(nmodel,i)
        ENDDO

C--- Select the aerosol LUT corresponding to alphaC and ws
C--- Selection of the LUTs corresponding to alphaC
         DO i=1,NBAND
          DO j=1,NAOT
          sa(i,j) = spha1(nmodel,i,j)
           DO k=1,NMU
           ttot(i,j,k)  = T_tot1(nmodel,i,j,k)
           ttot2(i,j,k) = T_tot21(nmodel,i,j,k)
            DO m=1,NRAA
             DO l=1,NMU
             rad1(i,j,k,l,m) = Lup1(nmodel,i,j,k,l,m)
             ENDDO
            ENDDO
           ENDDO
          ENDDO
         ENDDO

C--- Loop on the MERIS bands
        DO iband=1,NBAND

        No_aot(iband) = No_aot2

        lambda = twvl(iband)*1.D3

C--- Correction for the smile (Rayleigh only)
        dwvl = wvlidec(idec,iband)-lambda
        dP = -4*P0*dwvl/lambda
        PP = Pe + dP
        ROTS(iband)=ROT(iband)*PP/P0

        Tdirect(iband) = EXP(-(aot(iband)+ROT(iband))*
     &                  (1.D0/xmus+1.D0/xmuv))

        Tdirect2(iband) = EXP(-(aot(iband)+ROT(iband))*
     &                   (1.D0/xmuv))

        Tdirect_ray(iband) = EXP(-ROT(iband)*
     &                   (1.D0/xmuv))

        glint(iband)=Tdirect(iband)*xlg/xmus
```

```
        ENDDO

        write(6,*) 'iband Smile_effect_(nm) tauA tauR taur_S'
        DO iband=1,NBAND
        write(6,1001) iband,abs(wvlidec(idec,iband)
     &                          -(twvl(iband)*1.D3)),
     &                aot(iband),ROT(iband),ROTS(iband)
        ENDDO
        write(6,*)

C--- Interpolation of the signal components
        CALL Interpol_L(xmus,xmuv,0.,phi,No_ray,No_sza,
     &                  No_vza,No_phi,rad1,
     &                  rho_ray)

        CALL Interpol_L(xmus,xmuv,aoti,phi,No_aot,No_sza,
     &                  No_vza,No_phi,rad1,
     &                  rho_ATM)

        CALL Interpol_T(xmus,aoti,No_aot,No_sza,ttot,
     &                  Tdown)

        CALL Interpol_T(xmus,aoti,No_aot,No_sza,ttot2,
     &                  Tup)

        CALL Interpol_T(xmus,0.,No_ray,No_sza,ttot2,
     &                  Tup_ray)

        CALL Interpol_S(aoti,No_aot,Sa,
     &                  Sai)

        write(6,*) 'iband rhoATM rhoa rho_r rhor_corr. ',
     &             'Glitter Td Tu Tdu_aer Tdu_ray Saa Sar '

         DO iband=1,14

C -------------------------------------------------------------
C Compute the diffuse transmittances for the adacency effects
C-------------------------------------------------------------

        Td_up(iband) = Tup(iband) - Tdirect2(iband)
        Td_ray_up(iband) = Tup_ray(iband) - Tdirect_ray(iband)

        IF (iband .NE. 11) THEN

        write(6,1001) iband,rho_ATM(iband),
     &      rho_ATM(iband)-rho_ray(iband),rho_ray(iband),
     &      rho_ray(iband)*Pe/P0,glint(iband),Tdown(iband),
     &      Tup(iband),Td_up(iband)-Td_ray_up(iband),
     &      Td_ray_up(iband),sai(iband)-sa(iband,1),
     &      sa(iband,1)

        ENDIF

        ENDDO
        write(6,*)

C --------------------------------------------------------------------
C Formats
C --------------------------------------------------------------------

 1001  FORMAT(I2,1X,15(F12.8,1x))

        STOP
        END

C ***************************************************************
```

```
C
*******************************************************************************
************************************************
C *****                                                          *****
C *****             READING the LUTs                             *****
C *****                                                          *****
C        This program reads the grid point values (geometry
C        and AOT used to generate the LUTs
C        The initial LUTs were generated for ONE aerosol type
C        This program combined the 16 aerosol types
C        The computation is for one wind speed
C ******
C ***************************************************************

       subroutine read LUTs(ifaer,iws,
     & rho_up, T_tot_down,T_tot_up,sphalb


C ---------------------------------------------------------------------
C Parameters declaration
C ---------------------------------------------------------------------

       INTEGER NAOT,NMU,NRAA,NBAND,NAER
       PARAMETER (NRAA   = 25)     ! max nb of user azimuthal angles
       PARAMETER (NAOT   = 16)     ! nb of AOT's at 550nm
       PARAMETER (NMU    = 25)     ! nb of Gaussian angles used in SO
       PARAMETER (NBAND  = 15)     ! nb of MERIS spectral bands
       PARAMETER (NAER   = 16)     ! nb of IOPA models


C ---------------------------------------------------------------------
C Variables declaration
C --------------------------------------------------------------------

C      inputs for one aerosol type

       REAL rad1(NBAND,NAOT,NMU,NMU,NRAA) !TOA atmospheric reflectance
       REAL ttot(NBAND,NAOT,NMU) !upward total transmittance
       REAL ttot2(NBAND,NAOT,NMU)  !downward total transmittance
       REAL sa(NBAND,NAOT)! spherical albedo

C      outputs for one aerosol family

       REAL rho_up(NAER,NBAND,NAOT,NMU,NMU,NRAA)
       REAL T_tot_down(NAER,NBAND,NAOT,NMU)
       REAL T_tot_up(NAER,NBAND,NAOT,NMU)
       REAL sphalb(NAER,NBAND,NAOT)


C ---------------------------------------------------------------------
C Read data from LUTs binary file
C ---------------------------------------------------------------------
C ---- Read TOA radiances and transmittances for 16 IOPA models
       OPEN(1,FILE='input/LUT_IOPA144cc_ws5',FORM='unformatted')
C the example is fot the IOPA family with no absorption
C and a wind speed of 5 m/s.

       DO ii=1,NAER !loop on the aerosol type
       READ(1) rad1!normalized radiance
       READ(1) ttot,sa! total transmittance down and spherical albedo
       READ(1) ttot2!total transmittance up
       DO i=1,NBAND
        DO j=1,NAOT
        sphalb(ii,i,j) = sa(i,j)
         DO k=1,NMU
         T_tot_up(ii,i,j,k) = ttot(i,j,k)
         T_tot_down(ii,i,j,k) = ttot2(i,j,k)
          DO m=1,NRAA
```

```
            DO l=1,NMU
            rho_up(ii,i,j,k,l,m) =  rad1(i,j,k,l,m)
            ENDDO
           ENDDO
          ENDDO
         ENDDO
        ENDDO
        ENDDO
        CLOSE(1)

        STOP
        END


C ***********************************************************************
C ******************** - E N D   O F   C O D E  - ********************
C ***********************************************************************


C ***********************************************************************
C ***********************************************************************

        SUBROUTINE SUN_GLINT(sza,vza,dphi,ws,xlg)

C +++++++++++++++++++++++++++++++++++++++++++++++++++++++++++++++++++++++
C
C Notes:
C -----
C  This subroutine returns the sun glint (direct to direct path
C  radiance) contribution xlg(phi,vza) computed at TOA over a wind-
C  roughened sea surface induced by an input wind-speed (ws), and
C  for a given input solar zenith angle (sza) and each angular value
C  from an input set of view zenith angles (vza[nvza]) and from an
C  input set of relative azimuth angle (dphi[nphi]). Extinction of
C  the direct path radiance in the atmosphere is computed using an
C  input AOT (tauA) and an input Rayleigh optical thickness (tauR).
C
C +++++++++++++++++++++++++++++++++++++++++++++++++++++++++++++++++++++++

        REAL c0,c1,cksi,cpsi,dphi
        REAL PI,prob,R1,rphi,sigma2
        REAL sza,vza,ws
        REAL xlg

C ---- Setting...
        PI=DACOS(-1.D0)
        sigma2=0.003D0+0.00512D0*ws
        c0=DCOS(sza*PI/180.D0)

C ---- Sun glint computations...
        c1=DCOS(vza*PI/180.D0)
        rphi=dphi*PI/180.D0
C ---- Compute probability density function, prob(c0,c1,rphi)
        CALL GLITTE(sigma2,c0,c1,rphi,prob)
C ---- Compute cosine of scattering angle (psi)
C ---- and cosine of angle (ksi) between the normal
C ---- to the facet and the incident radiation field
        CALL ANGLE(c0,c1,rphi,cksi,cpsi)
C ---- Compute terms of the Fresnel reflexion matrix (R1,R2,R3)
        CALL FRESNEL_GLITTER(cpsi,R1)
        xlg= R1*PI*prob

        RETURN
        END

C ***********************************************************************
C ***********************************************************************
```

```
      SUBROUTINE GLITTE(sig2,c0,c1,phi,p)

C +++++++++++++++++++++++++++++++++++++++++++++++++++++++++++++++++++++
C
C Notes:
C -----
C  This subroutine computes the probability density function of facet
C  slopes p(sza,vza,dphi) for input illumination and viewing configu-
C  rations (c0=cos(sza),c1=cos(vza),phi=dphi). Assuming an isotropic
C  distribution of the facet slopes (Cox-Munk model) independently of
C  the wind orientation, p(sza,vza,dphi) is expressed as:
C    p(sza,vza,dphi) = [1/(PI.sig2)] . exp[-tan(beta)^2/sig2 ]
C    with,
C         beta, the angle between the local normal and the normal to
C               the facet, computed as:
C               cos(beta) = (c0+c1)/[2.cos(omega)]
C               with cos(2.omega) = c0.c1
C                           -[sqrt(1-c0^2)].[sqrt(1-c1^2)].cos(phi)
C         sig2, the root mean square of the facet slope defined as:
C               sig2 = 0.003 + 5.12E-3.ws
C
C  This subroutine returns p(sza,vza,dphi) / (4.c1.cos(beta)^4)
C
C +++++++++++++++++++++++++++++++++++++++++++++++++++++++++++++++++++++

      REAL c0,c1,cosb,cosw,p,phi,PI,pp,sig2,x1,x2,xxx

C ---- Setting...
      PI=DACOS(-1.D0)

C ---- Compute cos(beta) with beta the angle between the local normal
C ---- and the normal to the facet
      x1=c0*c1
      x2=-SQRT(1.D0-c0**2.D0)*SQRT(1.D0-c1**2.D0)*COS(phi)
      cosw=SQRT(0.5D0*(1.D0+x1+x2))
      cosb=(c0+c1)/(2.D0*cosw)

C ---- Compute the probability density function of face slopes: pp
C ---- and return pp/(4.muv.cos4(beta))
      xxx=-(1.D0-cosb**2.D0)/(sig2*cosb**2.D0)
      p=0.D0
      IF (xxx.GE.-100.D0) THEN
        pp=(1.D0/(PI*sig2))*EXP(xxx)
        p =pp/(4.D0*c1*cosb**4.D0)
      ENDIF

      RETURN
      END

C ***********************************************************************
C ***********************************************************************

      SUBROUTINE ANGLE(c0,c1,phi,cksi,cpsi)

C +++++++++++++++++++++++++++++++++++++++++++++++++++++++++++++++++++++
C
C Notes:
C -----
C  This subroutine computes and returns for a given illumination and
C  viewing configurations (c0=cos(sza),c1=cos(vza),phi=dphi):
C    -the cosine of scattering angle (cpsi) defined as,
C        cpsi = -c0.c1 + [sqrt(1-c0^2)].[sqrt(1-c1^2)].cos(phi)
C    -the cosine of the angle (ksi) between the normal to the facet
C     and the incident radiation field defined as,
C        cksi = (+/-) [c1.cpsi+c0]/[sqrt(1-cpsi^2).sqrt(1-c1^2)]
C
C +++++++++++++++++++++++++++++++++++++++++++++++++++++++++++++++++++++
```

```
      REAL c0,c1,cksi,cpsi,phi,PI,s,z

C ---- Setting...
      PI=ACOS(-1.D0)
      s=1.D0
      IF (SIN(phi).GT.0.D0) s=-1.D0

C ---- Compute the cosine of scattering angle
      cpsi=-c0*c1+SQRT(1.D0-c0**2.D0)*SQRT(1.D0-c1**2.D0)*COS(phi)

C ---- Compute the cosine of angle (ksi) between the normal to the
C ---- facet and the incident radiation field
      z=s*SQRT(1.D0-cpsi**2.D0)*SQRT(1.D0-c1**2.D0)
      cksi=0.D0
      IF (ABS(z).GT.1.D-4) cksi=(c1*cpsi+c0)/z

      RETURN
      END

C *********************************************************************
C *********************************************************************

      SUBROUTINE FRESNEL_GLITTER(cpsi,R1)

C +++++++++++++++++++++++++++++++++++++++++++++++++++++++++++++++++++++
C
C Notes:
C -----
C  This subroutine returns terms of the Fresnel reflection coefficient
C  R1 at the 'air-water' interface for a given incident
C  radiation field (theta_i), assuming a constant water refractive
C  index whatever the wavelength (nw=1.34).
C
C  According to the Snellius-Fresnel laws, the reflection coefficients
C  of the amplitude of the incident electric field in the parallel
C  (rl) and the perpendicular (rr) directions to the incidence plane
C  are written as:
C
C      rl = -[tan(theta_i-theta_r)]/[tan(theta_i+theta_r)]
C      rr = -[sin(theta_i-theta_r)]/[sin(theta_i+theta_r)]
C
C      with, theta_i : the angle between the direction of incident
C                      radiation and the normal to the wave facet
C                      (i.e., the 'air-sea' interface),
C            theta_r : the angle between the direction of refracted
C                      radiation in water and the normal to the
C                      wave facet (i.e., the 'air-sea' interface).
C
C  Using the Descartes law (refractive index of air being equal to 1),
C
C      sin(theta_i) = nw . sin(theta_r)
C
C  with nw the refractive index of pure water.
C
C  The 2 Fresnel reflection coefficients (rl,rr) are expressed as:
C
C      rl = [(nw)^2.mu-x]/[(nw)^2.mu+x]
C      rr = [mu-x]/[mu+x]
C
C      with, mu = cos(theta_i),
C             x = SQRT[(nw)^2-(sin(theta_i))^2]
C
C      with, R1 = (1/2).[(rl)^2+(rr)^2]
C
C +++++++++++++++++++++++++++++++++++++++++++++++++++++++++++++++++++++

      REAL NW
      PARAMETER (NW=1.34D0)          ! refractive index of pure water
```

```
       REAL cpsi,nw2,R1,rl,rr,x,v,w

C ---- Compute Fresnel reflection coefficients: r_parallel (rl)
C ---- and r_perpendicular (rr)
       nw2=NW**2.D0
       w=SQRT(0.5D0*(1.D0-cpsi))
       v=0.5D0*(1.D0+cpsi)
       x=SQRT(nw2-v)
       rl=(nw2*w-x)/(nw2*w+x)
       rr=(w-x)/(w+x)

C ---- Compute terms of Fresnel reflexion coef.
       R1 = (rl**2.D0+rr**2.D0)/2.D0

       RETURN
       END

C ********************************************************************
C ********************************************************************

      SUBROUTINE Interpol_L(xmus,xmuv,aot,phi,No_aot,No_sza,No_vza,
     &                      No_phi,rad1,L_TOA)

C ---------------------------------------------------------------------
C ---- Determine upwelling radiance L_SP(mu) by linear interpolation
C ---- on AOT
C----- Approximation pour l'ensemble des couples (tetaS,tetaV,phi,AOT)=0.
C----- On postule que L(interpolï¿½) = L(aux points de grilles)
C ---------------------------------------------------------------------

       INTEGER NAOT,NMU,NRAA,NBAND
       PARAMETER (NRAA   = 25)     ! max nb of user azimuthal angles
       PARAMETER (NAOT   = 16)     ! nb of AOT's at 550nm
       PARAMETER (NMU    = 25)     ! nb of Gaussian angles used in SO
       PARAMETER (NBAND  = 15)     ! nb of MERIS spectral bands

       CHARACTER*50     Gauss_file
       INTEGER          No_sza,No_phi,No_vza,No_aot(NBAND)
       REAL slope1,slope2,slope3,slope4
       REAL rad1(NBAND,NAOT,NMU,NMU,NRAA)
       REAL L_TOA1(NBAND,NMU,NMU,NRAA)
       REAL L_TOA2(NBAND,NMU,NRAA),dummy
       REAL L_TOA3(NBAND,NRAA),rmu(0:NMU)
       REAL L_TOA4(NBAND),L_TOA(NBAND)
       REAL phi_OS(NRAA),AOT_OS(NAOT)
       REAL xmus,xmuv,aot,phi,PI

       PI=DACOS(-1.D0)

C ---- Set 25 azimut angles [deg.]
       DO i=1,NRAA
       phi_OS(i) = 7.5*(i-1)
       ENDDO

C ---- Set 16 AOTs
       DO k=1,NAOT
       AOT_OS(k)=(k-1)/10.
       ENDDO

C ---- Gauss quadrature (mu angles, weigths) for atmosphere
       Gauss_file='input/gauss25'
       OPEN(1,FILE=Gauss_file)
       rmu(0)=0.D0
       DO k=1,NMU
         READ(1,*) rmu(k),dummy
       ENDDO
       CLOSE(1)
```

```
C ---- Loop on the wavelenght
       DO iband=1,NBAND

          slope1 = (rad1(iband,No_aot(iband)+1,No_sza,No_vza,No_phi)-
     &              rad1(iband,No_aot(iband),No_sza,No_vza,No_phi))/
     &              (AOT_OS(No_aot(iband)+1)-AOT_OS(No_aot(iband)))
          L_TOA1(iband,No_sza,No_vza,No_phi) =
     &        slope1*(aot-AOT_OS(No_aot(iband)))+
     &        rad1(iband,No_aot(iband),No_sza,No_vza,No_phi)

!=============================================================

          slope2 = (rad1(iband,No_aot(iband),No_sza+1,No_vza,No_phi)-
     &              rad1(iband,No_aot(iband),No_sza,No_vza,No_phi))/
     &              (rmu(No_sza+1)-rmu(No_sza))
          L_TOA2(iband,No_vza,No_phi) = slope2*(xmus-rmu(No_sza))+
     &        L_TOA1(iband,No_sza,No_vza,No_phi)

!=============================================================

          slope3 = (rad1(iband,No_aot(iband),No_sza,No_vza+1,No_phi)-
     &              rad1(iband,No_aot(iband),No_sza,No_vza,No_phi))/
     &              (rmu(No_vza+1)-rmu(No_vza))
          L_TOA3(iband,No_phi) = slope3*(xmuv-rmu(No_vza))+
     &        L_TOA2(iband,No_vza,No_phi)

!=============================================================

          slope4 = (rad1(iband,No_aot(iband),No_sza,No_vza,No_phi+1)-
     &              rad1(iband,No_aot(iband),No_sza,No_vza,No_phi))/
     &              (phi_OS(No_phi+1)-phi_OS(No_phi))

          L_TOA4(iband) = slope4*(phi-phi_OS(No_phi))+
     &        L_TOA3(iband,No_phi)

!=============================================================

!          L_TOA(iband) = L_TOA4(iband)/PI      !! normalized radiance

          L_TOA(iband) = L_TOA4(iband)/xmus   !! conversion to reflectance

       ENDDO
       write(6,*)
       RETURN
       END

C *********************************************************************
C *********************************************************************

      SUBROUTINE Interpol_T(xmus,aot,No_aot,No_sza,
     &                      T_LUTs,T)
C ---------------------------------------------------------------------
C ---- Determine upwelling radiance L_SP(mu) by linear interpolation
C ---- on AOT
C----- Approximation pour l'ensemble des couples (tetaS,AOT)=0.
C----- On postule que T(interpolï¿½) = T(aux points de grilles)
C ---------------------------------------------------------------------

       INTEGER NAOT,NMU,NBAND
       PARAMETER (NAOT   = 16)     ! nb of AOT's at 550nm
       PARAMETER (NMU    = 25)     ! nb of Gaussian angles used in SO
       PARAMETER (NBAND  = 15)     ! nb of MERIS spectral bands

       CHARACTER*50     Gauss_file
       INTEGER          No_sza,No_aot(NBAND)
       REAL slope1,slope2
       REAL T_TOA1(NBAND,NMU)
```

```
       REAL T_TOA2(NBAND),T(NBAND)
       REAL rmu(0:NMU),dummy
       REAL T_LUTs(NBAND,NAOT,NMU)
       REAL AOT_OS(NAOT),xmus,aot

C ---- Set 16 AOTs
       DO k=1,NAOT
       AOT_OS(k)=(k-1)/10.
       ENDDO

C ---- Gauss quadrature (mu angles, weigths) for atmosphere
       Gauss_file='input/gauss25'
       OPEN(1,FILE=Gauss_file)
       rmu(0)=0.D0
       DO k=1,NMU
         READ(1,*) rmu(k),dummy
       ENDDO
       CLOSE(1)

C ---- Loop on the wavelenght
       DO iband=1,NBAND

          slope1 = (LOG(T_LUTs(iband,No_aot(iband)+1,No_sza))-
     &              LOG(T_LUTs(iband,No_aot(iband),No_sza)))/
     &              (AOT_OS(No_aot(iband)+1)-AOT_OS(No_aot(iband)))
          T_TOA1(iband,No_sza) =
     &    EXP(slope1*(aot-AOT_OS(No_aot(iband)))+
     &        LOG(T_LUTs(iband,No_aot(iband),No_sza)))

!=================================================================

          slope2 = (T_LUTs(iband,No_aot(iband),No_sza+1)-
     &             T_LUTs(iband,No_aot(iband),No_sza))/
     &             (1./rmu(No_sza+1)-1./rmu(No_sza))
          T_TOA2(iband) = slope2*(1./xmus-1./rmu(No_sza))+
     &                    T_TOA1(iband,No_sza)


       T(iband) = T_TOA2(iband)

       ENDDO

       RETURN
       END

C ********************************************************************
C ********************************************************************

      SUBROUTINE Interpol_S(aot,No_aot,Sa,
     &                      Sai)
C ---------------------------------------------------------------------
C ---- Determine upwelling radiance L_SP(mu) by linear interpolation
C ---- on AOT
C----- Approximation pour l'ensemble des couples (tetaS,AOT)=0.
C----- On postule que T(interpolï¿½) = T(aux points de grilles)
C ---------------------------------------------------------------------

       INTEGER NAOT,NBAND
       PARAMETER (NAOT   = 16)     ! nb of AOT's at 550nm
       PARAMETER (NBAND  = 15)     ! nb of MERIS spectral bands

       INTEGER No_aot(NBAND)
       REAL slope1
       REAL Sa(NBAND,NAOT)
       REAL Sai(NBAND)
       REAL AOT_OS(NAOT),aot

C ---- Set 16 AOTs
```

```
        DO k=1,NAOT
        AOT_OS(k)=(k-1)/10.
        ENDDO

C ---- Loop on the wavelenght
        DO iband=1,NBAND

        slope1 = (LOG(Sa(iband,No_aot(iband)+1))-
     &           LOG(Sa(iband,No_aot(iband))))/
     &           (AOT_OS(No_aot(iband)+1)-AOT_OS(No_aot(iband)))
        Sai(iband) =
     & EXP(slope1*(aot-AOT_OS(No_aot(iband)))+
     &     LOG(Sa(iband,No_aot(iband))))

        ENDDO

        RETURN
        END

C ********************************************************************
C ********************************************************************

        SUBROUTINE select_model(alphaC,nmodel)

        INTEGER nmodel,n
        REAL alpha_IOPA(16)
        REAL A,D,alphaC

        DATA alpha_IOPA /0., 0.15, 0.30, 0.45, 0.6, 0.75, 0.90, 1.05,
     &                   1.2, 1.35, 1.50, 1.65, 1.80, 1.95, 2.10, 2.25/

C look for the nearest corresponding alpha for IOPA modeles
        A = 1000
        DO n=1,16
        D = ABS(alphaC-alpha_IOPA(n))
        IF (D.LT.A) THEN
        A = D
        nmodel = n
        ENDIF
        ENDDO

        RETURN
        END

C ********************************************************************
C ********************************************************************

        SUBROUTINE indices(thetas,thetav,phi,aot,
     &                     xmus,xmuv,No_sza,No_vza,No_phi,No_aot)

C ---------------------------------------------------------------------
C Parameters declaration
C ---------------------------------------------------------------------

        INTEGER NAOT,NMU,NRAA,NBAND
        PARAMETER (NRAA   = 25)     ! max nb of user azimuthal angles
        PARAMETER (NAOT   = 16)     ! nb of AOT's at 550nm
        PARAMETER (NMU    = 25)     ! nb of Gaussian angles used in SO
        PARAMETER (NBAND  = 15)     ! nb of MERIS spectral bands

C ---------------------------------------------------------------------
C Variables declaration
C ---------------------------------------------------------------------

        INTEGER          No_sza,No_phi,No_vza,No_aot,n,nws
        CHARACTER*50     Gauss_file
        REAL thetas,thetav,phi
        REAL xmus,xmuv,phi_OS(1:NRAA)
```

```
      REAL PI,AOT_OS(1:NAOT),rmu(0:NMU)
      REAL D,A,aot,wind(3)

C ---- Gauss quadrature (mu angles, weigths) for atmosphere
      Gauss_file='input/gauss25'
      OPEN(1,FILE=Gauss_file)
      rmu(0)=0.D0
      DO k=1,NMU
        READ(1,*) rmu(k),dummy
      ENDDO
      CLOSE(1)

C ---- Set 16 AOTs
      DO k=1,NAOT
      AOT_OS(k)=(k-1)/10.
      ENDDO

C ---- Set 25 azimut angles [deg.]
      DO i=1,NRAA
      phi_OS(i) = 7.5*(i-1)
      ENDDO

C ---- Set some variables
      PI=DACOS(-1.D0)

C ---- Set wind speed default values
      DATA wind /1.0, 5.0, 10./

C ------------------------------------------------------------------------
C ---- Search for index No of Gaussian angle close by inferior value
C ---- to the input SZA,VZA,phi
C ------------------------------------------------------------------------

      xmus=DCOS(thetas*PI/180.D0)
      No_sza=1
      IF (xmus.GE.rmu(1)) GOTO 1
      IF (xmus.LE.rmu(NMU)) THEN
        No_sza=NMU-1
        GOTO 1
      ENDIF
      A = 1000
      DO n=1,NMU
      D = ABS(xmus-rmu(n))
      IF (D.LT.A) THEN
      A = D
      IF (xmus.GT.rmu(n).AND.rmu(n).NE.1.0) THEN
      No_sza = n-1
      ELSE
      No_sza = n
      ENDIF
      ENDIF
      ENDDO
    1 CONTINUE

C ------------------------------------------------------------------------
C ---- Search for index No of Gaussian angle close by inferior value
C ---- to the input VZA
C ------------------------------------------------------------------------

      xmuv=DCOS(thetav*PI/180.D0)
      No_vza=1
      IF (xmuv.GE.rmu(1)) GOTO 2
      IF (xmuv.LE.rmu(NMU)) THEN
        No_vza=NMU-1
        GOTO 2
      ENDIF
      A = 1000
      DO n=1,NMU
```

```
        D = ABS(xmuv-rmu(n))
        IF (D.LT.A) THEN
        A = D
        IF (xmuv.GT.rmu(n).AND.rmu(n).NE.1.0) THEN
        No_vza = n-1
        ELSE
        No_vza = n
        ENDIF
        ENDIF
        ENDDO
    2   CONTINUE

C ---------------------------------------------------------------------
C ---- Search for index No of azimut angle close by
C ---- inferior value to input phi angle (phi)
C ---------------------------------------------------------------------

        No_phi = 1
        IF (phi.LE.phi_OS(1)) GOTO 3
        IF (phi.GE.phi_OS(25)) THEN
          No_phi = NRAA-1
          GOTO 3
        ENDIF
        A = 1000
        DO n=1,NRAA
        D = ABS(phi-phi_OS(n))
        IF (D.LT.A) THEN
        A = D
        IF (phi.LT.phi_OS(n)) THEN
        No_phi = n-1
        ELSE
        No_phi = n
        ENDIF
        ENDIF
        ENDDO
    3   CONTINUE

C ---------------------------------------------------------------------
C ---- Search for index No of Gaussian scattering angle close by
C ---- inferior value to input OAT
C ---------------------------------------------------------------------

        No_aot = 1
        IF (aot.LE.AOT_OS(1)) GOTO 4
        IF (aot.GE.AOT_OS(NAOT)) THEN
          No_aot = NAOT-1
          GOTO 4
        ENDIF
        A = 1000
        DO n=1,NAOT
        D =ABS(aot-AOT_OS(n))
        IF (D.LT.A) THEN
        A = D
        IF (aot.LT.AOT_OS(n)) THEN
        No_aot = n-1
        ELSE
        No_aot = n
        ENDIF
        ENDIF
        ENDDO
    4   CONTINUE

C ---------------------------------------------------------------------
C ---- Search for index No close by inferior value to input WS
C ---------------------------------------------------------------------

!       A = 1000
!       DO n=1,3
```

```
!       D = ABS(ws-wind(n))
!       IF (D.LT.A) THEN
!       A = D
!       nws = n
!       ENDIF
!       ENDDO

       RETURN
       END

C ***********************************************************************
C ******************** - E N D   O F   C O D E  - ********************
C ***********************************************************************
```

Annex 2.3 : Outputs of the simulator

```
Enter Angstroem coefficient a(778/865):
 Enter the AOT at 560 nm:
 Enter the solar zenith angle [Deg.]:
 Enter the view zenith angle [Deg.]:
 Enter the solar azimut angle [Deg.]:
 Enter the view azimut angle [Deg.]:
 Enter the marine reflectance at 15 wavelenghts:
 Enter the detector index:
 Enter the barometric pressure [hPa]:

 RECALL OF THE INPUTS:
 ALPHA =   1.20000005
 AOT (560nm) =   0.200000003
 SZA =   58.5999985
 VZA =   58.5999985
 PHI (OS)=   90.
 BAROMETRIC PRESSURE =   1013.25
 IDETECTOR =  1

 num. indices: SZA VZA PHI AND AOT
 17 17 13 3

 iband Smile_effect_(nm) tauA tauR taur_S
 1   0.44263291   0.28020179   0.31527978   0.31392655
 2   0.31235218   0.26182261   0.23591024   0.23524414
 3   0.13820457   0.23488060   0.15515523   0.15498017
 4   0.07666969   0.22432840   0.13171376   0.13163456
 5   0.04669428   0.20000000   0.08991221   0.08994220
 6   0.13727283   0.17467621   0.05943336   0.05948599
 7   0.16408396   0.15845400   0.04472972   0.04477386
 8   0.16507626   0.15317960   0.04056213   0.04060145
 9   0.15644264   0.14495941   0.03455820   0.03458871
10   0.11397886   0.13342100   0.02694379   0.02696008
11   0.77254438   0.13159080   0.02592163   0.02581637
12   0.07513666   0.12803720   0.02361672   0.02362583
13   0.14195824   0.11508900   0.01545924   0.01544909
14   0.21027565   0.11333280   0.01409880   0.01408540
15   0.26632023   0.11232340   0.01317574   0.01316015



 iband rhoATM rhoa rho_r rhor_corr. Glitter Td Tu Tdu_aer Tdu_ray Saa Sar
 1   0.30235577   0.06551394   0.23684183   0.23684183   0.00000000   0.73072267
0.71221066   0.17279685   0.22053295   0.04130006   0.20125628
 2   0.25482419   0.06849106   0.18633313   0.18633313   0.00000000   0.77486366
0.75714749   0.19379205   0.17866784   0.04387140   0.16008508
 3   0.19788305   0.06952719   0.12835586   0.12835586   0.00000000   0.82601392
0.80941701   0.20885500   0.12754095   0.04673189   0.11270303
 4   0.17904037   0.06873594   0.11030443   0.11030443   0.00000000   0.84255260
0.82680327   0.21101868   0.11087185   0.04734772   0.09768605
 5   0.14188918   0.06519549   0.07669370   0.07669370   0.00000000   0.87470847
0.86091965   0.20873111   0.07894415   0.04770888   0.06929797
 6   0.11084955   0.05971083   0.05113872   0.05113872   0.00000000   0.90094465
0.88937169   0.19752038   0.05380112   0.04651987   0.04713452
 7   0.09409367   0.05553638   0.03855729   0.03855729   0.00000000   0.91514736
0.90472174   0.18656415   0.04108769   0.04513086   0.03593206
 8   0.08908511   0.05411585   0.03496926   0.03496926   0.00000000   0.91943949
0.90938812   0.18252248   0.03741372   0.04456162   0.03269243
 9   0.08166540   0.05187745   0.02978795   0.02978795   0.00000000   0.92597127
0.91650993   0.17591035   0.03206551   0.04341567   0.02798742
10   0.07194587   0.04874270   0.02320316   0.02320316   0.00000000   0.93458545
0.92595857   0.16570485   0.02518862   0.04170721   0.02192128
12   0.06764076   0.04731669   0.02032408   0.02032408   0.00000000   0.93843043
0.93019879   0.16059017   0.02215052   0.04089457   0.01923877
13   0.05760073   0.04433019   0.01327053   0.01327053   0.00000000   0.94752717
0.94029921   0.14732480   0.01461571   0.03921872   0.01258010
```

14 0.05582281 0.04372669 0.01209612 0.01209612 0.00000000 0.94910443
0.94203961 0.14566374 0.01334715 0.03887916 0.01145846

Annex 3.4: Reading the grid points

```
C*********************************************************************
C *****  main parameters
C *********************************************************************

C ---------------------------------------------------------------------
C Parameters declaration
C ---------------------------------------------------------------------

       INTEGER NAOT,NMU,NRAA,NBAND,NAER
       PARAMETER (NRAA   = 25)     ! max nb of user azimuthal angles
       PARAMETER (NAOT   = 16)     ! nb of AOT's at 550nm
       PARAMETER (NMU    = 25)     ! nb of Gaussian angles used in SO
       PARAMETER (NBAND  = 15)     ! nb of MERIS spectral bands
       PARAMETER (NAER   = 16)     ! nb of IOPA models

       REAL P0
       PARAMETER (P0 =1013.25D0)   ! standard surface pressure [hPa]

C ---------------------------------------------------------------------
C Variables declaration
C ---------------------------------------------------------------------



       REAL twvl(NBAND)
       REAL phi_OS(1:NRAA),AOT_OS(1:NAOT),rmu(0:NMU)
       REAL Qnorm(16,NBAND)

C ---------------------------------------------------------------------
C Data set
C ---------------------------------------------------------------------
C ---- Set 15 MERIS wavelengths [mic.]
       DATA twvl/0.41250D0,0.44250D0,0.49000D0,0.51000D0,0.56000D0,
     &           0.62000D0,0.66500D0,0.68125D0,0.70875D0,0.75375D0,
     &           0.7610D00,0.77875D0,0.86500D0,0.88500D0,0.90000D0/

C ---- Set 15 Rayleigh Optical Thickness
```

```
        DATA ROT/0.31527978, 0.23591024, 0.15515523, 0.13171376,
     &           0.08991221, 0.05943336, 0.04472972, 0.04056213,
     &           0.03455820, 0.02694379, 0.02592163, 0.02361672,
     &           0.01545924, 0.01409880, 0.01317574/

C ---- Set 16 AOTs
        DO k=1,NAOT
        AOT_OS(k)=(k-1)/10.
        ENDDO

C ---- Set 25 azimut angles [deg.]
        DO i=1,NRAA
        phi_OS(i) = 7.5*(i-1)
        ENDDO


C ---- Spectral dependence of the AOT
        OPEN(1,'input/Qnorm_IOPA')
        DO j=1,16
        READ(1,*) (Qnorm(j,k),k=1,NBAND)
        ENDDO
        CLOSE(1)
```

Annex 2.5: Reading the LUTS

```
*****************************************************************
C *****                                                       *****
C *****             READING the LUTs                          *****
C *****                                                       *****
C        This program reads the grid point values (geometry
C        and AOT used to generate the LUTs
C        The initial LUTs were generated for ONE aerosol type
C        This program combined the 16 aerosol types
C        The computation is for one wind speed
C ******
C *****************************************************************

       subroutine read LUTs(ifaer,iws,
     & rho_up, T_tot_down,T_tot_up,sphalb



C -------------------------------------------------------------------
C Parameters declaration
C -------------------------------------------------------------------

       INTEGER NAOT,NMU,NRAA,NBAND,NAER
       PARAMETER (NRAA   = 25)     ! max nb of user azimut angles
       PARAMETER (NAOT   = 16)     ! nb of AOT's at 550nm
       PARAMETER (NMU    = 25)     ! nb of Gaussian angles used in SO
       PARAMETER (NBAND  = 15)     ! nb of MERIS spectral bands
       PARAMETER (NAER   = 16)     ! nb of IOPA models



C -------------------------------------------------------------------
C Variables declaration
C -------------------------------------------------------------------

C      inputs for one aerosol type

       REAL rad1(NBAND,NAOT,NMU,NMU,NRAA) !TOA atmospheric reflectance
       REAL ttot(NBAND,NAOT,NMU) !upward total transmittance
```

```
        REAL ttot2(NBAND,NAOT,NMU)  !downward total transmittance
        REAL sa(NBAND,NAOT)! spherical albedo

C       outputs for one aerosol family

        REAL rho_up(NAER,NBAND,NAOT,NMU,NMU,NRAA)
        REAL T_tot_down(NAER,NBAND,NAOT,NMU)
        REAL T_tot_up(NAER,NBAND,NAOT,NMU)
        REAL sphalb(NAER,NBAND,NAOT)



C ---------------------------------------------------------------------
C Read data from LUTs binary file
C ---------------------------------------------------------------------
C ---- Read TOA radiances and transmittances for 16 IOPA models
        OPEN(1,FILE='input/LUT_IOPA144cc_ws5',FORM='unformatted')
C the example is fot the IOPA family with no absorption
C and a wind speed of 5 m/s.

        DO ii=1,NAER !loop on the aerosol type
        READ(1) rad1!normalized radiance
        READ(1) ttot,sa! total transmittance down and spherical albedo
        READ(1) ttot2!total transmittance up
        DO i=1,NBAND
         DO j=1,NAOT
         sphalb(ii,i,j) = sa(i,j)
          DO k=1,NMU
          T_tot_up(ii,i,j,k) = ttot(i,j,k)
          T_tot_down(ii,i,j,k) = ttot2(i,j,k)
           DO m=1,NRAA
            DO l=1,NMU
            rho_up(ii,i,j,k,l,m) =  rad1(i,j,k,l,m)
            ENDDO
           ENDDO
          ENDDO
         ENDDO
        ENDDO
```

```
      ENDDO
      CLOSE(1)

      STOP
      END


C ***********************************************************************
C ******************* - E N D   O F   C O D E  - *********************
C ***********************************************************************
```

Title	**ATBD for atmospheric correction**
Version	0.1
Author(s)	R. Santer
and affiliation(s)	ADRINORD
Modification history	First draft: 31/07/2010
	This version:
Distribution	Public report

Executive summary:

This ATBD describes an atmospheric correction scheme specific to coastal areas and applies on MERIS both FR and RR. The aerosol model retrieval accounts for the contribution in the near infra red over case 2 waters. In the vicinity of land, we also include the adjacency effect correction.

The verification of the processor implementation will be conducted with the help of a forward simulator.

A specific validation approach is proposed relying on AERONET ocean colour network and a accurate prediction of the atmospheric function is order to evaluate the accuracy of the AC processor.

1. Introduction

We propose here to develop an atmospheric correction algorithm based on an analytical approach. The formalism used to model the TOA reflectance has its roots in 5S (Vermote et al, 1997). The radiative transfert code, and associate inputs and outputs, to generate the atmospheric functions required by 5S are fully consistent with MEGS. Section 2 described both 5S and the generation of the required LUTs.

One clear need for studies in coastal waters is to account for the adjacency effects. The role of the current ICOL processor is to return MERIS L1 after AE correction. Our objective here is to modify ICOL in order to generate L2 products. This objective implies first to revisit in section 3 the ICOL formalism in order to improve the performances, second to include the sun glint which was not accounted for and third to generate more accurate LUTs. In terms of accuracy, the achievement of the atmospheric correction is more demanding because it concerns the main part of the TOA signal compare to the AE which are a second order term.

Section 4 describes the preparation module which first re-uses ICOL routines, second introduces the sun glint and third proposes to use additional aerosol models with absorption.

Conversely to ICOL, the aerosol model retrieval and the AC are done in absence of AE, section 5. Our aerosol retrieval scheme applies on case 2 waters. It is a simplified version to what is implemented in ICOL for case 2 waters. Once the aerosol model is known, the AC follows the 5S formalism of section 2.

The introduction of the AE in the AC, section 6, is based on the formalism introduced in section 3. We return a L2 product but also a L1 after AE to be used for other AC processors.

Section 7 illustrates the performances of the last ICOL version with results which are not included in the ICOL reports. It contributes to demonstrate the aerosol retrieval scheme performances.

One required output is to provide error bars. Section 8 addresses the different issues of the production of the error bars on the L2 product.

Sections 9 and 10 detail respectively the verification and the validation strategies.

2) Model of the TOA reflectance in absence of AE effect

2.1) The 5S like formalism: from above land to above water

When ignoring the AE effects, we can simply formulate the TOA signal. This formalism is the order zero of ICOL.

For a given atmosphere, we can predict ρ^* over land following 5S:

$$\rho^* = \rho^0_{atm} + \mathrm{T}_{atm}(\mu_s, \rho_s)\mathrm{T}_{atm}(\mu_v)\rho_s \qquad (1)$$

ρ^0_{atm} is the intrinsic atmospheric reflectance. It corresponds to the TOA signal observed over a dark surface.	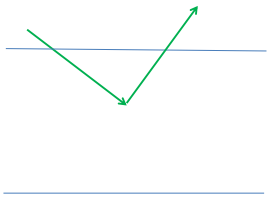

$\mathrm{T}_{atm}(\mu_s)$ is the total down-welling transmittance which includes by decreasing order of importance: (i) the direct irradiance at surface, (ii) the diffuse irradiance by the atmosphere, (iii) the diffuse irradiance corresponding to multiple interactions between the scattering and the surface reflection, if not null.	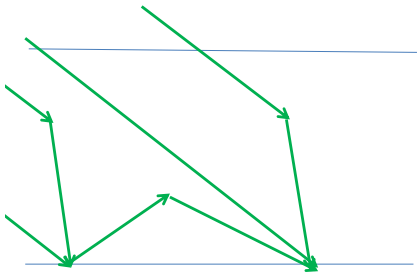

$\mathrm{T}_{atm}(\mu_v)$, the total upwelling transmittance corresponds to the attenuation on the direct path: pixel P to sensor; but also to the contribution of the surrounding pixel S by scattering.	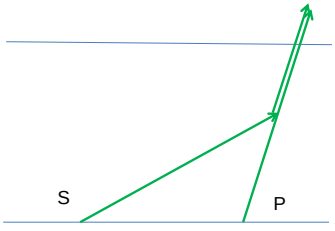

Over a dark surface, based on the principle of reciprocity, $\mathrm{T}_{atm}(\mu_s)$ and $\mathrm{T}_{atm}(\mu_v)$, are identical.

When we introduce a Lambertian and homogeneous surface, the multiple interactions between scattering and reflection are modeled in 5S as:

$$\mathrm{T}_{atm}(\mu_s, \rho_s) = \mathrm{T}_{atm}(\mu_s) / (1 - \rho_s * s_{atm}) \tag{2}$$

In which we introduce the spherical albedo s_{atm} of the atmosphere.

$$\rho^* = \rho^0_{atm} + \mathrm{T}_{atm}(\mu_s)\mathrm{T}_{atm}(\mu_v)\rho_s / (1 - \rho_s * s_{atm}) \tag{3}$$

ρ^0_{atm} and $\mathrm{T}_{atm}(\mu_s)$ are computed over a dark surface. By definition:

$$s_{atm} = 1 - 2\int_0^1 \mu T(\mu) d\mu \tag{4}$$

When the atmospheric properties are known, the 5S formalism in the homogeneous case is used to derive the surface reflectance:

$$\rho_s^C = (\rho^* - \rho_{atm}) / \mathrm{T}_{atm}(\mu_s)\mathrm{T}_{atm}(\mu_v) \tag{5}$$

$$\rho_s = \rho_s^c / (1 + \rho_s^c * s_{atm}) \tag{6}$$

Above the ocean, we have to introduce the Fresnel reflection.

We replace ρ^0_{atm} by ρ_{atm} where we add the coupling between atmospheric scattering and Fresnel reflection.	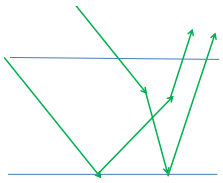

Even on a black sea, we have to add to compute the down welling irradiance the coupling between the Fresnel reflection and the atmospheric backscattering. We then get a down welling total transmittance T^F_{atm}	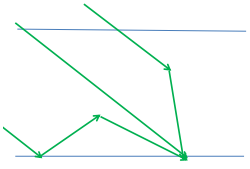

ρ_{atm} and T^F_{atm} are computed over the dark ocean but with the Fresnel reflection.

In presence of low and medium sunglint, we have to add ρ_G^* which corresponds to the sunglint reflection ρ_G at the surface attenuated by the atmosphere on the direct to direct path, using τ , the total optical thickness. ρ_G is computed using the Cox and Munk model associated to the ECMWF wind speed. Finally, we have:

$$\rho_w^* = \rho_{atm} + \mathrm{T}_{atm}^F(\mu_s)\mathrm{T}_{atm}(\mu_v)\rho_w / (1 - \rho_w * s_{atm}) + \rho_G \exp(-\tau(1/\mu_S + 1/\mu_V)) \quad (7)$$

The aerosol model is known from the NIR. For the "ocean colour" spectral bands, after subtracting the direct sunglint, we get ρ_w through equations (5) and (6).

In MEGS_8.0, we do not introduce the spherical albedo. According to equation (6); we introduce a relative bias on ρ_w of - ρ_w s_{atm}. We reported in table 1, s_{atm} for a standard atmosphere (standard pressure and a continental model with a visibility of 23 km). Relative errors are small at 412 nm for clear water, of the order of one percent… but why not to include the spherical albedo?

λ (nm)	412	443	490	520	560
s	0.27	0.24	0.19	0.17	0.14

Table 1: spherical albedo for a standard atmosphere in different MERIS spectral bands

2.2) Computation of the atmospheric functions

2.2.1) The radiative transfer code

The vertical distribution of the molecules is described by the altitude (z) dependence of the optical thickness:

$$\tau_R(z) = \tau_R \cdot \exp(-z / H_R), \quad (8)$$

with H_R the molecular vertical scale height, fixed here to a standard value of 8 *km*.

The aerosol vertical distribution will follow the same dependence but with H_a the aerosol vertical scale height. Alternatively, we can have a 3 layers of aerosols (see below).

The boundary condition is the Fresnel reflection. The state of the sea surface is described by the Cox and Munk (1954) wave slope distribution model.

The successive order of scattering (Deuzé et al, 1989) is the code of reference for MERIS because it includes the polarization. A vector code is a requirement for accurate computations of the radiance.

2.2.2) The ICOL option

The land approach (Santer et al, 199), implemented in MEGS, is based on decoupling the Rayleigh and the aerosol scattering. The molecular atmosphere is entirely above the aerosols. The coupling between Rayleigh and aerosol scatterings was described by the 5S approximation.

The land approach was used:

(i) To respond to the first AO for ICOL which required to first make a Rayleigh correction.

(ii) To include the lakes at any elevation for the Rayleigh correction because the only input is the ROT not the wavelength. Inland water is not a requirement in Coast Colour.

(iii) To ensure a spectral flexibility because the only input to the aerosol correction is the AOT not the wavelength. This spectral flexibility is no longer an advantage if you develop your software for one specific sensor.

(iv) The coupling scattering and reflection was approximated for the Rayleigh based on the primary scattering combined to a specular reflection. A similar approach was used for the aerosols.

The 26 aerosol models correspond to a power law:

$$n(r) \approx r^{\alpha - 3}, \tag{9}$$

where *r* is the particle radius and α is the *Angström* exponent which describes the wavelength dependency of the AOT ($\tau_a(\lambda)$):

$$\alpha(\lambda, \lambda') = \frac{\log(\tau_a(\lambda) / \tau_a(\lambda'))}{\log(\lambda / \lambda')}, \tag{10}$$

They present the advantages of the simplicity and of the optical continuity between two consecutive models. The major disadvantage is for the small aerosols as reported by Aznay and Santer (2009): the use of a power law over estimates the atmospheric correction.

2.2.3) The IOPA option

Instead of using aerosol models derived from the micro physics, the IOPA models (Zagolki et al, 2007) are based on the restitution of the optical properties using extinction and sky radiance measurements made available through AERONET (Holben et al, 1998).

The classification of the models is based on the Angstroem coefficient between 670 nm and 870 nm which ensures the continuity of the optical properties.

A specific generation of aerosol IOPs was made for Coast Colour and reported in a TN by Santer et al, 2010. 16 aerosol types are proposed for all the CC ROIs. In additions, we will activate for some of the ROIs and for turbid atmosphere a set of 16 additional aerosol models with absorption.

The routines exist at ADRINORD to process new AERONET data in order to provide “regional aerosol climatology” as it is required at the end of the project.

The IOPA models can be processed as well by MERISAT as for the regular MERIS SAMs. At the end, we have the MEGS LUTs and the computation of the atmospheric functions is described in the MERIS DPM. This module should be available to public through ODESA.

Alternatively, we propose to generate a SOS code (Deuzé et al, 1989) data base and to provide BC with the fortran routines which computes the atmospheric functions. This more direct computation and accurate because we fully account for all the coupling terms: Rayleigh –aerosol scattering, atmospheric scattering and Fresnel reflection.

2.2.5) Rescale the Rayleigh to the barometric pressure

The LUTs are generated for the standard barometric pressure of 1013 hPa at the central wavelength of the nominal MERIS spectral bands. We need to account for the actual barometric pressure as provided in the MERIS auxiliary file as well as the smile effect.

Rayleigh and barometric pressure

The Rayleigh computation of the optical thickness τ_R^0, of the reflectance ρ_R^0 and of the transmittances total T_R^0 and diffuse t_R^0 are conducted for a standard surface pressure P_0 and we used the ECMWF pressure P of the auxiliary data file. We directly have:

$$\tau_R = \tau_R^0 \; P \; / P_0 \tag{11}$$

Or

$$d\tau_R = \tau_R^0 \; dP \; / P_0 \tag{12}$$

Following Antoine and Morel, 1999, we have:

$$\rho_R(P) = \rho_R(P_0) \; (1 - \exp(\tau_R P / (\mu P_0)) / \; (1 - \exp(\tau_R / P_0) \tag{13}$$

Where μ is the cosine of the VZA.

Following Gordon and Wang, we have:

$$T_R = T_R^0 \; \exp(-0.5 * d\tau_R / \mu) \tag{14}$$

Which gives:

$$t_R = t_R^0 + 0.5 * d\tau_R / \mu \tag{15}$$

Rayleigh and smile

The Rayleigh scattering functions are computed for each band *i* for the nominal central wavelength λ_0^i ignoring the smile. To each detector *j* corresponds one central wavelength λ_j^i with for each spectral band:

$$d\tau_R^{i,j} = -4\tau_R^{i,0} d\lambda^{i,j} / \lambda^{i,0} \tag{16}$$

Which is equivalent to an additional pressure variation of:

$$dP^{i,j} = -4P_0 \, d\lambda^{i,j} / \lambda^{i,0} \tag{17}$$

Allowing using directly (11) to (15)

Rayleigh and atmospheric scattering functions

The atmospheric reflectance and transmittances becomes:

$$\rho_a = \rho_a^0 + d\rho_R \tag{18}$$

$$T_a = T_a^0 \; \exp(-0.5 * d\tau_R / \mu) \tag{19}$$

$$t_a = T_a \; - \exp(-(\tau_R + \tau_a) / \mu) \tag{20}$$

3) Modeling of the TOA reflectance in the presence of AE effect

3.1) The TOA reflectance over water in presence of AE effect

Following 5S, equation (7) becomes:

$$\rho^{*} = \rho_{atm} + \mathrm{T}_{atm}(\mu_s)(\rho_w(\exp(-M\tau) + < \rho_{Ray} > t_{Ray}(\mu_v)) + < \rho_{aer} > t_{aer}(\mu_v)) +$$

$$\rho_G \exp(-\tau(1/\mu_s + 1/\mu_v)) \quad (21)$$

Compare to equation (7), we have:

(i) The atmospheric reflectance ρ_{atm} can be reduced by the so-called land Fresnel mask (and cloud Fresnel mask).

(ii) We assume than the solar irradiance at surface is the same in the AE window (same $\mathrm{T}_{atm}(\mu_s)$).

(iii) The water reflectance is weighted by the attenuation on the direct upward path

(iv) We decouple the Rayleigh and aerosol adjacency effects. For each of them, the diffuse transmittance of the aerosols $t(\mu_v)$ weights the mean reflectance $< \rho >$

When the LFM reduces the coupling between the Fresnel reflection of the solar beam and it coupling with the atmospheric scattering. We decouple Rayleigh and aerosol scatterings:

$$\rho_{atm} = C_{Ray}^{F}\ \rho_{Ray} + C_{aer}^{F}\ \rho_{aer} \quad (22)$$

$$C_{Ray}^{F} = (1 + r(\mu_v) + r(\mu_s)(1 - \exp(-Z_{\max} / H_{Ray})) / (1 + r(\mu_v) + r(\mu_s)) \quad (23)$$

$$C_{aer}^{F} = (1 + PFB(r(\mu_v) + r(\mu_s)(1 - \exp(-Z_{\max} / H_{aer}))) / (1 + PFB(r(\mu_v) + r(\mu_s))) \quad (24)$$

For the aerosols, C_{aer}^{F} account for the ration PFB of the aerosol phase function between the forward and the backward scatterings. The land Fresnel mask introduces Z_{max} as in ICOL_1.0. (Santer and Zagolski, 2009)

In absence of LFM, we have $C_{Ray}^{F} = C_{aer}^{F} = 1$ and we define ρ_{aer} as ρ_{atm} - ρ_{Ray}

3.2) Computation of $< \rho >$ in absence of direct sunglint

$< \rho >$ is defined as the convolution of the BOA reflectance matrix $\tilde{\rho}_s$ by the weighting matrix $\tilde{W}$.

The 5S formalism in the homogeneous case, equation (5), is used to derive the surface reflectance. Because $\rho_{atm}, \mathrm{T}_{atm}(\mu_s), \mathrm{T}_{atm}(\mu_v)$ are assumed to be constant in the AE window and because $\tilde{W}$ is normalized to one, we have:

$$< \rho_s >=< \rho^* > / \mathrm{T}_{atm}(\mu_s)\mathrm{T}_{atm}(\mu_v) - \rho_{atm} / \mathrm{T}_{atm}(\mu_s)\mathrm{T}_{atm}(\mu_v) \quad (25)$$

Equation (21) becomes:

$$\rho^*_{nG} = \rho_{atm} CA + \mathrm{T}_{atm}(\mu_s)\rho_w \exp(-\tau/\mu_v) + (< \rho^*_{aer} > t_{aer}(\mu_v) + < \rho^*_{Ray} > t_{Ray}(\mu_v))/T_{atm}(\mu_v) \quad (26)$$

With:

$$CA = 1 - t_{atm}(\mu_v)/T_{atm}(\mu_v) \quad (27)$$

3.3 $< \rho >$ in presence of direct sunglint

To (21), we need to subtract $< \rho_G > \exp(-M\tau) / \mathrm{T}_{atm}(\mu_s)\mathrm{T}_{atm}(\mu_v)$. Assuming that in the AE window, the AOT is constant and that the total air mass *M* varies slowly, we have then:

$$< \rho_G > = \tilde{\rho}_G \otimes \tilde{WF} \otimes \tilde{W} \quad (28)$$

Where: $\tilde{\rho}_G$ is the sunglint reflectance matrix, $\tilde{WF}$ the water flag matrix and $\tilde{W}$ the AE matrix for the Rayleigh or for the aerosols.

(26) becomes:

$$\rho^* = \rho^*_{nG} - \exp(-M\tau)(< \rho^G_{aer} > t_{aer}(\mu_v) + < \rho^G_{Ray} > t_{Ray}(\mu_v))/T_{atm}(\mu_v) + \rho_G \exp(-M\tau) \quad (29)$$

3.4 Limitations to the above formalism

The basic geophysical assumption is that the atmosphere is homogeneous on the window used to achieve the adjacency effect correction. We do more by simplification because (25) assumed that the atmospheric functions are the same over water and land. Over water, we ignore the

possible reduction of ρ_{atm} by the land Fresnel mask. Over land, we should use ρ_{atm}^{0} instead of ρ_{atm}

and $T_{atm}(\mu_s)$ is slightly under estimated because of the coupling between scattering and surface reflection is certainly larger over land than over water.

At the end, it is a first order approximation to the AE effect and a second order approximation in the signal formalism.

4) Preparation module

4.1) The BEAM flags and TOA reflectance

ρ^{*} has been corrected from the gaseous transmittance.

4.2) The ICOL flags

ICOL is applied only when the water AE flag is raised (defined as water pixel distant by less than 30 RR pixels from the coast line for the Rayleigh *(F_AE_Ray)* and 10 RR pixels for the aerosols *(F_AE_aer)*.

In order to apply ICOL, we need to extend this area by 30 RR pixels for the Rayleigh over any type of pixels (water, land or cloud) in the computation of $<\rho_R>$, flag: *F_romean_Ray*.

In order to apply ICOL, we need to extend this area by 10 RR pixels for the aerosols over any type of pixels (water, land or cloud) in the computation of $<\rho_a>$, flag: *F_romean_aer*.

4.3) Prepare the inputs

sunglint

The direct sunglint reflectance ρ_G is computed with the Cox and Munk model associated to the measured wind speed.

If $\rho_G > \rho_G^{\max}$, the high sunglint flag, HSGF, is raised and the AC is abandoned. $\rho_G^{\max}$ is by default set to 0.1.

If $\rho_G < \rho_G^{\min}$, the low sunglint flag, LSGF, is raised and the sunglint is not accounted in the formulation of the signal. $\rho_G^{\min}$ is by default set to 0.0001.

Rayleigh adjustment

$d\tau_R$, $d\rho_R$, $\exp(-0.5*d\tau_R/\mu_s)$ and $\exp(-0.5*d\tau_R/\mu_v)$ are compute for the pressure adjustment in the 13 MERIS spectral bands for each pixel.

5) The atmospheric correction in absence of AE

HSGF is used. When not raised we activate this module.

5.1) The turbid atmospheric flag: TAF

We use equation (7) over the dark water to compute the TOA reflectance in B13 for the 16 aerosol models and an AOT=1.5. We take the maximum and if MERIS TOA reflectance is above the simulation, we raise the turbid atmospheric flag and stop the process.

5.2) The absorbing dust flag: ADF

The risk of the presence of absorbing dust is linked to specific ROIs.

We use equation (7) over the dark water to compute the TOA reflectance in B13 for the 16 aerosol model and an AOT=0.5. For a given aerosol type, if MERIS TOA reflectance is above the simulation, we use for this aerosol type, the LUTs for absorbing aerosols.

5.3) The aerosol model retrieval

If the LSGF is raised, we do not include the sunglint in equation (7) we use to model the TOA reflectance.

The three unknowns: AOT_865, α and ρ_W (708) are determined using the TOA reflectance ρ^* at 708, 778 and 865 nm. In MEGS, the case 2 water is divided into

The approach to retrieve the aerosol model is similar to what we described in ICOL D6 (Santer, 2010) with the noticeable difference that we use the TOA reflectance instead of the BBR.

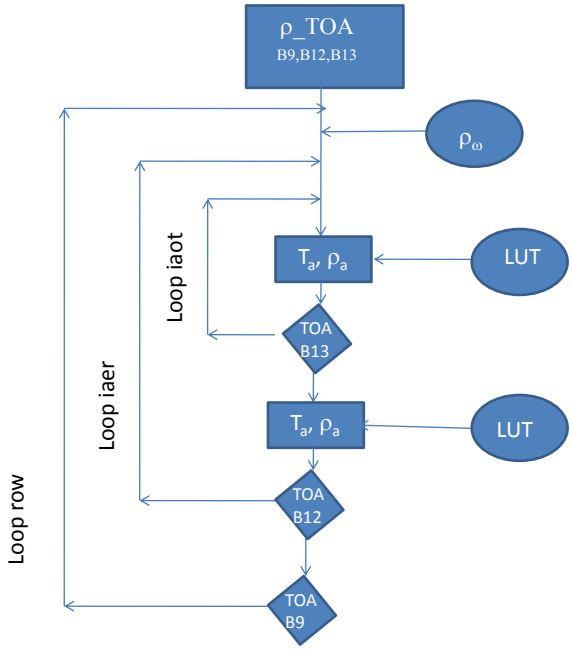

Figure 1: Flow chart for the aerosol model retrieval in case 2 water no glint and no AE

The external loop is on the water reflectance starting by 0 for the case 1.

We then loop on the aerosol type *iaer* with the reading of the atmospheric LUTs to predict ρ^* in B13 following (7). The atmospheric LUTS are first interpolated in the cosine of the zenith angle and in the azimuth angles. They are Rayleigh adjusted. When the LSGGF is not raised the direct sun glint is added with the direct to direct attenuation both for the molecule and for the aerosols.

The loop on the AOT at 550 nm (*iaot=0 to 15 for AOT_550=0 to 1.5*) allows to bracket ρ^* MERIS in B13 between *jaot* and *jaot-1*. For each aerosol type, by linear interpolation between $\rho^*(jaot-1)$ and $\rho^*(jaot)$, we get one AOT_550 for each aerosol type: AOT_550(*iaer*).

The aerosol type is retrieved in B12 by matching MERIS. Two aerosol types , *jaer* and *jaer-1,* bracket ρ^* in B12. By linear interpolation between $\rho^*(jaot-1)$ and $\rho^*(jaot)$ in B12, we get α. The aerosol model is α and the AOT_865.

With this aerosol model, we predict ρ^* in B9 which should be below MERIS when the water is dark.

The schematic determination of α and ρ^* in B9 is represented below in figure 2. The key parameter for these two linear interpolations is the mixing ratio defined in B12 on the TOA reflectance as:

$$M = (\rho(jaer) - \rho^*_{MERIS})/(\rho(jaer) - \rho(jaer-1)) \quad (30)$$

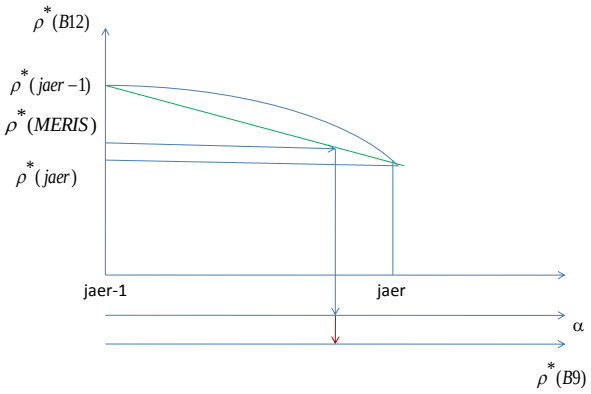

Figure 2: schematic representation of the linear interpolation on the MERIS TOA reflectance in B12 in order to determine α and the MERIS TOA reflectance in B9.

If so, we loop on ρ_W as far as in B9 we predict ρ^* above MERIS. If so, we derive by interpolation on ρ^* in B9 between the two successive values of ρ_W to get the best estimate of ρ_W .

Last aerosol retrieval is made with this ρ_W value.

5.4) The atmospheric correction

There are done from B1 to B8. If the LSGF is not raised, we first remove the direct sunglint ($\rho_G \exp(-M\tau)$) from ρ^* . ρ_G is wavelength independent. The AOT in any band is computed first for the two bracketed aerosol types. Second the mixing ratio M is used for a linear interpolation following figure 2.

To use equations (5) and (6) to get the water reflectance, we extrapolate the atmospheric functions first computed for the two bracketed aerosol types and second interpolated using *M*..

6) The atmospheric correction in presence of AE

HSGF is used. When not raised and if *F_AE_Ray* is raised, we activate this module.

6.1) The aerosol model retrieval

The scheme is the same than for §5.1 to §5.3 except than we use equation (29) instead of equation (7).

For B9, B12 and B13, we need to compute $< \rho^*_{aer} >, < \rho^*_{Ray} >$ in the same way than for ICOL2.0 except that:

(i) we have 16 aerosol models instead of 26.

(ii) we use the TOA reflectance instead of the BRR.

The effective reflectance to compute $< \rho^*_{aer} >, < \rho^*_{Ray} >$

The introduction of the bright clouds in the AE computation

The bright cloud flag *F_BC* is raised. Following ICOL D4, (Santer et al, 2009), we simply replace ρ^*_c for the Rayleigh computation by:

$$\rho^*_{c,Ray} = \rho^*_c P_C / P_O \,. \tag{31}$$

P_C is the CTP and P_O the ECMWF sea level pressure.

For the aerosols we consider the optical thickness above the clouds. The CTP is converted into a cloud top altitude (in km) with:

$$z_c = 8.\ln(P_o / P_c) \tag{32}$$

With a vertical scale height $H_a = 3\ km$, the aerosol optical thickness above the cloud was:

$$\tau_a^C = \tau_a \exp(-z_C / H_a) \tag{33}$$

Following D4, we simply replaced ρ^*_c for the aerosol computation by:

$$\rho^*_{c,aer} = \rho^*_c \,.\, \tau_a^C / \tau_a \tag{34}$$

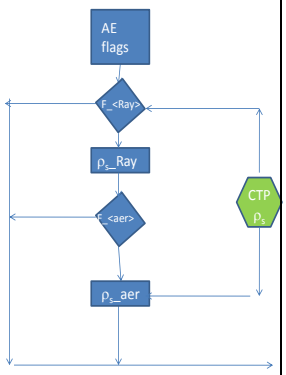

Compute ρ_s^R

If *F_romean_Ray* is raised, we generate in a MERIS band a Rayleigh surface reflectance composed over land and over water of the surface reflectance and over cloud of the cloud reflectance weighted by the ratio CTP/(surface pressure)

Compute ρ_s^a

If *F_romean_aer* is raised, we generate as above except that the cloud reflectance is weighted by the ratio of the AOT above the cloud to the total AOT.

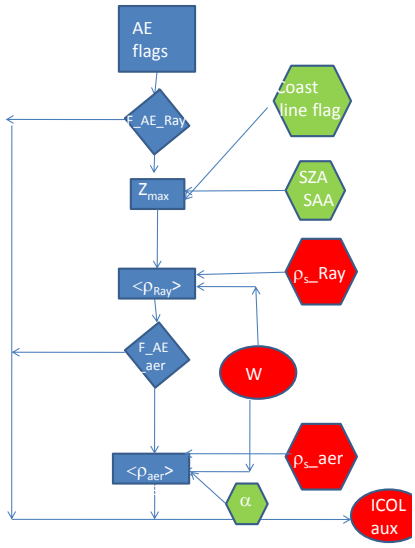

Compute Z_{max}

If *F_AE_Ray* is raised, Z_{max}, the distance to the coast line in the principal plane, is computed and will be used for the Land Fresnel mask and for the cloud Fresnel mask.

Compute $< \rho_R^* >$

If *F_AE_Ray* is raised, we compute $< \rho_R >$ in 3+8 MERIS bands

Compute $< \rho_a^* >$

If *F_AE_aer* is raised, we compute in B9, B12 and B13 $< \rho_a >$ for 2 values of α (-0.6 and -1.6); iaer=5 and 12.

For the AC, $< \rho_a >$ is computed for the aerosol model *jaer* in from B1 to B8.

NB: Green polygons are BEAM parameters. Blue is new process, Red is ICOL or new outputs. The first module produces the AE flags.

The Fresnel masks (land and cloud), equations (23) to (25) are wavelength independent.

6.2) The atmospheric correction

We have the aerosol model with which we can compute the atmospheric functions in all the MERIS bands. The wind speed is an input for the coupling between atmospheric scattering and Fresnel reflection.

If the direct sunglint is not negligible, we use equation (29) to correct it.

We have to compute in the 8 MERIS bands $< \rho^*_{Ray} >$ and $< \rho^*_{aer} >$ for *jaer*, which corresponds to the selected aerosol type by excess.

Using equation (26), we finally get:

$$\rho_w = (\rho^*_{nG} - \rho_{atm} CA - (< \rho^*_{aer} > t_{aer}(\mu_v) + < \rho^*_{Ray} > t_{Ray}(\mu_v))/T_{atm}(\mu_v))/$$

$$(\mathrm{T}_{atm}(\mu_s)\rho_w \exp(-M\tau)) \qquad (32)$$

Again, in equations (32) and (6), the atmospheric functions: $\rho_{atm}, CA, t_{aer}(\mu_v), T_{atm}(\mu_v)$, $(\mathrm{T}_{atm}(\mu_s), \tau, sa$, are computed for the two bracketed aerosol types and are interpolated with *M*.

6.3) The L1 product

Having the aerosol model, we use the current ICOL to provide a corrected L1 product.

6.4) The L2 product

We first need to include the L1 flags and the L2 classification flags. We have the MERIS standard L2 geophysical products. We add, table 1 is a list of new parameters which are break points relevant to this algorithm.

acronym	use	nature	unit	default
HSGF	High sun glint	Flag	NU	0
LSGF	Low sun glint	Flag	NU	0
TAF	Turbid atmosphere	Flag	NU	0
ADF	Absorbing dust	Flag	NU	0

F_AE_Ray	Apply AE for Rayleigh	Flag	NU	0
F_AE_aer	Apply AE for aerosol	Flag	NU	0
F_romean_Ray	Pixel for $<\rho_R>$computation	Flag	NU	0
F_romean_aer	Pixel for $<\rho_a>$computation	Flag	NU	0
Z_{max}	Altitude of the Fresnel mask	Distance	km	999
$9<\rho_R>$		Reflectance	NU	0
$9<\rho_a>$		Reflectance	NU	0

Table 2: Content of the ICOL break points

7) The ICOL heritage

7.1) (Near) case 1 water

The first version of ICOL assumed dark water in B12 and B13. The two aerosol parameters are determined from the best fit with the MERIS TOA reflectance.

We selected, in figure 3, a MERIS image collected off shore of Sweden. The first row corresponds to the initial version of ICOL. The second row corresponds to the three band algorithm described in §5.2.

The AOT are scaled from black to white from 0 to 0.5 and α from -2.5 to 0. The water reflectance in B9 is small and corresponds to suspended matter content less than 5 mg/l which are acceptable values in those waters. For these quasi case 1 waters, the introduction of the water reflectance in the algorithm slightly impacts on the aerosol product: the AOT decreases and α indicates whiter aerosols. Both trends were expected.

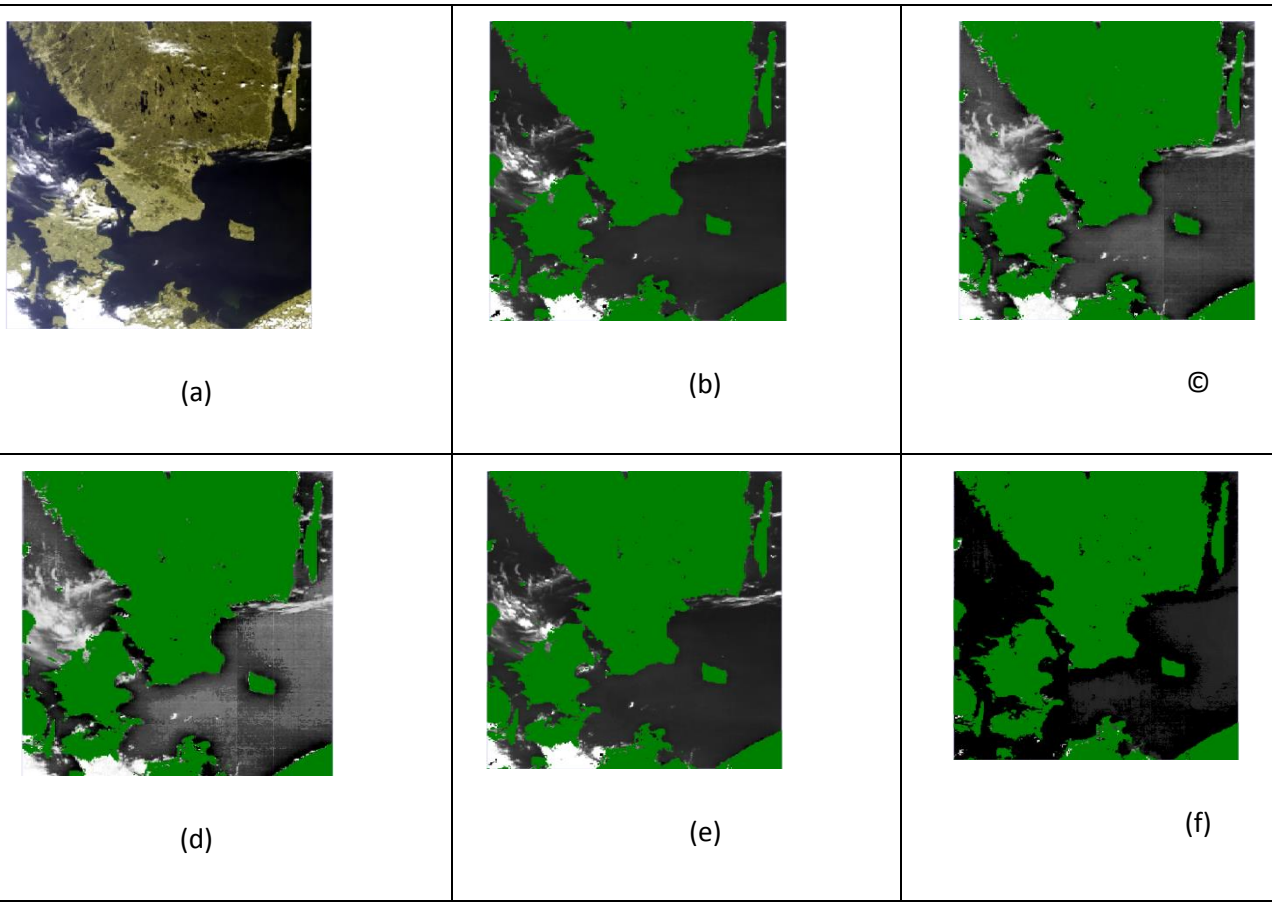

Figure 3: ICOL on the Swedish waters: (a) RGB; case 1 water aerosol product (b) AOT and (c) α; case 2 water: water reflectance in B9 (d) aerosol product (e) AOT and (f) α;

7.2) Case 2 water

With the same two ICOL algorithms, we now move to turbid waters in the Mouth of the Thames River. If we neglect the contribution of the water reflectance on the aerosol product, first row of figure 4, we clearly bias it with mainly an artificial increase of the AOT with follows the structure of the river plume. With the case 2 algorithm, second row, we decouple the water turbidity from the water one with the introduction of larger aerosols with a decrease of the AOT.

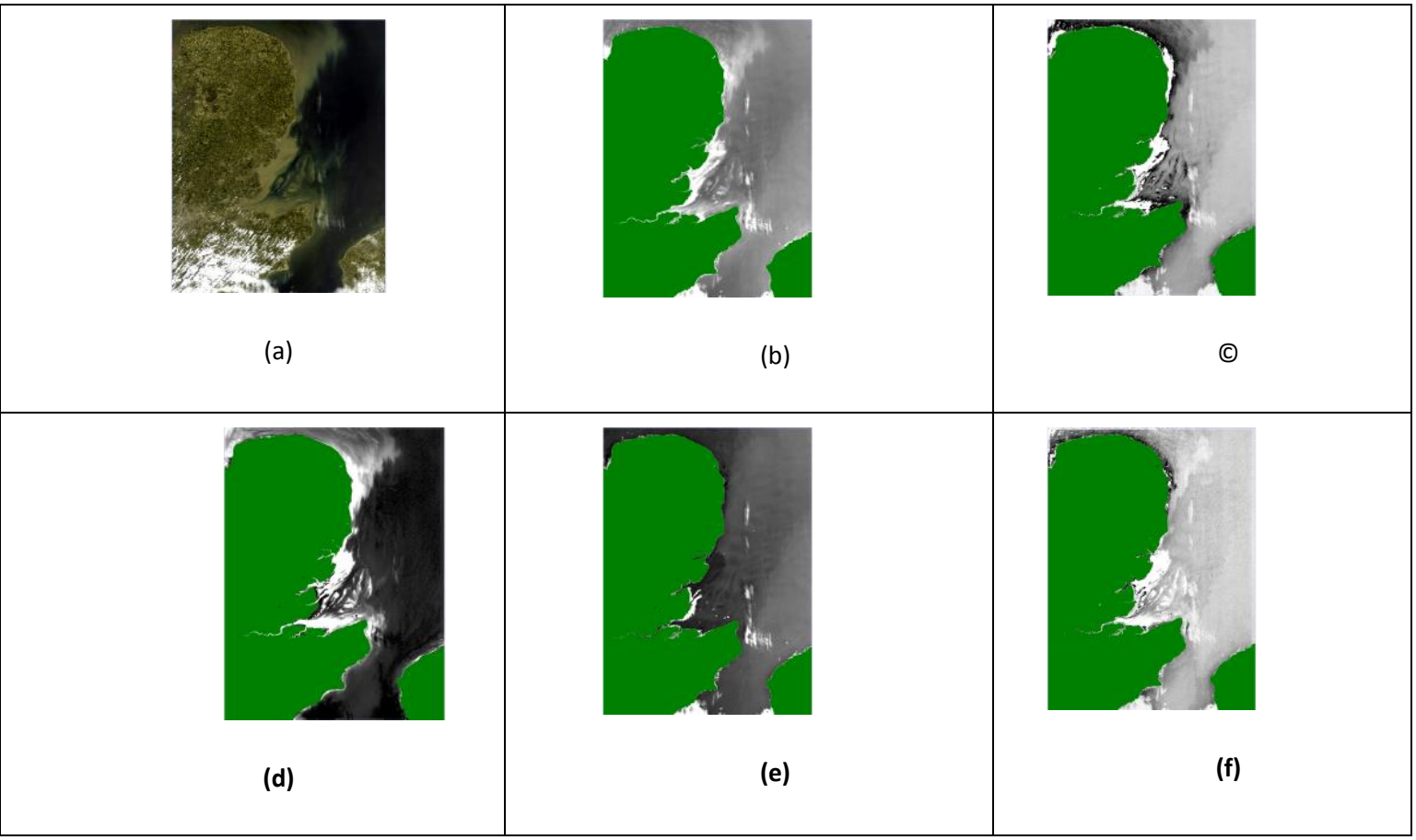

Figure 4: ICOL on the Southern North Sea with the same plots than for figure 3. :

8) Error analysis

8.1) Source of errors

It is the first task to undertake but not an easy one because this *a priori* classification between sustematic error and random error can be arbitrary.

8.1.1) Systematic errors

The radiometric and the spectral calibrations go first.

Then, we have the pixel classification which is driven by a decision matrix feeds by threshold values…which are subject to errors.

The computation of the atmospheric functions relies on aerosol standard models. There are different families reported in the literature and implemented in operational atmospheric correction algorithms. One assumption is also on the aerosol vertical distribution.

The wave slope distribution model used for the Fresnel reflection is quite arbitrary as well.

For aerosol remote sensing, we need over case 2 water a reference model for the water reflectance. We also ignore the influence of the foam.

8.1.2) Random errors

For a given algorithm applies to a defined L1 product and auxiliary data (LUTs for example), we need to consider the random errors on the inputs:

(i) Gaseous content (O3 and water vapour).

(ii) Barometric pressure.

(iii) Wind speed

(iv) Water reflectance in the NIR.

We will not consider the error on the adjacency effect correction, a domain which is by far too complex to be introduced, except for the relative weights of the direct and diffuse transmittances on the pixel and surrounding reflectances.

8.2) Sensitivity study

This sensitivity study will be based on the use of the TOA reflectance simulator described in annex 2. The nominal case to this sensitivity study will correspond to:

(i) Three MERIS bands: 442 nm, 708 nm and 865 nm.

(ii) 3 SZA: 30°, 60°, 75°.

(iii) 2 VZA: 0° and 30°.

(iv) 3 AA: 0°, 90° and 180°.

(v) Mid latitude summer and winter models.

(vi) 2 IOPA models corresponding to α=-1.2 and -1.95.

(vii) One aerosol vertical distribution with a scale height of 3 km.

(viii) 2 wind speed 3 m/s and 10 m/s

The outputs of the simulator will be used as input of the AC processor. Table 3 is the first attempt to set errors on the inputs. The accuracy on the calibrations is a consensus. For bright clouds, the influence of the threshold should be secondary because the too bright pixels will be rejected downstream. The Cirrus cloud flag is raised above 700 hPa, 100 hPa is reasonable amplitude. The other errors on the inputs are indicative and can be consider as a first guess.

The sensitivity study will focus on the water reflectance in B2 and on the aerosol product.

Name	**Tool**	**Input error**
Radiometric calibration	Simulator	+/- 2 percent relative
Spectral calibration	Simulator	+/- 0.2 nm
Cloud flag	Processor	TBD
Cirrus cloud flag	Processor	100 hPa
Aerosol families	Simulator	Junge and IOPA
O3 content	Simulator	+20 DU
H2O content	Simulator	+0.2 cm
Pressure	Simulator	+5 hPa
Aerosol vertical distribution	Simulator	1 km instead of 3 km
Wind speed	Simulator	+2 m/s
Water reflectance in the NIR	Simulator	20 percent relative

Table 3: Inputs to the error analysis

8.3) Error bars

The systematic errors will be not included in the error bars attached to the product because:

(i) Leading to a complex algorithm and/or to a substantial increase of the processing time.

(ii) Of the absence of a strong scientific consensus on the amplitude.

On the aerosol model

The aerosol model retrieval is conducted in the NIR in B12 and B13. Over case 1 water, the main source of error is the Rayleigh (through the barometric pressure) in the restitution of aerosol reflectance ρ_{aer}:

$$d\rho_{aer}^{Ray} = -\rho_{Ray}\, dP/P \quad (33)$$

A good guess for the relative error on the barometric pressure being 2 percent.

Over case 2 waters, we consider the error on ρ_w and it impact on ρ_{aer}:

$$d\rho_{aer}^{w} = -d\rho_w \; \mathrm{T}_{atm}(\mu_s)\mathrm{T}_{atm}(\mu_v) \quad (34)$$

In presence of direct sunglint, we recomputed this term adding 2 m/s to the wind speed to get:

$$d\rho_{aer}^{G} = d\rho_G \; \exp(-\tau(1/\mu_s + 1/\mu_v)) \quad (35)$$

The total error is the quadratic sum:

$$d\rho_{aer} = d\rho_{aer}^{Ray} \oplus d\rho_{aer}^{w} \oplus d\rho_{aer}^{G} \quad (36)$$

At first order in B13, ρ_{aer} is proportional to the AOT, τ_{aer}:

$$d\tau_{aer}^{B13} / \tau_{aer}^{B13} = d\rho_{aer}^{B13} / \rho_{aer}^{B13} \qquad (37)$$

The selection of the aerosol type is based on the Gordon coefficient between B12 and B13:

$$\varepsilon = \rho_{aer}^{B12} / \rho_{aer}^{B13} \quad (38).$$

And we have:

$$d\varepsilon / \varepsilon = d\rho_{aer}^{B12} / \rho_{aer}^{B12} - d\rho_{aer}^{B13} / \rho_{aer}^{B13} \qquad (39),$$

Or, going back to the Angstroem coefficient:

$$d\alpha = (d\varepsilon / \varepsilon) / \ln(778) / \ln(865) \qquad (40)$$

On the water reflectance

We have a new barometric pressure, a new aerosol model, a new wind, we go to §5.3 or to §6.2. For the correction of the AE effect, $< \rho^*_{Ray} >$ and $< \rho^*_{aer} >$ are not recomputed.

9) Verification

9.1) In absence of adjacency effect

We will use the set of cases reported in §8.2. A first QC will bring on the atmospheric functions (reflectance and transmittances) and on the direct sunglint. The TOA simulator will be then used with gaseous absorption as an input to the ICOL processor.

9.2) ICOL traceability

In the presence of adjacency effects, the CC processor will be clearly an improvement of the current ICOL version. It remains that first some ICOL subroutines will be re used and a new implementation can be validated. Second, an additional QC is to follow the evolution of ICOL.

9.3) Understand the outputs

We will define test scenes to process and based on a scientific expertise, we will evaluate the L2 product with of course an inter-comparison with MEGS and the second CC algorithm.

10) Validation

The validation of the atmospheric correction relies on the use of the AERONET ocean colour network for which we have a consistent set of data with:

(i) the water leaving radiance (or converted value in reflectance)

(ii) a full description of the atmospheric optical properties through the solar extinction measurement and through the sky radiance measurements.

The principle of the validation is to predict the MERIS TOA reflectance thanks to:

(i) The barometric pressure for the Rayleigh.

(ii) The wind speed for the Fresnel reflection

(iii) The measured AOT by the CIMEL instrument.

(iv) The retrieved aerosol phase function after inversion of the sky radiance measurements. The WOPAER software package is one option.

(v) The MERIS water reflectance, regardless of their origin: MEGS, CC or other AC processor.

(vi) A radiative transfer code. The SOS code is one option as well as 6S.

At the end, we have the best description and computation of all the atmospheric functions, and if the L2 water reflectances are correct, we should have an accurate retrieval of the MERIS TOA.

The way to conduct the validation is to detail the protocol and to illustrate it. In order to make it accessible, the realization with the support of ESA of a tool box is a strong recommendation.

11) Conclusion

We will not process B10, B11, B14 and B15 which are devoted to pressure and water vapour determinations. This new AC processor which includes the AE is clearly a CC requirement. It implies major changes in the ICOL processor. Nevertheless, these changes reflect more a reorganization of existing modules or functions than the introduction of new routines. At the end, it will be less time consuming than the current ICOL because:

(i) We do not apply a standard Rayleigh correction.

(ii) We use only 11 spectral bands instead of 13.

If we compare this new algorithm with the previous approach (ICOL at L1 and AC at L2), it will be faster are more consistent.

The introduction of errors is a key issue we decouple in errors:

(i) On the aerosol product we conduct in an analytical way

(ii) On the water reflectance for which we re-conduct an AC with a new aerosol model.

Different modules are devoted to the generation of the atmospheric functions. The 5S formalism is used to build a TOA simulator which can be used to validate the AC processor in absence of AE. The traceability of the different ICOL versions will help for verification.

Our validation strategy is based on AERONET OC using the atmospheric measurements to compute all the atmospheric functions. The water leaving signal proposed by MERIS L2 is the other input to a RTC to predict the TOA radiance. Comparison to MERIS L1 accesses the quality of the AC scheme. We will demonstrate this approach.

The possibility to have a regional algorithm is based on the implementation of new LUTS. The LUTs for regional aerosol can be generated based on new aerosol IOPs. For case 2 waters, new set of water reflectance in the NIR can be computed for the IOPs, including the BRDF.

11) Acknowledgments

We thank O. Danne for the ICOL processing of MERIS images and P. Santer Limerez for the editing.

12) References

Aiken J. & G. Moore (2000) ATBD 2.6. CASE 2 (S) BRIGHT PIXEL ATMOSPHERIC CORRECTION http://envisat.esa.int/instruments/meris/pdf/atbd_2_06.pdf

Antoine, D., and A. Morel, 1999. "A multiple scattering algorithm for atmospheric correction of remotely sensed ocean color (MERIS instrument): Principle and implementation for atmospheres carrying various aerosols including absorbing ones", *International Journal of Remote Sensing*, 20 (9), pp. 1875-1916.

Aznay O. and Santer R.,(2009) MERIS atmospheric correction for over coastal waters: Validation of the MERIS aerosol models using AERONET". International Journal of Remote Sensing, January 2008. .

Cox, C., and W. Munk, 1954. Measurements of roughness of the sea surface from photographs of the sun glitter, *Journal of Optical Society in America*, 44 (11): 838-888.

Deuzé, J.L., M. Herman, and R. Santer, 1989. Fourier series expansion of the transfer equation in the atmosphere-ocean system, *Journal of Quantitative Spectroscopy & Radiative Transfer*, 41 (6): 483-494.

Holben, B., T. Eck, I. Slutsker, D. Tanré, J.P. Buis, A. Setzer, E. Vermote, J. Reagan, Y. Kaufman, T. Nakajima, F. Lavenu, I. Jankowiak, and A. Smirnov, 1998. AERONET – A federated instrument network and data archive for aerosol characterization, *Remote Sensing of Environment*, 66: 1-16.

Santer R., Carrere V., Dubuisson P., & Roger J.C. (1999). Atmospheric correction over land for MERIS, International Journal of Remote Sensing, Vol. 20. Issue 9, p 1819-1840.

Santer R. (2009) *D4: ICOL+ , Nadir view; ATBD for MERIS and Landsat ETM+*. Internal report, this current ICOL contract.

Santer R. (2010) *D6: ICOL+ , case 2 and off nadir view; ATBD for MERIS*. Internal report, this current ICOL contract.

Santer R., Aznay O. and Santer-Limerez P. (2010). The inherent optical properties of the aerosols. Technical note to Coast Colour.

Shettle, E.P., and R.W. Fenn, 1979. Models for the aerosols of the lower atmosphere and the effects of humidity variations on their optical properties, *Air Force Geophysical Laboratory, Technical Report AFGL-TR-79-0214*, Hanscom Air Force Base (Mass.).

Vermote, E., D. Tanré, J.L. Deuzé, M. Herman, and J.J. Morcrette (1997). Second simulation of the satellite signal in the solar spectrum, 6S: an overview, *I.E.E.E. Transactions on Geoscience and Remote Sensing*, 35 (3), 675-687.

Zagolski F., Santer R., Aznay O., (2007). A new climatology for atmospheric correction based on the aerosol inherent optical properties**.** Journal of Geophysical Research, *Vol. 112, No. D14, D14208*

Annex 3